SCUOLA DI DOTTORATO
UNIVERSITÀ DEGLI STUDI DI MILANO-BICOCCA

Department of Earth and Environmental Sciences (DISAT)

PhD program Chemical Geological and Environmental Sciences (SCGA)

Cycle XXXVIII

Curriculum in Terrestrial and Marine Environmental Sciences

UNDERWATER BIOMATERIALS FOR THE TREATMENT OF CORAL DISEASES AND CONSERVATION OF REEF BIODIVERSITY

SCRIBANO VINCENZO

Registration number 897088

Tutor: Prof. GALLI PAOLO

Supervisor: Prof. MONTANO SIMONE
Co-Supervisor: Dr. ATHANASSIA ATHANASSIOU, Dr. MARCO CONTARDI

Coordinator: Prof. MALUSA' MARCO GIOVANNI

ACADEMIC YEAR A.A. 2024/2025

This chapter is based on a published manuscript and has been adapted with permission from the authors.

Chapter 1 – State of the art

Corals are marine invertebrates functioning as holobionts, engaging in complex symbiotic relationships with their hosts, such as dinoflagellate algae (primarily from the *Symbiodinaceae* family) and bacteria (Bourne et al., 2009; Nancy Knowlton & Forest Rohwer, 2003), archaea, protozoa, fungi, and viruses. Dinoflagellates and bacteria represent a significant component of the coral microbiome and play an essential role in maintaining holobiont homeostasis (Liu et al., 2024). *Symbiodinaceae* are endosymbiotic algae that live inside the coral and are the primary source of nutrients for corals. Upon stress, these algae are expelled from the coral tissue as a defensive mechanism of the host, inducing the loss of pigmentation of the coral tissue and producing so-called 'bleaching' (Voolstra et al., 2024). On the other hand, symbiotic bacteria are anatomically compartmentalized and their shift in abundance is directly correlated to responses to stress, age, environment, and seasonality, with their distribution and community composition varying depending also on the bacterial species considered (Apprill et al., 2016; Pollock et al., 2018; Voolstra et al., 2024). An example of that is the bacterium from the genus *Reugeria*, which seems to be associated with many coral species (Huggett & Apprill, 2019) and their abundance is correlated to the presence of stressors, such as diseases (Rubio-Portillo et al., 2021).

However, not all symbionts have solely beneficial effects on corals. Out of the 138 culturable bacterial genera, almost 100 of these are part of the phylum *Proteobacteria*, among which 25.5% were associated with diseased coral colonies (Sweet et al., 2021). Within this phylum, genera like *Reugeria*, *Photobacterium*, *Alteromonas*, *Pseudomonas*, *Pseudoalteromonas*, *Vibrio*, and *Pseudovibrio* have been commonly isolated, although it is worth mentioning that most of the isolates deriving from diseased coral colonies belong to the *Vibrionaceae* family (Sweet et al., 2021).

In particular, it was recently observed that several bacteria from the genus *Vibrio spp.* presented a correlation between their growth and the upshift in temperatures, with some, like *V. coralliilyticus*, even modifying their metabolomic pathways and virulence factors (Sheikh et al., 2022).

Despite the correlation between disease and a single bacterium presented some significant results, even following Koch's postulates, some more recent theories highlighted the possibility that diseases may be caused more by a pathobiome, a consortium of microorganisms, which may play a direct role in the causation of diseases (Sweet & Bulling, 2017).

Some bacteria can induce harmful disease per se, whereas others, such as opportunistic strains (e.g., *V. coralliilyticus*), can leverage favorable community dynamics to thrive and disrupt the holobiont equilibrium following environmental changes like increased seawater temperatures (Apprill, 2017;

Fox-Kemper et al., 2021; Pinzón et al., 2015; Sheikh et al., 2022; Sweet & Bulling, 2017). Pinzón et al discussed how bleaching on corals presents long-term effects that may lead to easier disease appearance, even after 1 year from the event (Pinzón et al., 2015).

In recent years, the spread of coral diseases has drastically increased, and it is estimated that by 2100, nearly 80% of corals will be infected (Burke et al., 2023). Such escalation might be addressed to the corals' genomic inability to withstand pathogen attacks, as well as the higher frequency of environmental perturbations imposed by climate change that may cause rapid shifts in microbiome bacterial communities (Mydlarz et al., 2009; Pinzón et al., 2015; Pollock et al., 2019; Rosales et al., 2019; Voolstra et al., 2024).

Environmental factors affecting disease rate

Climate change is significantly affecting the reefs' homeostasis. Often, these environmental perturbations affect the coral microbiome and the coral immune system, making them more susceptible to pathogens (Burke et al., 2023; Muller et al., 2018; Thurber et al., 2020). An increase in drastic environmental-derived stress seems to be directly related to the increased number of diseased colonies in the reefs (Mera & Bourne, 2018). Increasing temperatures are the major driver and the most studied of disease dynamics influencing intervals in which corals could be infected or transmitted, and the time at which they could undergo recovery (Burke et al., 2023; Thurber et al., 2020). Pathogens from different classes, such as bacterial, protozoal, and fungal, may benefit from changes in seawater temperatures, provoking diseases such as white syndromes, black and yellow band diseases (Cervino et al., 2008; Harvell et al., 2009; Heron et al., 2010; Maynard et al., 2015; Maynard et al., 2011; Muller & van Woesik, 2012, 2014). Despite that, in many cases, the direct link between disease and temperature is still unknown (Thurber et al., 2020). In nature, as many environmental factors are interconnected, it becomes difficult to separate the single environmental stress influence. Whereas in the laboratory, where environmental stimuli can be induced singularly, it is easier to discern among different stresses and observe how each influences the disease. For instance, Sato et al. found that an increase in light amount determined an increased progression rate for the black band disease, whereas an increase in temperature did not seem to affect the velocity progression (Sato et al., 2011). In the same way, other environmental stressors have been demonstrated to influence coral diseases in the field after disastrous events, such as increased nutrient availability (e.g., rainfall in inshore reefs) (Haapkylä et al., 2011; Thurber et al., 2014) or cyclones and storms (Beeden et al., 2015; Brandt et al., 2013).

Another abiotic factor connecting ocean warming and air pollution to the increased coral bleaching is the rising concentrations of CO_2 in the atmosphere due to anthropogenic factors, which promote

ocean acidification and a reduction in coral skeletal bulk structure (Prada et al., 2017), however, the role of ocean acidification in the alteration of the coral microbiome is still debated (Barreto et al., 2021).

On the other side, direct anthropogenic factors such as increased pollutants (Lamb et al., 2016; Redding et al., 2013; Rice, Maher, et al., 2019) with a particular focus on plastic debris (Beloe et al., 2022; Browne et al., 2015), have been considered as primary effectors of an increased prevalence of coral disease in the reefs (Moriarty et al., 2020), even if insufficient evidence on the direct involvement of plastic debris in the rising rate of diseases in the reef has been published so far (Beloe et al., 2022). Among the anthropogenic actions, tourism and overfishing seem to directly and indirectly influence the increased rate of coral infections (Lamb et al., 2014; Lamb et al., 2015; van de Water et al., 2015; Zaneveld et al., 2016), resulting in the significant alteration of coral-algal competition or the coral microbiome destabilization (Rice, Ezzat, et al., 2019).

The interaction microbiome-host

The increased susceptibility to diseases is not solely related to the unfavorable environmental conditions caused by climate change. Coral diseases can be determined by different pathogens, including bacteria, protozoa, but also fungi, and viruses (Gleason et al., 2017; Roik et al., 2022; Sweet & Bythell, 2017). However, to a relatively large number of diseases (up to 40 different coral diseases identified worldwide), a low number of phenotypical responses to distress is shown (discoloration, tissue loss, growth anomalies), making it a challenge to correctly identify diseases exclusively by the morphological observation of the infection (Akmal et al., 2023; Meyer et al., 2025; Moriarty et al., 2020). The main methodology for the identification of the leading pathogen causing the disease was the reinfection of healthy corals using the cultured suspected pathogen to observe if the same disease was shown and the pathogen re-isolated (Koch's postulates) (Meyer et al., 2025). Several researchers debated the results found following this method (Kellogg et al., 2013; Lesser & Jarett, 2014; Pantos et al., 2003; Thurber et al., 2020; Toledo-Hernández et al., 2008).

Such complexity in understanding the etiopathology of a specific infection also relies on identifying the entire microbiome community present during dysbiosis, which may affect the coral health.

During a disease, the microorganisms inhabiting the host change in composition and in the ratio of populations; generally, some family of bacteria, such as *Vibrionaceae,* prevail over others (e.g., *Endozoicomonaceae*) (Rubio-Portillo et al., 2021; Thurber et al., 2009). In particular, it has been hypothesized that in some cases, an entire consortium of microorganisms participates rather than being a single actor causing the infection (Sweet & Bulling, 2017). This was already often observed in the past, such as in the case of the Black Band Disease (BBD) (Meyer et al., 2017): a

cyanobacterium is usually leading the disease (Miller & Richardson, 2011), followed by other phylogenetic groups (*Gammaproteobacteria*, *Deltaproteobacteria* and *Firmicutes*), responsible of sulfide production, toxic for the host and typical of the disease, which however does not harm the cyanobacterium leading the disease (Meyer et al., 2015; Miller & Richardson, 2011).

Multiple infections may also happen simultaneously, where some bacteria act as primary pathogens while others work as opportunists and rely on the weakened immune system of the coral to further exacerbate the equilibrium of the microbiome and leverage the dysbiosis (Meyer et al., 2025; Sweet & Bulling, 2017). This is particularly true in the case of the interaction between *Pseudoalteromonas piratica* and a pre-existing diseased *Montipora capitata* affected by Montipora white syndrome. In this case, the interaction of *P. piratica* with the already infected host exacerbates the disease, switching from the chronic to the more aggressive acute condition (Silvia Beurmann et al., 2017). Another interesting example is the increased pathogenicity of *Vibrio coralliilyticus* and *Vibrio mediterranei* when cocultured in competing conditions. It has been observed how these bacteria increased the production of biofilms and induced significant changes in the microbiome of *Oculina patagonica*, favoring coral tissue damage (Rubio-Portillo et al., 2020).

Although most spotted microorganisms causing diseases are bacteria because of their simpler cultivation in the laboratory, the pathogens causing diseases to corals are multiple and differentiated. Other diseases, such as the Skeletal Eroding Band (SEB) and the Brown Band disease (BrB), which are widely distributed in the Indo-Pacific area, seem to be caused by ciliated protozoa (Akmal et al., 2023; Moriarty et al., 2020), whereas the so-called aspergillosis was associated with the fungus *Aspergillus sydowii* in the fan coral *Gorgonia ventalina* (Byers, 2021; Ward et al., 2007). Another example is the stony coral tissue loss disease (SCTLD), an aggressively spreading disease that has affected most Caribbean reefs, the etiopathology of which is still unknown and/or not confirmed, but is supposed to be transmitted and caused by multiple vectors, either bacteria or viruses (Papke et al., 2024; Precht et al., 2016; Work et al., 2021).

The abundance and variety of pathogens among different reigns (Barton et al., 2020; Byers, 2021; Thurber et al., 2020), the imprecise disease classification due to reduced ways for a coral to display diseases (Work & Aeby, 2006), which names also tend to vary based on regionality and coral species involved (e.g., white syndromes) (Willis et al., 2004), and the unclear etiopathology of most diseases, together with the genomic variability that conceals the hosts (Thurber et al., 2020), it makes identifying proper treatments to face coral diseases extremely challenging.

Coral diseases in aquacultures

In recent decades, coral trading became an important industry providing up to 1.5 million dollars per year and allowing the development of proper coral aquacultures, either close to the reef (also called *in situ* or mariculture) or in deputed closed systems such as aquaria (*ex situ*) (Khodzori et al., 2024). This market covers the production for the restoration activities, the pharmaceutical sector, and the hobbyists (Tagliafico et al., 2018). Despite these facilities being set to allow optimal coral growth, they may also face several diseases, and due to their high rearing density, diffusion of pathogens is favored, risking the destruction of entire production lines (Sheridan et al., 2013).

Maricultures are usually set by lagoons or shallow waters, in natural environments, so that the growing conditions resemble, at best, the conditions in the reefs. However, this poses a risk to the possible exposure to all the biotic and abiotic stresses present in the reefs (Sheridan et al., 2013).

On the other hand, ex situ coral aquaculture is more protected and controlled from pathogens as corals are reared in tanks. Here, water can be supplied through two different systems: flow-through aquaculture system (FTAS), where the water is pumped directly from and to the ocean and filtered (mechanically and chemically), or recirculating aquaculture system (RAS), where the water is in a full closed system and recirculates constantly (Sheridan et al., 2013). However, if the filtration is not actuated correctly, there is the risk of pumping pathogens and vectors from the natural environment, or in the case of the RAS, where the water is mostly recirculating, an imbalance in the nutrients present in water (e.g., trace elements) may impair coral health and growth (Sheridan et al., 2013).

In this context, corals in mariculture have experienced dysbiosis due to a sudden change in environmental conditions, favoring the spreading of diseases that resemble those found in reefs (Khodzori et al., 2024). However, even an equipment dysfunction may produce a change in the water condition, which may turn into diseases, as disease-associated pathogens, such as *Vibrio coralliilyticus*, were also observed in healthy coral tissues, and whatever shift in the coral microbiome may alter the pathogen concentration and promote an infection (Sheridan et al., 2013; Thurber et al., 2009).

There have been some attempts to connect or associate diseases in nature with those observed in aquaculture facilities (Sweet et al., 2012), but the incomplete etiopathology of most of them (Moriarty et al., 2020; Sweet & Bulling, 2017), brought the researchers to classify most of them as separate diseases, despite the similarity that has been found (Sweet et al., 2012).

An example of this is the Rapid Tissue Necrosis (RTN) or shutdown reaction, which is characterized by a quick tissue detachment from the coral skeleton and has been found associated with *Vibrio harveyi* (Luna et al., 2007). However, it is worth mentioning that *Vibrio harveyi* was observed to be the causative agent of white syndromes as well (Luna et al., 2010), even if this bacterium was not the

only one that was associated with white syndromes. Indeed, other bacteria, such as *Aurantimonas* coralicida (Denner et al., 2003), as well as others from the Vibrio family (Sussman et al., 2008), and even some ciliates have been hypothesized to be the primary vectors (Sweet & Bythell, 2012).

The uncertainty on the leading cause of diseases brings the attention more on the pathogen involved rather than the disease caused, as this seems to vary also based on multiple other factors, such as coral infected, geography location, biological (e.g., genotype, microbial community present, etc.), and environmental conditions (e.g., temperature, light, pollution, etc.) (Meyer et al., 2025). Hence, the development of identification methods for analyzing pathogens in coral diseases should be supported by very precise and versatile or wide-spectrum technology to arrest the disease and prevent pathogen diffusion.

Methods against coral diseases

In the last 30 years, several methods have been reported to attempt diseases treatment of some of the most common diseases, such as the Black Band Disease or the Yellow Blotch Disease, mainly focusing on the usage of suction methods to remove the infected band and cover up using clays to prevent the spreading (Bruckner, 2002; Bruckner & Bruckner, 1999; Hudson, 2000).

Some of those methods are still used in more recent times to prevent the spread of the disease (Ruiz-Diaz et al., 2016), but the increasing occurrence of diseases induced researchers to evolve the techniques to prevent coral infection.

The mechanical removal of the lesion (infected coral tissue), administration of probiotics, phage therapy, or active molecules are all methods that have been recently or are currently used (Beurmann et al., 2017; Neely et al., 2021; Roger et al., 2023; Thatcher et al., 2022) and that may need some more investigation.

For instance, mechanical separation of the infected site from the healthy coral, despite resulting in success for some coral types such as *Gorgonia ventalina* (Ruiz-Diaz et al., 2016). Instead, in *Montipora capitata*-infected corals, this treatment did not prevent the reinfection, probably because of the production of new lesions and entry points for other pathogens present in the surrounding environment (S. Beurmann et al., 2017). Most probably, the success of this technique is mediated by the pathogen causing the disease or by its vector, determining the modality of reinfection.

Phage administration is a ready-to-use method to attack a pathogenic agent causing a specific infection (Cohen et al., 2013). The phage specificity for a determined bacterium, such as *V. coralliilyticus*, is a great advantage in controlling the treatment. Viruses are obligate parasites, and their proliferation depends on the host's presence. Moreover, many phages have already been observed in the coral (Rubio-Portillo et al., 2024) and have presented some astonishing results in the

field as well (Atad et al., 2012). However, the high specificity of this technique and the lack of information regarding the etiopathology of many coral diseases make this approach inefficient for use on uncharacterized diseases. Also, as much as for antibiotics, there is the chance that bacteria would develop resistance to that phage, and the maintenance of large-scale stable phage formulations is highly demanding and, to date, not yet produced, despite they present significant consideration as a future direction toward the development of aquaculture treatments (Strathdee et al., 2023).

Technologies for the delivery of probiotics

Due to the recent mass bleaching events (Neely et al., 2024; Reimer et al., 2024), the study and administration of Beneficial Microorganisms for Corals (BMCs) has become a trending treatment for coral bleaching in recent years, trying to mitigate these catastrophic phenomena (Delgadillo-Ordoñez et al., 2024; Dörr et al., 2025; Garcias-Bonet et al., 2025; Peixoto et al., 2017; Reshef et al., 2006; Rosado et al., 2019).

Surfing this wave, the idea to treat diseases with potential probiotics by direct administration or by the usage of delivery methods has been recently explored (Delgadillo-Ordoñez et al., 2024; Demko et al., 2025; Pitts et al., 2025; Ushijima et al., 2023). In particular, it is worth mentioning the first successful trial of a targeted delivery method that efficiently reduced coral damage by about 5-fold compared to the control (Pitts et al., 2025). This was performed through multiple administrations of the bacterial strain McH1-7 using incubating bags to avoid probiotic dispersion and then improving coral uptake.

Administering probiotics seems to be a promising technique to slow down coral disease progression even in the long term (up to two years (Pitts et al., 2025)). However, it presents challenges that still need to be addressed. Probiotics can be coral species-specific, and the potentially unpredictable effects on the local marine bacterial community still need to be fully understood (Sweet et al., 2017; Thatcher et al., 2022). Moreover, the repeated delivery can be pretty expensive and time-consuming, and the production of a scalable quantity of probiotics that could be preserved for the long term may pose a problem that still needs to be addressed. Further research is encouraged, and the positive feedback obtained so far promotes investments in this direction.

Technologies for the delivery of active molecules

Despite the other techniques seeming to have a good grasp on the development of new technology for the treatment delivery of diseased corals, the delivery of active molecules, such as antibiotics, seems to be the most straightforward method to treat coral disease on a reef scale (Toth et al., 2024).

It is worth mentioning that alternatives to antibiotics have been spotted, such as the usage of chlorine or potential natural extracts from either algae or bacterial sources (Aeby et al., 2015; Cotas et al., 2020; Sang et al., 2019). However, the efficacy of these treatments is relative to the disease and, more importantly, to the pathogen that is intended to be eradicated (Forrester et al., 2024). Despite the alternatives, the massive use of antibiotics in the field to fight what is one of the most lethal coral diseases ever faced seems to be the most effective solution (Forrester et al., 2024; Neely et al., 2020; Neely et al., 2021; Toth et al., 2024). However, many concerns regarding the development of antibiotic resistance, the alteration of the holobiont community, and potential cascading effects such as dysbiosis and the spread of opportunistic pathogens have been raised (Meyer et al., 2025; Sweet et al., 2014).

Such doubts come from the current methodology of antibiotics delivery, which nowadays focuses on direct application to the coral infection site via topical pastes (Neely & Hower, 2019; Neely et al., 2020; Neely et al., 2021; Shilling et al., 2021; Sweet et al., 2012; Toth et al., 2024).

Paying more attention to the delivery system used so far, it is noticeable that the antibiotic-loaded pastes are applied as a single, uniform, and continuous layer directly onto the infected area, ensuring its coverage. The parameters influencing drug diffusion from a matrix, including dissolution into the environment, are noteworthy as they involve Fick's laws (concentration, dispersion), the hydrophobic/hydrophilic properties of the material, crosslinking, and other water-related parameters such as swelling, erosion, temperature, pH, and ionic strength (Lehner, 1979; Paul et al., 2014; Saranjampour et al., 2017). Among them, the quantity of water in contact with the material plays a crucial role in drug diffusion and the linked phenomenon of matrix erosion, especially when a material is applied as a mono-layer on corals (Visan et al., 2021). Indeed, at the interface between the coral tissue/infected area and the active material surface, a very low amount of water will be present, especially compared to the quantity of water in the sea. The difference in volume between the two exposed sides of the mono-layered paste could represent an obstacle to the diffusion of the drug toward the infected coral site, reducing efficacy and, thus, potentially inhibiting the effectiveness of the treatment (Liu et al., 2019; Smith, 2005; Wu & Grainger, 2006). Indeed, at the interface between the active material and the external marine environment, the drug diffusion and the erosion of the matrix mediated by seawater are theoretically enhanced, compared to the internal interface. This difference may favor the diffusion of the antibiotic in the environment (Shilling et al., 2021; Sweet et al., 2014). Approaches like this one can foster the previously mentioned concerns regarding the use of antibiotics (Connelly et al., 2022; Connelly et al., 2023; MacVittie et al., 2024; Vizcaino et al., 2010).

In the past, similar challenges faced in treating human infections have been resolved through the dedicated design of topical drug delivery systems. These deliver antibiotics directly to the infected area, ensuring drug availability at the proper concentrations throughout the treatment period. The constant and localized administration enhances the overall healing rate while minimizing interaction with non-involved tissue (Adebisi, 2023; Wu & Grainger, 2006). Specifically, in buccal infections, the delivery system releases the drug unidirectionally by having a hydrophilic layer loaded with the drug that comes in contact with the buccal tissue (both infected or healthy), and a covering hydrophobic external layer to avoid the dispersion of the drug in the external wet environment made of the mouth, saliva, sublingual area, etc. (Sonawane et al., 2017). This scenario is somewhat similar to the coral infection case. Hence, an ideal underwater drug delivery system should focus its intervention on the infected region, focusing the drug delivery on one single spot and avoiding the dispersion of drugs in the surrounding environment (Contardi et al., 2020; Sonawane et al., 2017). Moreover, the ideal system should present suitable mechanical properties such as flexibility, moldability, and adhesivity, as well as be user-friendly (Zych et al., 2024). Finally, the underwater drug delivery system should promote coral tissue growth, and its dispersion in the environment should not damage the environment itself (Contardi et al., 2023; Contardi et al., 2020).

Recently, Contardi *et al.* proposed the first *in-situ* drug-delivery system for coral wounds, using a hydrophilic polymeric film to deliver antiseptics to the wounded site and a sealing thermoplastic to separate the covered wound from the surroundings, leading the way to underwater coral drug-delivery (Contardi et al., 2020). Inspired by previous research on the design of buccal delivery systems to treat human infection in wet environments and the previous works from my group, I developed a new strategy for treating coral disease.

Knowledge gap

Actual limitations in underwater drug delivery

To date, the unknown pathogenicity of many diseases is probably the most significant issue determining the bottleneck to the development of new treatments (Meyer et al., 2025). The uncertain causation, as well as the nonspecific signs of disease, are a significant challenge to whoever tries to develop a new treatment for a specific disease, hence mining the effectiveness of the proposed system (Meyer et al., 2025; Sweet & Bulling, 2017). To compensate for the uncertainty of the disease etiology, methods such as the use of wide-spectrum antibiotics are employed (Neely & Hower, 2019; Neely et al., 2020). On the other hand, this application found the bases for the concerns regarding the development of antibiotic resistance in the bacteria interacting with sublethal concentrations of antibiotics (Andersson & Hughes, 2014).

A first design of a potential unidirectional underwater drug delivery system was proposed by (Contardi et al., 2020). However, in this first work, the unidirectionality of the drug diffusion was not proven. Moreover, the inapplicability of such systems in situ limits considerably their application.

In the following chapters, I will try to overcome the knowledge gap presented here through the development of possible solutions for the treatment of coral diseases.

Chapter 2 – Aim of the thesis

Numerous factors endanger reefs and the environments related to them due to climate change, and diseases are setting the final point on their disappearance. Outbreaks with exponentially increasing frequency occur, related to rising seawater temperatures, pollution, and alteration of the ecosystems because of tourism and overfishing.

To prevent reef destruction, intense restoration programs are undertaken to protect and rebuild reefs using artificial constructions to resemble the coral 3D structures and aquacultures to refurbish the dead areas of the reefs. However, corals, especially when freshly transplanted, tend to be more susceptible to diseases, and the mortality rate is high. To prevent reef desertification due to outbreaks, environmentally friendly solutions should be presented to preserve one of the most important ecosystems in the world.

This doctoral project aimed at the development of eco-friendly solutions for the treatment of coral diseases, focusing on infection determined by bacteria of the *Vibrio* family, some of which are coral pathogens known to develop a virulent behavior at temperatures high enough to impair the coral immune system, and hence are highly infective and virulent, which could cause outbreaks. Moreover, a further goal was posed during this Ph.D.: avoiding the pollution of the environment. To do so, the obtained technologies were designed to be fully biodegradable, focusing also on the concept of underwater targeted drug delivery and, hence, preventing the spread of active molecules in the surrounding environment, such as antibiotics.

The final achievements of these solutions were then further optimized, singularly isolating and improving each of the main features of the leading technology, focusing on the improvement of applicability of the technology underwater, in particular on the adhesivity and the sealing of the infection, and on the development of antibiotic-free alternatives for the treatment of bacterial-determined coral diseases.

Chapter 3 – Eco-friendly active film and sealant for underwater drug delivery to diseased corals

This chapter is a readaptation of *Scribano et al. "Eco-friendly active film and sealant for underwater drug delivery to diseased corals." One Earth 8.7 (2025).*

Introduction

Active compounds such as antibiotics, which are widely available and possess broad-spectrum activity, have been considered a straightforward option for treating coral diseases caused by unidentified pathogens (Vega Thurber et al., 2025). A clear example is the treatment recently developed for stony coral tissue loss disease (SCTLD). Although the causative agent remains unknown, the disease has been managed with a combination of the antibiotic amoxicillin and a silicon-based product, Base2b (Neely et al., 2020; Neely et al., 2021; Shilling et al., 2021; Toth et al., 2024). However, concerns remain regarding the potential development of antibiotic resistance, disruption of the coral holobiont, and downstream effects such as dysbiosis or the rise of opportunistic pathogens (Sweet et al., 2014).

For example, *Serratia marcescens*, the bacterium responsible for serratiosis in Acropora palmata, developed resistance after repeated exposure to antibiotics used in human treatments (Tavares-Carreon et al., 2023).

These concerns are valid, yet antibiotics—when delivered with precision—can still be highly effective in maintaining coral health (Vega Thurber et al., 2025). Furthermore, the likelihood of resistance can be reduced by ensuring sufficiently high doses are administered, so that even partially resistant populations are eradicated (Roberts et al., 2008).

Traditionally, antibiotics have been applied directly to infection sites by incorporating them into hydrophobic pastes, which are then placed on the advancing disease front (Neely et al., 2020; Neely et al., 2021). This technique, however, could be optimized as embedding an antibiotic within a hydrophobic or highly crosslinked matrix, such as silicon-based materials, that forms a uniform and continuous coating over the lesion, may ensure adequate coverage of the diseased area but simultaneously expose the antibiotic-loaded matrix to the surrounding seawater.

Drug release from matrices is influenced by various parameters, including Fick's diffusion laws (concentration gradients, dispersion), hydrophobic/hydrophilic balance of the carrier, degree of crosslinking, and water-related factors such as swelling, erosion, temperature, pH, and ionic strength (Lehner, 1979; Paul et al., 2014; Saranjampour et al., 2017). In particular, the amount of water in contact with the material strongly affects diffusion and matrix erosion, especially when the formulation is applied as a monolayer to corals (Visan et al., 2021). At the interface between the coral

lesion and the active material, water availability is relatively low compared to the surrounding seawater. This imbalance may hinder diffusion toward the infected tissue, decreasing treatment effectiveness (Liu et al., 2019; Smith, 2005; Wu & Grainger, 2006). By contrast, drug diffusion and matrix erosion are enhanced at the material–seawater boundary, favoring drug loss to the environment (Shilling et al., 2021; Sweet et al., 2014). Such leakage not only diminishes treatment efficacy but could also contribute to antibiotic resistance and potentially encourage pathogens, such as *Vibrio spp*., to colonize adjacent tissues (Connelly et al., 2022; Connelly et al., 2023; MacVittie et al., 2024; Pearson-Lund et al., 2025; Vizcaino et al., 2010).

Comparable challenges in human medicine have been addressed through the careful design of localized drug delivery systems. These platforms deliver antibiotics directly to infection sites, maintaining therapeutic concentrations throughout treatment while limiting exposure of healthy tissues (Adebisi, 2023; Wu & Grainger, 2006). Inspired by strategies developed for buccal infections—which also occur in wet environments—we designed a similar system for coral disease management. In buccal applications, a hydrophilic, drug-loaded layer is placed against the tissue, while a protective hydrophobic outer layer prevents drug loss into the oral environment (Sonawane et al., 2017). This scenario closely parallels coral infections, where an ideal underwater system should ensure targeted drug release to the diseased tissue while preventing environmental dispersion (Contardi et al., 2020; Sonawane et al., 2017). In addition to controlled release, the system should possess mechanical characteristics such as flexibility, moldability, and adhesiveness, while also being easy to apply in situ (Zych et al., 2024). Ideally, it should support coral tissue regeneration and have no adverse environmental impacts if dispersed (Contardi et al., 2023; Contardi et al., 2020).

Recently, Contardi and colleagues introduced the first in situ drug delivery approach for coral wounds, using a hydrophilic polymeric film to apply antiseptics, combined with a thermoplastic sealant to protect the treated site from seawater (Contardi et al., 2020). While pioneering, the system was not tested for unidirectional drug release in diseased corals, and the requirement to melt the thermoplastic before use posed practical challenges in field applications.

Here, we present an improved two-part strategy for treating coral infections. The method involves sequential application of a hydrophilic, antibiotic-loaded film onto the active disease front, followed by a hydrophobic sealant to encapsulate it. This design enables controlled, unidirectional drug release toward the lesion, while preventing antibiotic loss to the environment and reducing the risk of resistance development. In vitro, the treatment was effective against *Vibrio coralliilyticus*, and in vivo, it successfully treated corals with tissue necrosis-like disease. This dual-component approach introduces a new framework for underwater drug delivery and could inspire future therapeutic tools for coral disease management.

Materials and methods

Materials:

Linseed Oil (LO, CAS-No: 8001-26-1), Beeswax (BW, CAS-No: 8012-89-3), Chitosan (C, CAS-No: 9012-76-4), and polyvinylpyrrolidone (360 kDa) (P, CAS-No: 9003-39-8) were obtained from Sigma-Aldrich and used without further modification. Acetic Acid (CAS-No: 64-19-7), Ciprofloxacin (Cipro, CAS-No: 85721-33-1), and Gentamicin Sulfate (Gent, CAS-No: 1405-41-0) were also sourced from Sigma-Aldrich. Marine Broth 2216 (Product No.: 76448-500g) was purchased from Millipore and used as recommended. Deionized water was supplied by a Milli-Q Advantage A10 ultrapure water purification system (Merck-Millipore, Darmstadt, Germany). Polyglycerol-10 was provided by SPIGA NORD S.p.A. (Batch No.: PG10_20221021_0945). Sunflower Oil (SFO) was purchased as a commercial product (Lot. N.: L309323) ("Olio di semi di Girasole Coop,"). The Sylgard-184 kit (Product No.: 761028) was purchased from DOW Corning Corporation (Midland, Michigan, USA). *Vibrio coralliilyticus* (strain ATCC BAA-450) was obtained from DSMZ (Braunschweig, Germany).

Preparation of Sealant:

Beeswax was combined with either LO or SFO, chosen for their different levels of unsaturated fatty acids, at a weight ratio of 4:1 (BW:Oil). The resulting formulations were named BW4LO1 and BW4SFO1, respectively. Mixtures were melted in aluminum cups at 90 °C for 5 minutes, then cooled. For rapid solidification, samples were cooled in a dry ice bath and stirred to room temperature—these were designated as “DIC” (Dry Ice Cooled). Samples cooled without dry ice were allowed to solidify at room temperature and referred to as “not DIC”.

Preparation of Films:

Polyvinylpyrrolidone (P) and Chitosan (C) were mixed at two ratios: 1:1 (50P-50C, 1050 mg each) and 7:3 (70P-30C, 1470 mg P and 630 mg C). The polymers were dispersed in 20 mL of 8% v/v aqueous acetic acid. Antibiotics (Gentamicin or Ciprofloxacin) were separately dissolved in 8% v/v acetic acid to 10 mg/mL. Polyglycerol-10 was prepared in the same solvent at 50 mg/mL. 8.4 mL of the polyglycerol solution and 2.542 mL of the antibiotic solution were added to the polymer mixture. For control (no-drug) films, the same volume of acetic acid solution was used instead of the antibiotic. The final mixture volume was adjusted to 35 mL with 8% v/v acetic acid. Solutions were homogenized, stirred at 55 °C for 2 hours, then cast into square Petri dishes (120 × 120 mm²) lined with Sylgard-184 silicone. Films were dried under airflow (0.5 L/min, 16–20 °C, 40–50% RH) for 48 h, yielding ~ 2.55 g per film. 50P-50C final composition: 41.25% P, 41.25% C, 16.5% polyglycerol-

10, and 1% antibiotic. 70P-30C final composition: 57.75% P, 24.75% C, 16.5% polyglycerol-10, and 1% antibiotic.

Scanning Electron Microscopy:

Morphologies of films and sealants were examined with a JOEL JSM-649LA scanning electron microscope (JEOL, Tokyo, Japan), operating at 5 kV in high vacuum. Samples were sputter-coated with 10 nm gold (Cressington Sputter Coater – 208 HR, UK).

ATR-FT-IR spectroscopy:

Fourier transform infrared spectra (4000–600 cm^{-1}, resolution 4 cm^{-1}, 64 scans) were acquired using a Bruker Vertex 70v FT-IR spectrometer coupled with a MIRacle ATR diamond crystal (PIKE Technologies).

Thermal analysis:

Thermogravimetric analysis (TGA) was performed with a TGA Q500 (TA Instruments, USA). Samples (7–12 mg) were heated from 30–800 °C at 10 °C/min under nitrogen (50 mL/min). Weight loss and derivative curves were recorded and normalized to the initial mass at 30 °C.

Differential Scanning Calorimetry (DSC):

Sealants (~5 mg each) were analyzed with a Discovery DSC 250 system (TA Instruments) equipped with a Discovery RCS90 cooling system. Samples underwent the following program: equilibration at 20 °C, rapid cooling to –20 °C (1 min isothermal), heating to 100 °C, cooling back to –20 °C, and a second heating cycle to 100 °C (10 °C/min). Deconvolution of melting peaks was performed using Origin 2022 (version 9.9.0.225) with the “Peak Analyzer” tool, ensuring $R^2 \geq 0.99$.

Dynamic Mechanical Thermal Analysis (DMTA):

Sealants BW4SFO1–DIC, BW4SFO1–not DIC, BW4LO1–DIC, and BW4LO1–not DIC were tested with a DMTA TA Q800 (compression clamp, frequency sweep mode). Samples were subjected to a 1 °C/min ramp between 15–50 °C (n = 3), with 10 Hz oscillation frequency and 5 µm amplitude after a 1 N preload. Storage modulus, loss modulus, and tan δ were recorded.

Tensile test:

Films were cut into dog-bone specimens (4 mm width, 25 mm length). Tests were performed at 20 mm/min on an Instron 3365 universal testing machine. Young’s modulus, maximum tensile stress,

and elongation at break were derived from stress–strain curves. At least 7 specimens per film were analyzed at 25 °C and 44% RH.

Water contact angle:

Sealant hydrophobicity was evaluated using an OCA-20 goniometer (DataPhysics Instruments, Germany) at 16–20 °C, 40–50% RH. Seawater droplets (5 µL) were deposited, and static WCA was measured. A minimum of 14 replicates per sample were collected. For films, dynamic WCA (DWCA) was recorded every second for 5 min (3 replicates per sample).

Sealant temperature variation test:

Temperature changes during mixing were monitored using a Greisinger GMH 3250 thermocouple. BW4LO1–DIC was hand-mixed at room temperature (20 °C) in air, and in seawater at 20 °C and 25 °C. Internal paste temperature was recorded until stable.

Unidirectional drug release test:

A transwell system (VWR® Tissue Culture Plate Inserts, 6.5 mm diameter, 0.4 µm PET membrane) was used to simulate drug release. Films containing Ciprofloxacin (6 mm) were placed in the inserts, followed by sealant disks (7 mm) and 0.25 mL seawater. The insert was then positioned in a well containing 1 mL seawater, creating two compartments: the bottom (simulated coral lesion) and the top (marine environment). Seawater was collected from Old Harbor, Genoa (Italy), filtered to 1.2 µm. Tests were conducted at 25 °C. Ciprofloxacin release was monitored by UV–Vis spectrophotometry (CARY 300 Scan), using absorbance at 330 nm. Gentamicin release was not evaluated because it does not present aromatics or double bonds that makes it visible within the spectra considered. Samples were collected up to 168 h (7 days). Experiments were run in triplicate.

Biochemical Oxygen Demand (BOD):

Following ISO 23977-2:2020, 50 mg of film or sealant was incubated in 432 mL seawater (Old Harbor, Genoa). Oxygen demand over 30 days was measured using OxiTop®-IDS sensors. Values were corrected for seawater blanks and expressed as mg O_2/100 mg material.

Minimal Inhibitory Concentration:

MIC tests were carried out in 12-well plates, each containing 2 mL of sterilized marine broth inoculated with *Vibrio coralliilyticus* at 1.7×10^6 CFU (OD_{600} = 0.01). Serial dilutions of Ciprofloxacin (Cipro) and Gentamicin (Gent) were prepared, ranging from 0.125 to 64 µg/mL. After

24 hours of incubation at 28 °C with constant shaking (100 rpm), bacterial growth was quantified by measuring OD_{600}. Stock solutions were prepared as follows: 10 mg Gentamicin in 1 mL milliQ water, and 10 mg Ciprofloxacin in 980 µL milliQ water with 20 µL acetic acid. Susceptibility categories (Resistant, Intermediate, Susceptible) were assigned according to the guidelines (*The European Committee on Antimicrobial Susceptibility Testing - EUCAST 2025*).

Disk Diffusion Assay:

Disk diffusion tests were performed on marine agar Petri dishes seeded with *V. coralliilyticus* (200 µL at 3.4×10^{10} CFU, $OD_{600} = 0.2$). Three 6 mm film disks were placed on each plate and incubated for 24 hours. Inhibition zones were measured using ImageJ, with the 90 mm Petri dish diameter as a scale. Control disks were prepared with sterile filter paper loaded with either growth medium (negative control) or Apramycin (5 mg/mL, positive control). Statistical analysis of inhibition zone diameters was performed using one-way ANOVA followed by Bonferroni post-hoc testing, with $\alpha = 0.05$. Groups not sharing a common letter were considered significantly different.

Growth analysis in liquid:

To further test antibacterial efficacy, growth inhibition was evaluated in liquid culture. *V. coralliilyticus* ($OD_{600} = 0.01$, $\sim 1.7 \times 10^6$ CFU) was exposed to UV-sterilized films at three concentrations (1.0, 2.5, and 5.0 mg/mL; triplicates for each). Cultures (2 mL marine broth) were incubated for 24 hours at 28 °C with 100 rpm shaking. Initial OD_{600} was measured at T0, and after incubation, surviving CFUs were quantified by plating 10 µL aliquots.

Statistical comparisons of bacterial counts after 24 h were conducted using two-way ANOVA followed by Bonferroni post-hoc analysis ($\alpha = 0.05$). Inert Teflon films were used as positive controls, and a blank broth culture (no antibiotics, no films) served as a growth control but was excluded from statistical analysis since it lacked comparable film treatments.

Maintenance and Growth Condition of Corals:

Experiments were conducted with *Stylophora pistillata*, a reef-building coral maintained at the Genoa Aquarium. Fragments from three diseased colonies were used. Corals were fed twice weekly with a suspension of *Tetraselmis* sp. algae and rotifers.

Daytime conditions used a semi-open system: water (25 °C) was pumped from 50 m depth, filtered through sand, UV-sterilized, and circulated at 0.3 m^3/h. At night, a closed system recirculated seawater through a sand filter (0.4 mm, Astralpool ARTIC) and UV sterilizer (Panaque 750 s, 4 × 40 W lamps), with a pump circulation of 10–13 m^3/h (full turnover every 25 minutes). Lighting was

provided by HQI lamps (400 W, 10,000 K Nepturion BLV, 12:12 light–dark), at 250 µmol photons m^{-2} s^{-1}. To enhance calcification, 50 L of $Ca(OH)_2$ solution (18 g/L) was dripped nightly. For infection experiments, 20 *S. pistillata* fragments were isolated in a separate 400 L tank (25 °C, 13:11 light–dark, 200 µmol photons m^{-2} s^{-1} LED light, 62 W, 5000 K) with complete water renewal every hour, under the same filtration and heating setup described by (Contardi et al., 2023).

Characterization of tissue necrosis-like disease

Fragments of *Stylophora pistillata* were categorized into three groups: "apparently healthy", "intermediate", and "diseased". The *apparently healthy* samples were taken from tissue showing no visible signs of bleaching or lesions, at least 1.5 cm above the advancing white band. The *intermediate* group included fragments with tissue immediately above and below the white band threshold. The *diseased* samples consisted of bleached, necrotic tissue directly adjacent to the white band.

DNA extraction:

Nine coral fragments (3 from each category, ~1 × 2 cm each) were ground, and total DNA was extracted using the FastDNA™ Spin Kit for Soil (MP Biomedicals, USA). To prevent degradation, DNA was purified with the Monarch® Genomic DNA Purification Kit (New England BioLabs, UK).

PCR amplification:

The bacterial 16S rRNA gene (V5–V6 hypervariable regions) was amplified using barcoded primers, enabling multiplexing of samples during sequencing, following the methods described in (Ambrosini et al., 2019).

High-throughput sequencing (HTS):

Amplicons were sequenced on an Illumina MiSeq platform (2 × 300 bp paired-end protocol). Sequence processing was conducted using the DADA2 pipeline (Callahan et al., 2016), as in (Costanzo et al., 2022). Amplicon Sequence Variants (ASVs) shorter than expected were verified with BLAST and discarded if they did not match bacterial sequences. Non-bacterial ASVs (archaea or unclassified domains) were also removed. ASVs identified as *Vibrio* were further examined and, when possible, tentatively assigned to species level by BLAST, with up to four best-hit species selected per ASV based on the lowest E-value.

Statistical analysis:

The proportion of *Vibrio* sequences in each group (apparently healthy, intermediate, diseased) was compared with one-way ANOVA, followed by Bonferroni post-hoc testing ($\alpha = 0.05$).

Application of the two-component system on infected corals:

Twenty coral fragments were collected from three diseased mother colonies. Fragments were randomly assigned to four groups (n = 5 per group): untreated control, sealant only (BW4LO1–DIC), sealant + 70P-30C-Cipro film, and sealant + 70P-30C-Gent film. Treatments were applied directly onto the white disease band. Hydrophilic films were cut into small pieces with sterile blades, adhered to the coral surface, and then sealed with hand-warmed BW4LO1–DIC paste. Application extended at least 1 cm beyond lesion margins to ensure full coverage.

Throughout the four-month trial, colonies were photographed biweekly to monitor disease progression. At the end, fragments were classified as either “unstopped infection/dead” or “not infected”. Statistical significance of treatment was assessed using Chi-square analysis ($p < 0.05$).

Results

This work proposes a two-component strategy to treat diseased corals while minimizing environmental impact. The system consists of a hydrophilic, antibiotic-loaded film applied directly to the affected coral tissue, which is then covered with a natural hydrophobic, paste-like sealant. This configuration ensures that the drug is released exclusively toward the coral. All acronyms used in this study are summarized in Table 1.

BW	Beeswax
LO	Linseed Oil
SFO	Sunflower Oil
DIC	Dry Ice Cooling
not DIC	Not Dry Ice Cooling
P	Polyvinylpyrrolidone
C	Chitosan
Cipro	Ciprofloxacin
Gent	Gentamicin
BW4LO1-DIC	Sealant with Beeswax and Linseed oil, prepared with Dry Ice cooling method
BW4LO1-not DIC	Sealant with Beeswax and Linseed oil, prepared without Dry Ice cooling method
BW4SFO1-DIC	Sealant with Beeswax and Sunflower oil, prepared with Dry Ice cooling method
BW4SFO1-not DIC	Sealant with Beeswax and Sunflower oil prepared without Dry Ice cooling method
50P-50C Cipro	Film with 50% Polyvinylpyrrolidone, 50% Chitosan, and Ciprofloxacin

70P-30C Cipro	Film with 70% Polyvinylpyrrolidone, 30% Chitosan, and Ciprofloxacin
50P-50C Gent	Film with 50% Polyvinylpyrrolidone, 50% Chitosan, and Gentamicin
70P-30C Gent	Film with 70% Polyvinylpyrrolidone, 30% Chitosan, and Gentamicin

Table 1. List of acronyms used in this paper.

Sealant characterization

The preparation process of the natural beeswax/plant-based sealant is schematically illustrated in Figure 1A and detailed in the Methods section. Briefly, beeswax—chosen for its ability to be molded at relatively low temperatures—was melted with oil (either LO or SFO) in a 4:1 ratio. The mixture was rapidly cooled using the DIC method to enhance oil miscibility within the beeswax matrix. Four different sealants were produced, named according to their composition and processing method: BW4LO1-DIC, BW4LO1–not DIC, BW4SFO1-DIC, and BW4SFO1–not DIC. These formulations were tested to compare composition, preparation method, and overall performance. The resulting pastes had a yellowish color similar to raw beeswax and were morphologically assessed by SEM, which provides high-contrast 2D images of surface morphology—a critical factor influencing material properties such as mechanical behavior and degradation (Donald, 2003; Inkson, 2016). Sealants containing LO (BW4LO1 in Figure 1C) displayed an inhomogeneous surface with distinct zones, whereas those with SFO (BW4SFO1 in Figure 1D) appeared more homogeneous and closely resembled pristine beeswax (BW in Figure 1B).

Hydrophobicity was analyzed via water contact angle measurements, which are essential to understand material–water interactions (Zych et al., 2024). The mean water contact angles of BW4SFO1–DIC, BW4LO1–DIC, BW4SFO1–not DIC, and BW4LO1–not DIC were 108.2°, 137.7°, 133.1°, and 134.5°, respectively (Figure 1E). All surfaces exhibited hydrophobic behavior, a necessary property for preventing seawater infiltration and avoiding outward drug release. Fourier Transform Infrared spectroscopy (FT-IR) confirmed that no new chemical interactions occurred during sealant fabrication, as no changes were observed in the functional groups of the components (Figure 1F; (Contardi et al., 2021)).

Thermal stability was investigated using thermogravimetric analysis (TGA) and differential scanning calorimetry (DSC). TGA provides insights into thermal degradation expressed as weight loss (Contardi, Heredia-Guerrero, et al., 2019). Derivative TGA curves showed that the main degradation peaks of BW4LO1-DIC and BW4SFO1-DIC (Figures 1G-I) were located between those of the oils and beeswax. Specifically, BW degraded at 369.4 °C, LO at 405.3 °C, and SFO at 392.4 °C, while BW4LO1–DIC and BW4SFO1–DIC peaked at 372.4 °C and 376.4 °C, respectively. Sealants prepared without DIC showed slightly higher degradation peaks—376.3 °C for BW4LO1–not DIC and 382.4 °C for BW4SFO1–not DIC—suggesting differences in oil–beeswax interactions.

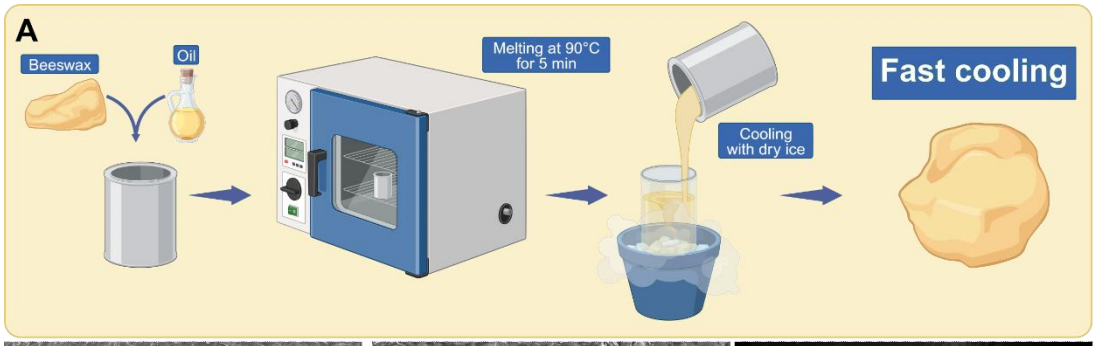
A
Beeswax
Oil
Melting at 90°C for 5 min
Cooling with dry ice
Fast cooling

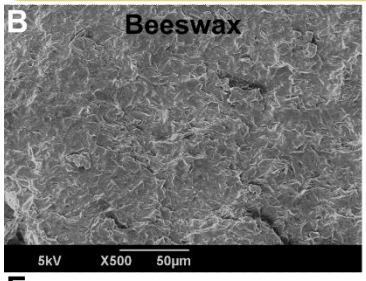
B
Beeswax
5kV X500 50µm

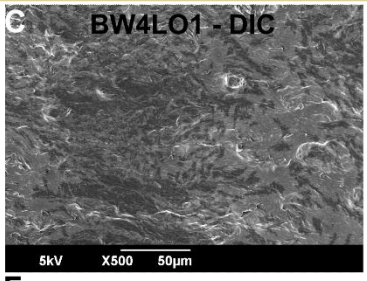
C
BW4LO1 - DIC
5kV X500 50µm

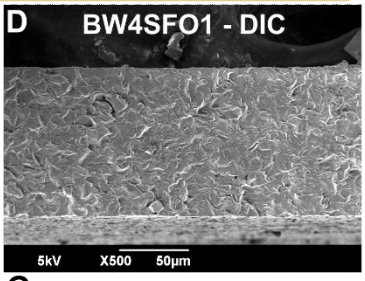
D
BW4SFO1 - DIC
5kV X500 50µm

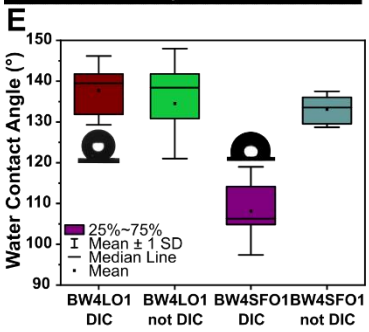
E
Water Contact Angle (°)
25%~75%
Mean ± 1 SD
Median Line
Mean
BW4LO1 DIC
BW4LO1 not DIC
BW4SFO1 DIC
BW4SFO1 not DIC

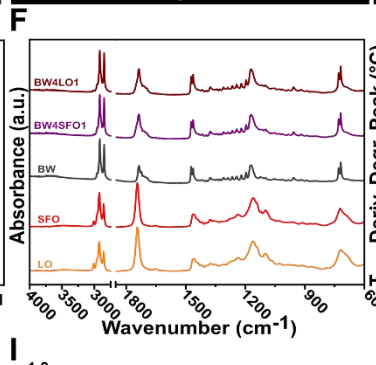
F
Absorbance (a.u.)
BW4LO1
BW4SFO1
BW
SFO
LO
Wavenumber (cm-1)

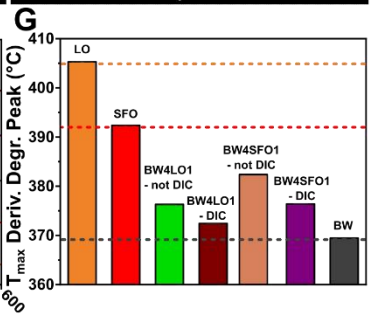
G
Deriv. Degr. Peak (°C)
Tmax
LO
SFO
BW4LO1 - not DIC
BW4LO1 - DIC
BW4SFO1 - not DIC
BW4SFO1 - DIC
BW

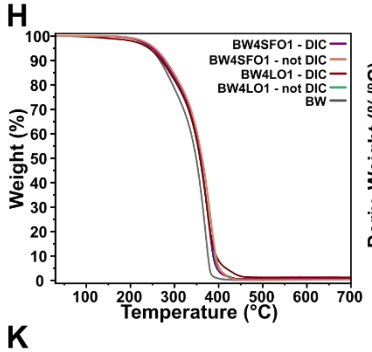
H
Weight (%)
BW4SFO1 - DIC
BW4SFO1 - not DIC
BW4LO1 - DIC
BW4LO1 - not DIC
BW
Temperature (°C)

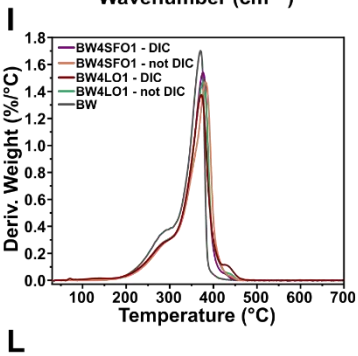
I
Deriv. Weight (%/°C)
BW4SFO1 - DIC
BW4SFO1 - not DIC
BW4LO1 - DIC
BW4LO1 - not DIC
BW
Temperature (°C)

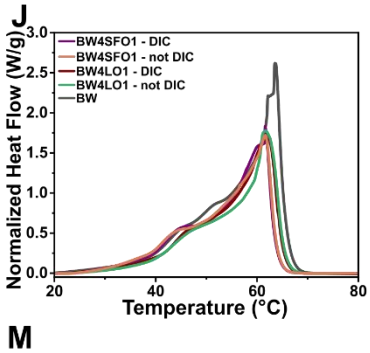
J
Normalized Heat Flow (W/g)
BW4SFO1 - DIC
BW4SFO1 - not DIC
BW4LO1 - DIC
BW4LO1 - not DIC
BW
Temperature (°C)

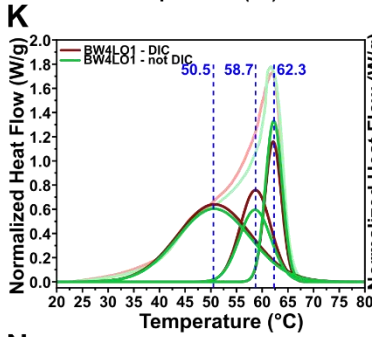
K
Normalized Heat Flow (W/g)
BW4LO1 - DIC
BW4LO1 - not DIC
50.5
58.7
62.3
Temperature (°C)

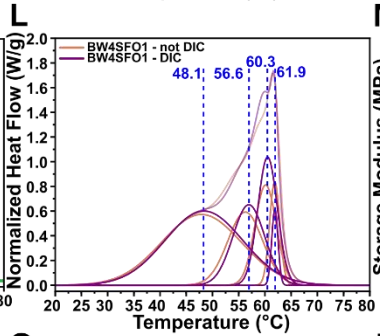
L
Normalized Heat Flow (W/g)
BW4SFO1 - not DIC
BW4SFO1 - DIC
48.1
56.6
60.3
61.9
Temperature (°C)

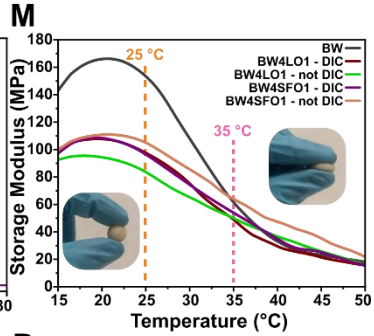
M
Storage Modulus (MPa)
25 °C
35 °C
BW
BW4LO1 - DIC
BW4LO1 - not DIC
BW4SFO1 - DIC
BW4SFO1 - not DIC
Temperature (°C)

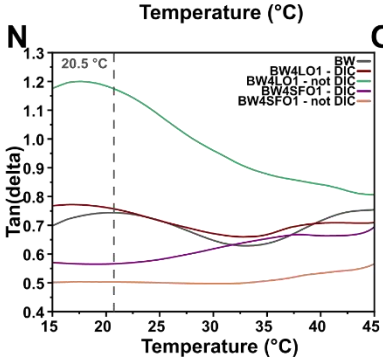
N
20.5 °C
Tan(delta)
BW
BW4LO1 - DIC
BW4LO1 - not DIC
BW4SFO1 - DIC
BW4SFO1 - not DIC
Temperature (°C)

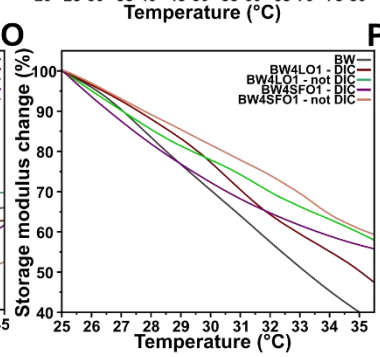
O
Storage modulus change (%)
BW
BW4LO1 - DIC
BW4LO1 - not DIC
BW4SFO1 - DIC
BW4SFO1 - not DIC
Temperature (°C)

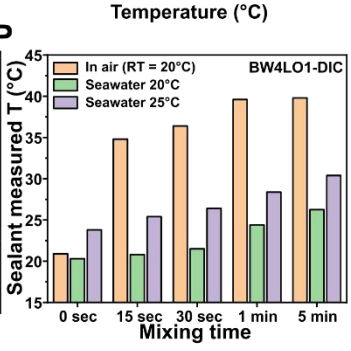
P
Sealant measured T (°C)
In air (RT = 20°C)
Seawater 20°C
Seawater 25°C
BW4LO1-DIC
0 sec
15 sec
30 sec
1 min
5 min
Mixing time

Figure 1. ***Sealant characterization.*** *A, schematic representation of the sealant preparation. B, C, D, SEM images of BW, BW4LO1–DIC, and BW4SFO1–DIC sealants, respectively. E, Water contact angle of the sealants BW4LO1–DIC, BW4LO1–not DIC, BW4SFO1–DIC and BW4SFO1–not DIC; the inserts in the figure are images representative of the shape of water droplets on the material surface. F, FT-IR normalized spectra of the two pastes (BW4LO1-DIC, BW4SFO1–DIC) and the relative single reagents (BW, SFO, LO). G, temperatures at which each sample tested loses most of its mass in TGA analysis; dotted horizontal lines represent the temperature degradation of the reagents LO, SFO, and BW. H,I, respectively thermogravimetric curve and the first derivative of the pristine BW and the paste sealants BW4LO1–DIC, BW4SFO1–DIC, BW4LO1–not DIC, BW4SFO–not DIC. J, 1st melting round (endo up) of DSC of BW, BW4SFO1–DIC, BW4LO1–DIC, BW4SFO1–not DIC, BW4LO1–not DIC. K, deconvolved curves of DSC 1st melting round (endo up) of BW4LO1–DIC and BW4LO1–not DIC; L, DSC deconvolution of BW4SFO1–DIC and BW4SFO1–not DIC; the semi-transparent curves represent the raw curves, and the more saturated curves are the obtained deconvolved peaks, dashed lines indicate the temperature at which the deconvoluted curves have their peak center. M, mechanical dynamical transition of the storage modulus relative to temperature variations of BW and the four pastes; inserts are a visual representation of the hardness of the sealant produced. N, tan(delta) of pastes and BW as a function of the temperature. O, Stiffness variation of the sealants in the range of temperature between 25 and 35°C. P, BW4LO1-DIC sealant temperature at different time points upon hand-mixing in air and seawater (RT = Room Temperature).*

DSC was used to further explore the internal structure of the sealants (Figures 1J-L). In DSC, materials are exposed to a thermal ramp, and heat absorption (endothermic) or release (exothermic) is recorded, providing insights into crystallinity, amorphous phases, and glass-transition behavior. The area under the first melting cycle was 27.85 for BW, compared to 21.49, 22.01, 21.53, and 20.50 for BW4SFO1–DIC, BW4SFO1–not DIC, BW4LO1–DIC, and BW4LO1–not DIC, respectively. This reduction suggests that oil incorporation lowered the energy needed for melting. Deconvolution analysis highlighted preparation-dependent differences: BW4LO1–DIC required higher energy to melt semi-crystalline structures at 50.5 and 58.7 °C compared with BW4LO1–not DIC, while the latter showed higher enthalpy at 62.3 °C (Table 2). A similar pattern was observed for BW4SFO1–DIC and BW4SFO1–not DIC (Figure 1L, Table 3). These differences likely stem from cooling rates: slower cooling in the “not DIC” samples allowed fewer nucleation points and growth of larger crystals, leading to less uniform oil distribution.

Sample Name	**Peak at 50.5 °C**	**Peak at 58.7 °C**	**Peak at 62.3 °C**
BW4LO1–DIC	**11.48**	**5.65**	**4.66**
BW4LO1–not DIC	**10.72**	**4.58**	**5.45**

Table 2. Area of deconvolved peaks for BW4LO–DIC and BW4LO1–not DIC. The enthalpy (area under the curve, measured as J/g) of the peaks of the 1st melting round deconvolved curves obtained by the residuals 1st derivative method.

Sample Name	Peak at 48.1 °C	Peak at 56.6 °C	Peak at 60.3°C	Peak at 61.9 °C
BWSFO1–DIC	11.15	4.97	4.84	0.92
BW4SFO1–not DIC	10.93	4.94	4.14	2.02

Table 3. **Area of deconvolved peaks for BW4SFO – DIC and BW4SFO1 – not DIC**. Enthalpy (area under the curve, measured as J/g) peaks of the 1st melting round deconvolved curves for BW4SFO1 – DIC and BW4SFO1 – not DIC.

Since reef-building corals typically inhabit waters at 25–30 °C, but can also survive between 15 and 36 °C (Howells et al., 2016; Pohl et al., 2014), the sealants' mechanical properties were tested across this range using dynamic mechanical thermal analysis (DMTA) (Zych et al., 2024). As shown in Figure 1M, BW4LO1-DIC reached a storage modulus maximum of 108.0 MPa at 19.4 °C, BW4LO1–not DIC peaked at 95.7 MPa at 18.0 °C, BW4SFO1–DIC at 84.2 MPa at 17.2 °C, and BW4SFO1–not DIC at 111.3 MPa at 20.7 °C. Pristine BW, however, exhibited a much higher modulus (166.7 MPa at 20.5 °C), indicating greater stiffness. Between 25 °C and 35 °C, all samples softened, with BW decreasing from 108.1 MPa at 30 °C to 61.7 MPa at 35 °C. Sealants showed comparable decreases: BW4LO1–DIC dropped to 75.3 MPa at 30 °C and 48.9 MPa at 35 °C, BW4LO1–not DIC to 65.3 and 50.0 MPa, BW4SFO1–DIC to 74.4 and 54.0 MPa, and BW4SFO1–not DIC to 85.6 and 64.0 MPa. Thus, stiffness peaked near 20 °C and declined toward 30 °C, giving the sealants temperature-responsiveness suitable for coral application.

Tan(δ) values plotted against temperature (Figure 1N) indicated a glass-transition temperature (Tg) of 20.5 °C for BW, while BW4LO1–DIC and BW4LO1–not DIC had Tg values of 19.4 °C and 17.5 °C, respectively. BW4SFO1–DIC and BW4SFO1–not DIC did not show clear Tg peaks within the measured range, likely due to oil incorporation. Collectively, TGA, DSC, and DMTA results demonstrated that DIC treatment enhanced oil dispersion within the beeswax matrix and increased thermo-mechanical responsiveness compared to untreated sealants and pristine BW. Among all formulations, BW4LO1–DIC stood out as the softest at 35 °C (Figure 1M), exhibited the largest reduction in storage modulus between 25 °C and 35 °C (approximately 49.9%, Figure 1O), and was the most hydrophobic (Figure 1E). Consequently, it was chosen for subsequent experiments to test the coral treatment system.

For real-world coral application, the sealant is designed to be hand-mixed and warmed to ~35 °C (human skin temperature) before underwater use, where tropical corals live at ~25 °C. To simulate this, the internal temperature of BW4LO1–DIC was monitored using a thermocouple during mixing (Bajzek, 2005). When mixed in air at 20 °C, the internal temperature peaked at 39.8 °C after one minute. In seawater at 20 °C, the sealant reached 27.2 °C after five minutes, while in 25 °C seawater, it reached 30.8 °C after five minutes (Figure 1P). In all cases, BW4LO1–DIC became sufficiently soft for molding and application.

Characterization of the drug-loaded films

Films with different weight ratios of P and C (50:50 and 70:30, Figure 2A), prepared with Poly-gly-10 as a plasticizer and loaded with either Cipro or Gent, were fabricated by solvent casting (Contardi, Heredia-Guerrero, et al., 2019; Contardi, Russo, et al., 2019). Their preparation procedure is schematically shown in Figure 3A. The films were named according to their polymer composition and drug loading: 50P-50C-no drug, 50P-50C-Cipro, 50P-50C-Gent, 70P-30C-no drug, 70P-30C-Cipro, and 70P-30C-Gent. Macroscopically, the films were optically transparent (Figure 2A). SEM analysis revealed a homogeneous morphology on both the surface and cross-section, regardless of polymer ratio or drug loading (Figures 2B, 3B-I), suggesting that both antibiotics were well-dispersed within the polymer matrix (Contardi et al., 2017).

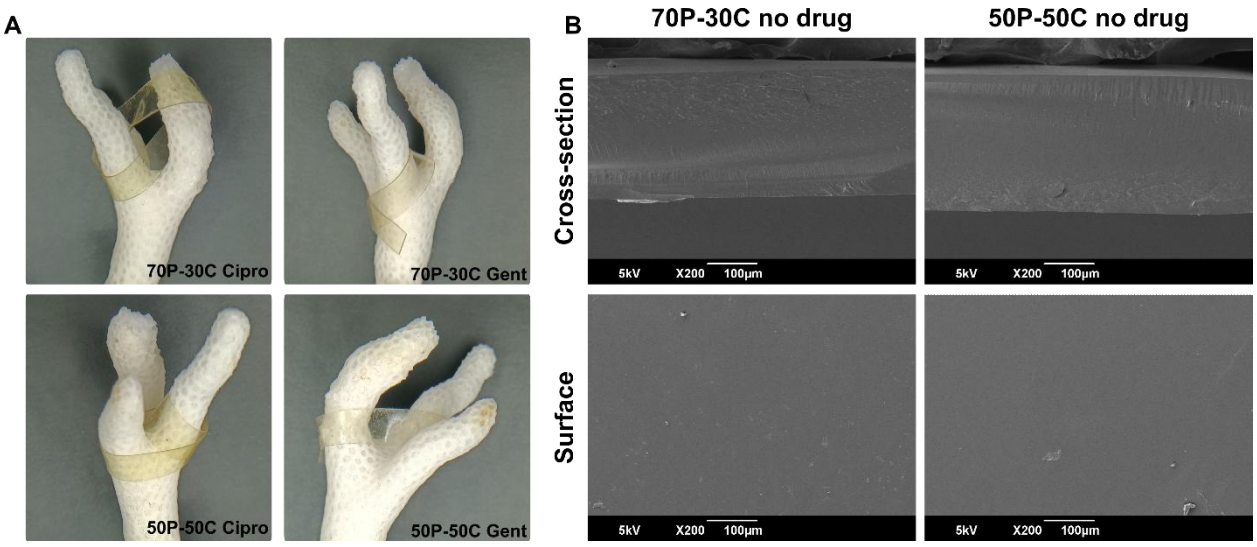

Figure 2. ***Macroscopical and microscopical film images.*** **A**, *representative photos of the film used;* **B**, *SEM acquisitions of the 70P-30C and 50P-50C without drugs loaded.*

Chemical characterization was performed using FT-IR spectroscopy to detect possible interactions among polymers and drugs (Figure 4A). The spectra were dominated by the polymer signals: characteristic alcohol (C–O–H) and ether (C–O–C) stretching bands of chitosan were observed between 1150 and 950 cm^{-1}, overlapping with similar vibrations from poly-gly-10 (Figure 4A). For P, the most prominent signal was the carbonyl (C=O) stretching at 1652 cm^{-1}. Drug-specific peaks were not detectable, likely due to the low drug content (1% w/w) and overlap with polymer vibrational modes (Contardi et al., 2022).

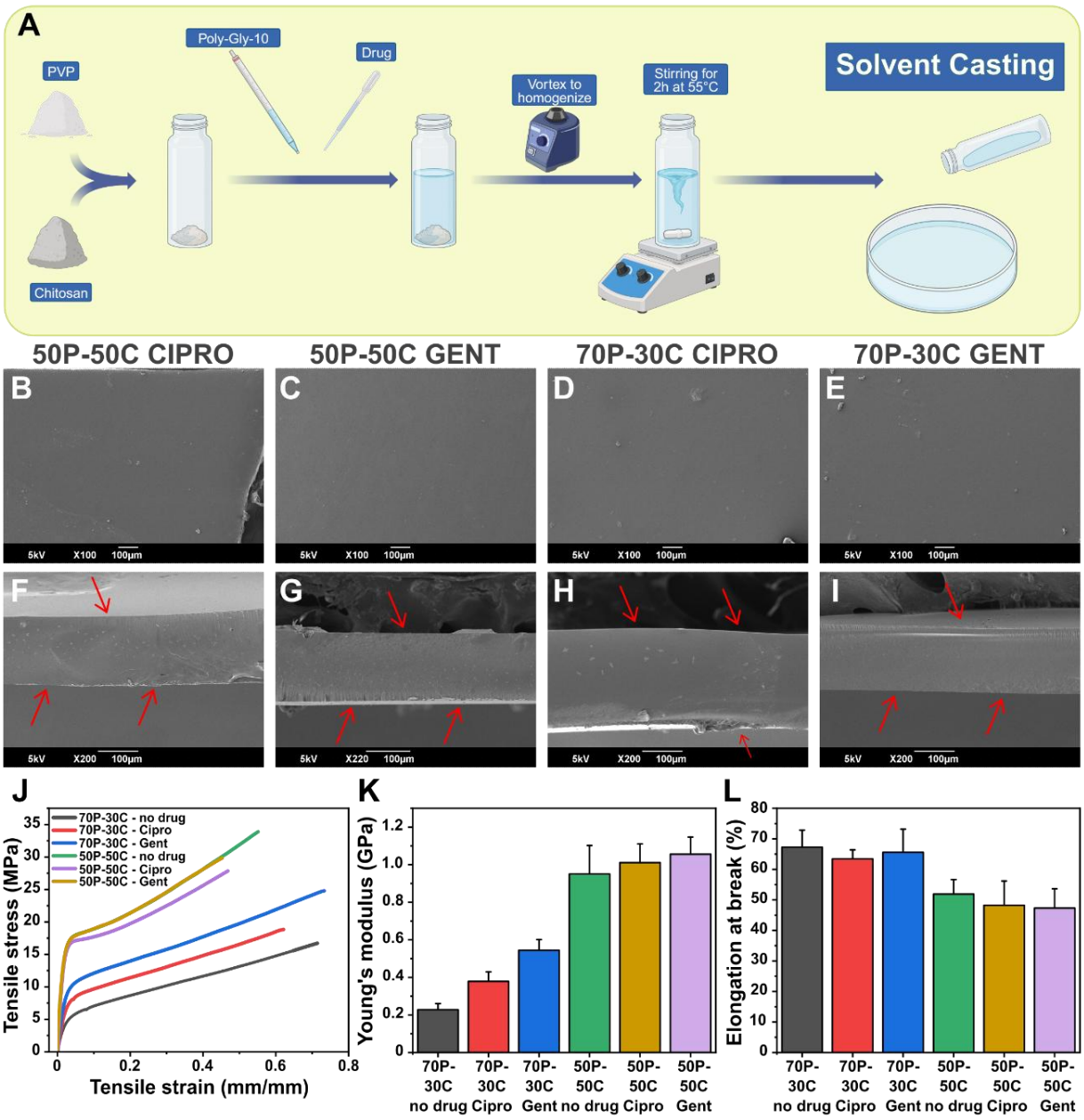

*Figure 3.**Films and two-component system characterization.** **A**, schematic representation of the films' production. **B**, **C**, **D**, **E**, top-view SEM images of 50P-50C-Cipro, 50P-50C-Gent, 70P-30C-Cipro, and 70P-30C-Gent films, respectively. **F**, **G**, **H**, **I**, cross-sections SEM images of 50P-50C-Cipro, 50P-50C-Gent, 70P-30C-Cipro, and 70P-30C-Gent films, respectively; red arrows indicate the extremities of the films. **J**, stress-strain curves of the films' mechanical tensile stress/strain. **K**, Mean Young's Modulus and relative standard deviation of the films. **L**, Mean elongation at break and relative standard deviation of the films.*

Mechanical properties varied according to composition. Increasing the chitosan fraction resulted in higher stiffness (higher Young's modulus) but reduced stretchability (Figure 3J). These values were obtained by tensile stress analysis, a standard method to measure elasticity and tensile strength (Davis, 2004; Nardi et al., 2024). For 50P-50C films, the mean Young's modulus was 0.95 GPa for the no-drug sample, 1.01 GPa for Cipro-loaded, and 1.05 GPa for Gent-loaded, which were 2–5 times higher

than those of the 70P-30C films (Figure 3K). The 70P-30C samples showed significantly lower moduli: 0.23 GPa (no drug), 0.38 GPa (Cipro), and 0.54 GPa (Gent). Interestingly, drug incorporation slightly increased stiffness, with Gent-loaded films consistently showing the highest values.

This trend reversed for elongation at break (Figure 3L). The 70P-30C formulations—both drug-loaded and drug-free—exhibited greater stretchability (~65%) than the 50P-50C films (~50%). This behavior appeared unaffected by the drug presence. Tensile stress at maximum load (Figure 4B) further differentiated the groups. The 70P-30C-no drug, -Cipro, and -Gent films had mean values of 19.05 MPa, 17.95 MPa, and 24.47 MPa, respectively, while the 50P-50C films were stronger: 30.83 MPa (no drug), 25.71 MPa (Cipro), and 28.46 MPa (Gent). Despite these variations in stiffness and strength, all films maintained adequate stretchability, a critical property for conformal wrapping around coral branches at infected sites (Figure 2A). Based on their balance of flexibility and handling, the 70P-30C films were chosen for *in vivo* experiments.

Dynamic water contact angle (WCA) measurements were carried out to study the interaction between the films and seawater during the first 5 minutes of contact (Tagliaro et al., 2024), with results shown in Figure 4C. As a reference, Teflon displayed a stable WCA of 102°, with negligible change in droplet volume during the test. In contrast, the films showed initial WCA values between 95° and 105°, but the angles rapidly decreased as the films absorbed the droplets, leading to complete water uptake within ~30 seconds. This behavior reflects the strong hygroscopic nature of polyvinylpyrrolidone and chitosan, both of which are known for their high swelling capacity (Han et al., 2023; Murgia et al., 2020). Significantly, hygroscopicity directly influences drug release kinetics in aqueous environments (Wójcik-Pastuszka et al., 2023), with higher hygroscopicity linked to faster drug release—a desirable feature for rapid antibacterial action (Briggs et al., 2022).

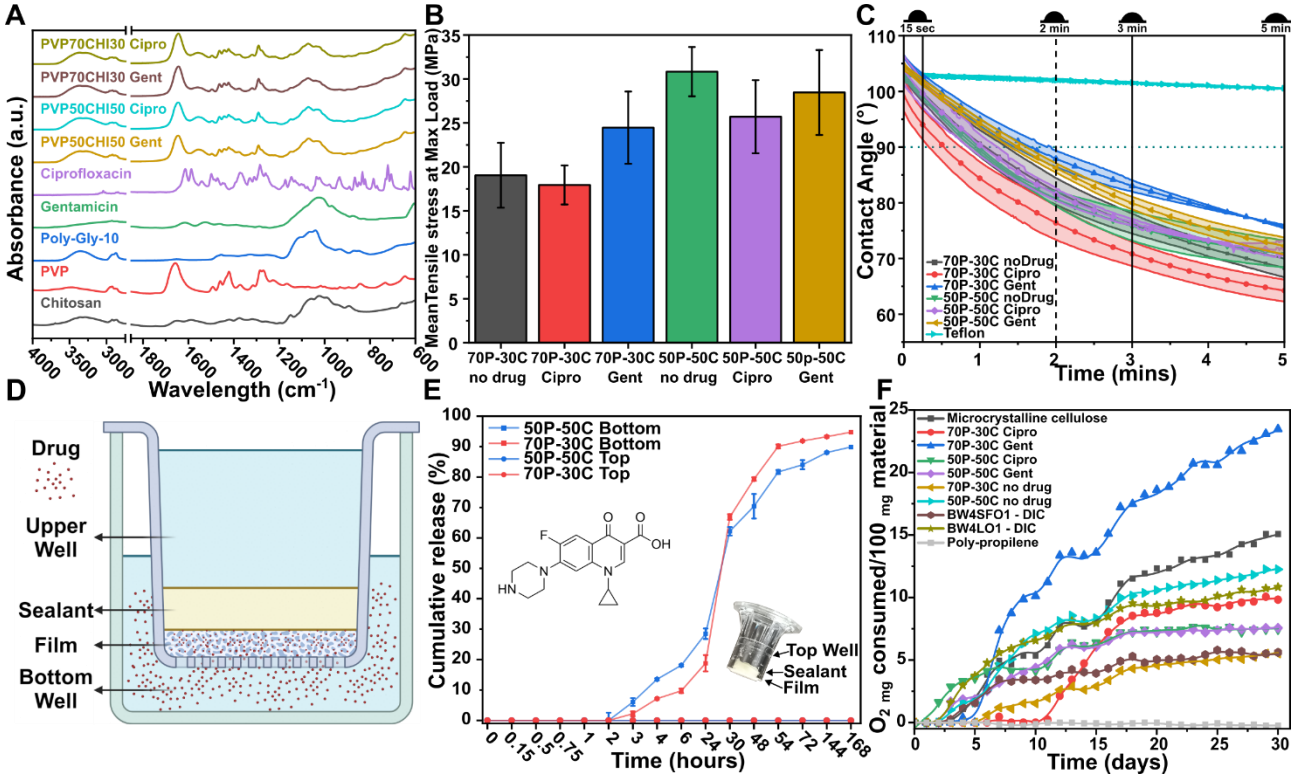

Figure 4. ***Characterization of the films, the transwell model, and BOD degradation.*** **A**, *FT-IR spectra of the films 70P-30C and 50P-50C and their single components.* **B**, *mean tensile stress at the maximum load of the films.* **C**, *Dynamic Water Contact Angle of the two different film compositions in the presence/absence of the drugs (either Cipro or Gent). Teflon is used as a control.* **D**, *schematic representation of the transwell model.* **E**, *cumulative release of Cipro from the transwell model for the 50P-50C-Cipro (blue lines) and 70P-30C-Cipro (red lines) films in the top and bottom wells (circle and square, respectively); the inset shows a photo of the transwell setup.* **G**, *biochemical degradation activity within 30 days of the films 70P-30C-Cipro, 70P-30C-Gent, 50P-50C with Cipro and Gent, and the paste sealant BW4LO1–DIC, BW4SFO1–DIC; Microcrystalline cellulose and Polypropylene are added as positive and negative controls, respectively.*

Unidirectional release and biodegradability of the two-component system

To ensure that antibiotics embedded in the films are delivered directly to the coral lesion without dispersing into the surrounding seawater, the release behavior of the two-component system (film + sealant) was evaluated. A transwell setup was employed to mimic the positioning of the system on an infected coral surface at the interface with seawater. As schematically shown in Figure 4D, the film and sealant were placed inside the transwell insert, forming a separate compartment in the upper portion (Figure 4E). This arrangement prevented seawater diffusion between the upper (external) and lower (internal) compartments.

In this model, the upper chamber represented the marine environment, while the lower chamber simulated the infected coral site. The film was placed in contact with the lower chamber, the sealant with the upper chamber, and the two layers were in contact with one another. Cipro release into both compartments was monitored over 168 hours (7 days) (Figure 4E). In both 70P-30C and 50P-50C

films, Cipro began to diffuse into the lower compartment after 2–3 hours. Over 60% of the antibiotic was released within the first 24–30 hours, with slower release continuing to day 6. Minor differences were observed between the two formulations during the first 24 hours, with higher chitosan content leading to a faster initial release, likely due to the greater swelling ability of chitosan relative to polyvinylpyrrolidone. Importantly, no drug diffusion was detected in the upper chamber throughout the experiment, confirming the sealing efficiency of BW4LO1–DIC.

Because an additional design requirement was environmental compatibility, the biodegradability of the films (with and without antibiotics) and the sealant was assessed using Biochemical Oxygen Demand (BOD). Results are presented in Figures 4F. The test was conducted by immersing the materials in seawater for 30 days, with oxygen consumption serving as a proxy for biodegradation (ISO 23977-2:2020). Microcrystalline cellulose was used as a positive control (15.1 mg O_2/100 mg), and polypropylene as a negative control (0.0 mg O_2/100 mg). The BW4LO1–DIC sealant began degrading after three days, reaching a final oxygen consumption of 10.8 mg O_2/100 mg. All films were confirmed biodegradable, with oxygen consumption ranging from 7.4 to 23.5 mg O_2/100 mg (Figures 4F).

Antibacterial properties

The antibacterial potential of the films was next investigated. Minimal Inhibitory Concentration (MIC) assays were performed to determine the lowest concentration of antibiotic needed to inhibit Vibrio coralliilyticus growth (Kadeřábková et al., 2024). As summarized in Table 4, *V. coralliilyticus* was more susceptible to Cipro (MIC = 0.5 µg/mL) than Gent (MIC = 32.0 µg/mL). These results confirmed that effective drug concentrations had been successfully loaded into films.

Tested drug	**MIC (µg/mL)**	0.125	0.25	0.5	1.0	2.0	4.0	8.0	16.0	32.0	64.0
Ciprofloxacin	Interpretative Category	R	I	S	S	S	S	S	S	S	S
Gentamicin	Interpretative Category	R	R	R	R	R	R	R	I	S	S

*Table 4. **Minimal Inhibitory Concentration (MIC)**. Concentrations of the drug tested on V. coralliilyticus; R- Resistant, I-intermediate, S-susceptible to the drug dose administered.*

To further evaluate antibacterial activity in a solid medium, a disk diffusion assay was carried out using the films in place of conventional paper disks (Contardi et al., 2017; Contardi, Russo, et al., 2019). Representative plates are shown in Figure 6A, with the mean inhibition diameters summarized in Figure 6B.

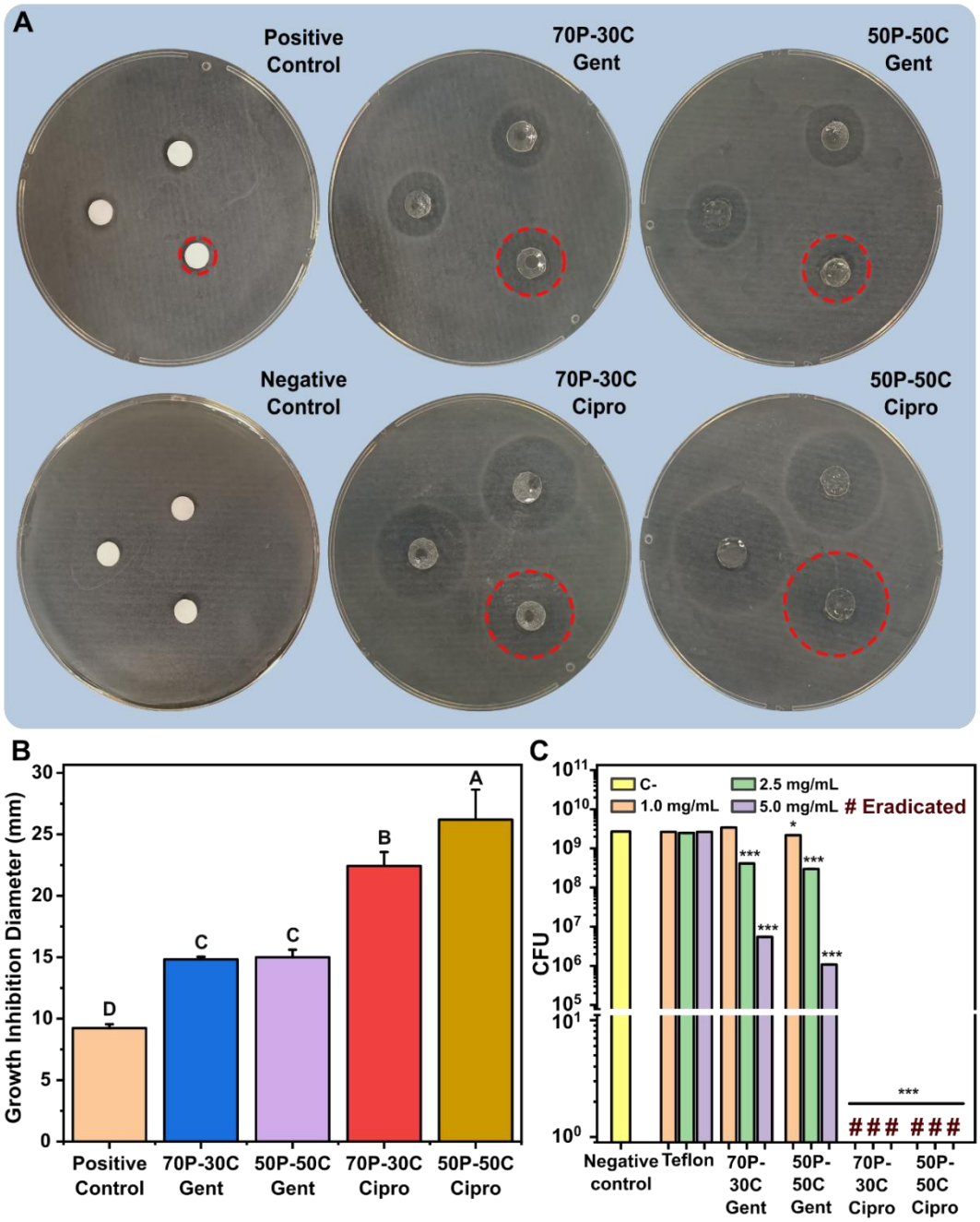

*Figure 2. Antibacterial properties. A, photographs of Petri dishes used in the disk diffusion assay with V. coralliilyticus of the positive control, 70P-30C-Gent, 50P-50C-Gent, negative control, 70P-30C-Cipro, and 50P-50C-Cipro samples; Red dotted rings are indicative of the inhibition growth ring on the different plates. B, Mean maximum diameter and relative standard deviation of the disk diffusion assay for the positive control, 70P-30C-Cipro, 70P-30C-Gent, 50P-50C-Cipro, and 50P-50C-Gent; One-way ANOVA followed by Bonferroni post-hoc: different letters on top of the histogram indicate significance ($p < 0.05$) among groups. C, Bactericidal effect of the films in the Marine Broth medium inoculated with V. coralliilyticus measured in colony-forming unit (CFU). # indicates that the bacterium was fully eradicated. Two-way ANOVA followed by Bonferroni post-hoc; Significant differences from the Teflon (Negative control) are highlighted as * = $p < 0.05$, ** = $p < 0.01$, *** = $p < 0.001$.*

All drug-loaded films produced larger inhibition zones compared to controls. One-Way ANOVA indicated significant overall differences among the groups ($p < 0.001$), and Bonferroni post-hoc tests

confirmed that nearly all pairwise comparisons were significant ($p < 0.05$). The only non-significant difference was between the two Gent-loaded films, which showed roughly identical inhibition diameters (14.8 mm for 70P-30C-Gent, 15.0 mm for 50P-50C-Gent). In contrast, the inhibition zones of 50P-50C-Cipro (26.2 mm) and 70P-30C-Cipro (22.4 mm) were significantly different ($p < 0.05$), suggesting a possible synergistic interaction between chitosan and Cipro (Contardi et al., 2017). The antibacterial activity was also assessed in liquid culture conditions to evaluate drug release and bactericidal efficacy over 24 hours. Films of different compositions (70P-30C-Gent, 50P-50C-Gent, 70P-30C-Cipro, 50P-50C-Cipro) were tested at three concentrations (1.0, 2.5, and 5.0 mg/mL). Results are shown in Figure 6C (Contardi, Russo, et al., 2019). Teflon films and untreated medium served as negative controls. *V. coralliilyticus* was inoculated at ~10^6 CFU at T0, and bacterial counts were assessed after 24 h (~10^9 CFU in controls).

Two-way ANOVA revealed highly significant differences across all tested factors ($p < 0.001$), and Bonferroni post-hoc tests further confirmed these outcomes (detailed in Table 5; simplified comparisons shown in Figure 6C). Films loaded with Cipro eradicated *Vibrio* at all tested concentrations (Teflon vs Cipro-loaded films: $p < 0.001$), consistent with the high bacterial susceptibility indicated by MIC assays. Gent-loaded films showed a concentration-dependent effect. At 1.0 mg/mL, 70P-30C-Gent showed no inhibition, whereas 50P-50C-Gent exhibited mild activity ($p < 0.05$). At the highest concentration (5 mg/mL), antibacterial efficacy was more pronounced: 70P-30C-Gent reduced bacterial counts by over 2 logs (~5.5×10^6 CFU, $p < 0.001$), while 50P-50C-Gent reduced counts by ~3 logs (~1.08×10^6 CFU, $p < 0.001$). These differences may be explained by the higher chitosan content in the 50P-50C films (Liang et al., 2021), contributing to antibacterial activity alongside the drug itself, although at higher concentrations the antibiotic dominated the inhibitory effect.

Film name	**Conc. mg/mL**	**Film name**	**Conc. mg/mL**	**Alpha**	**Significance**	**Prob**	**p-value**
50P/50C Cipro	1	TEFLON	1	0.05	1	8.92E-28	0.001
50P/50C Cipro	2.5	TEFLON	2.5	0.05	1	5.81E-27	0.001
50P/50C Cipro	5	TEFLON	5	0.05	1	8.92E-28	0.001
50P/50C Gent	1	TEFLON	1	0.05	1	1.76E-07	0.001
50P/50C Gent	1	50P/50C Cipro	1	0.05	1	3.05E-25	0.001
50P/50C Gent	2.5	TEFLON	2.5	0.05	1	2.58E-25	0.001
50P/50C Gent	2.5	50P/50C Cipro	2.5	0.05	1	8.40E-04	0.001
50P/50C Gent	5	TEFLON	5	0.05	1	9.03E-28	0.001

50P/50C Gent	5	50P/50C Cipro	5	0.05	0	1	1
70P/30C Cipro	1	TEFLON	1	0.05	1	8.92E-28	0.001
70P/30C Cipro	1	50P/50C Cipro	1	0.05	0	1	1
70P/30C Cipro	1	50P/50C Gent	1	0.05	1	3.05E-25	0.001
70P/30C Cipro	2.5	TEFLON	2.5	0.05	1	5.81E-27	0.001
70P/30C Cipro	2.5	50P/50C Cipro	2.5	0.05	0	1	1
70P/30C Cipro	2.5	50P/50C Gent	2.5	0.05	1	8.40E-04	0.001
70P/30C Cipro	5	TEFLON	5	0.05	1	8.92E-28	0.001
70P/30C Cipro	5	50P/50C Cipro	5	0.05	0	1	1
70P/30C Cipro	5	50P/50C Gent	5	0.05	0	1	1
70P/30C Gent	1	TEFLON	1	0.05	1	2.11E-12	0.001
70P/30C Gent	1	50P/50C Cipro	1	0.05	1	4.88E-31	0.001
70P/30C Gent	1	50P/50C Gent	1	0.05	1	3.82E-18	0.001
70P/30C Gent	1	70P/30C Cipro	1	0.05	1	4.88E-31	0.001
70P/30C Gent	2.5	TEFLON	2.5	0.05	1	1.22E-24	0.001
70P/30C Gent	2.5	50P/50C Cipro	2.5	0.05	1	3.22E-06	0.001
70P/30C Gent	2.5	50P/50C Gent	2.5	0.05	0	1	1
70P/30C Gent	2.5	70P/30C Cipro	2.5	0.05	1	3.22E-06	0.001
70P/30C Gent	5	TEFLON	5	0.05	1	9.49E-28	0.001
70P/30C Gent	5	50P/50C Cipro	5	0.05	0	1	1
70P/30C Gent	5	50P/50C Gent	5	0.05	0	1	1
70P/30C Gent	5	70P/30C Cipro	5	0.05	0	1	1

Table 5. Results of the Two-way ANOVA test followed by the Bonferroni post-hoc for all the comparisons among the materials tested in the antibacterial liquid test.

Characterization of the coral disease

Infected colonies of *S. pistillata* were selected for *in vivo* treatment. Colonies were identified as diseased based on the presence of the characteristic white band across coral tissue. Following identification, colonies were visually monitored, and confirmation of infection was obtained by assessing disease progression. The affected area, discoloration, and rate of tissue degradation suggested similarities with Rapid Tissue Necrosis (RTN) (Luna et al., 2007). Fragments showing advancing necrosis were isolated from three diseased colonies for microbiome analysis, aimed at identifying microorganisms associated with the condition. High-throughput sequencing yielded 67,257 retained sequences, with per-sample counts ranging from 507 to 27,474.

The genus *Vibrio* was consistently present across all samples, representing between 0.28% and 55.27% of the total bacterial community (Figure 7, Tables 6 and 7). One-Way ANOVA revealed no significant differences in *Vibrio* abundance among tissue categories ($p = 0.53$). Bonferroni post-hoc tests confirmed the absence of statistical differences in pairwise comparisons of apparently healthy (Stylo-H), intermediate (Stylo-I), and diseased (Stylo-D) tissues (Stylo-D vs. Stylo-H; Stylo-H vs. Stylo-I; Stylo-I vs. Stylo-D) (Table 6). Nevertheless, a consistent trend was observed: *Vibrio* proportions were elevated in intermediate tissues—defined as areas immediately above and below the white band threshold—while diseased areas displayed bacterial levels comparable to healthy tissues. Thus, the peak in *Vibrio* abundance was localized at the advancing margin of the lesion. Species-level analysis further revealed *Vibrio harveyi* as the predominant species detected (Table 7). These microbiome findings reinforced the similarity to RTN, allowing classification of the condition as a tissue necrosis-like disease (Luna et al., 2007; Sweet et al., 2012).

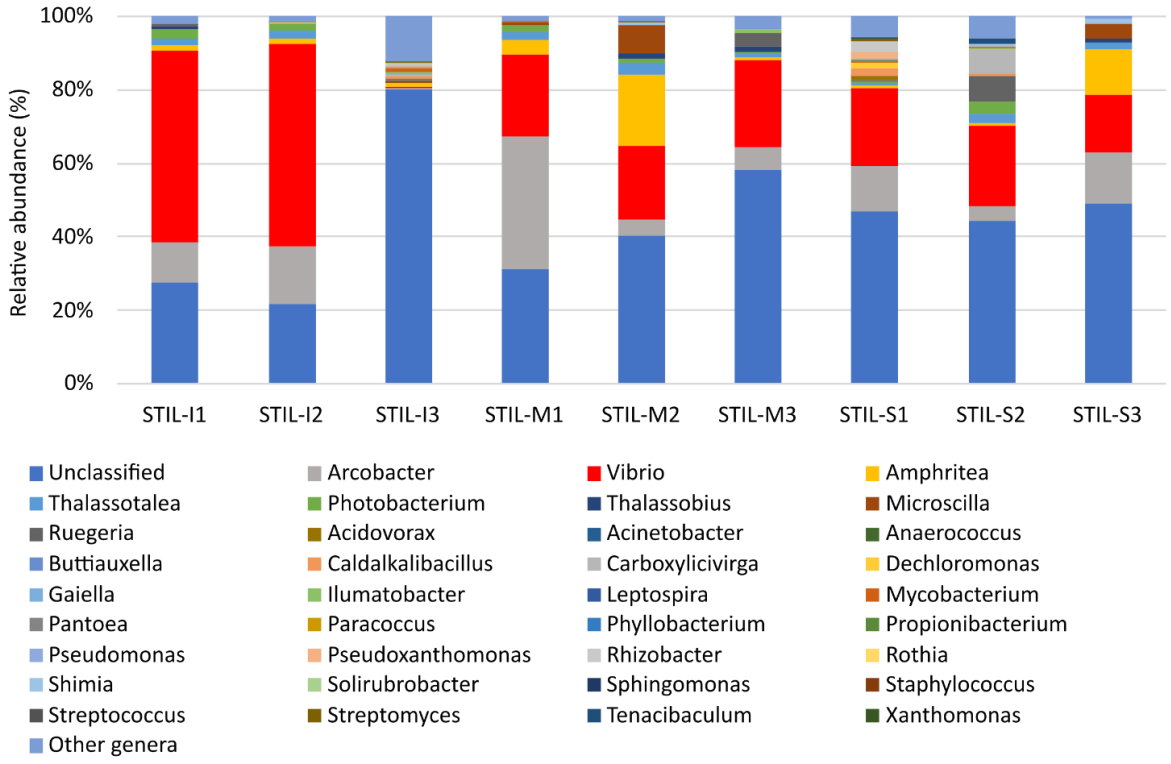

Figure 3. Microbiome analysis. Bar plots of the relative abundance of the most abundant genera in each sample; Genera with abundance < 1% in all samples were grouped in 'Other genera'. I1, I2, I3 indicate the intermediate condition, D1, D2, D3 indicate the "diseased" fragments, H1, H2, H3 indicate the "healthy" fragments. "STYLO" is indicative of the coral genus (Stylophora).

	I1	I2	I3	D1	D2	D3	H1	H2	H3
Vibrio	52.30	55.27	0.28	22.30	19.87	23.75	21.26	22.14	15.58
Mean ± SD	35.95 ± 30.93%			21.97 ± 1.96%			19.66 ± 3.56%		

Table 6. Percentage of sequences classified as Vibrio in each sample and average, and standard deviation for each sample group.

ASV	STYLO-I1	STYLO-I2	STYLO-I3	STYLO-D1	STYLO-D2	STYLO-D3	STYLO-H1	STYLO-H2	STYLO-H3	Best hit
ASV_30	45.19	49.30	0.26	19.33	15.95	21.51	19.35	19.51	12.82	*Vibrio harveyi/owensii/parahaemolyticus/alginolyticus*
ASV_580	3.59	3.26	0.02	2.17	2.28	1.30	1.01	1.42	2.76	*Vibrio alginolyticus/fluvialis/maritimus/furnissii*
ASV_1353	1.20	1.54	0.00	0.00	1.08	0.58	0.00	0.00	0.00	*Vibrio natriegens/rotiferianus/astriarenae/ishigakensis*
ASV_1994	1.26	0.87	0.00	0.72	0.42	0.26	0.87	0.00	0.00	*Vibrio gallaecicus/mediterranei/splendidus/echinoideorum*
ASV_4320	1.07	0.29	0.00	0.08	0.13	0.09	0.03	0.33	0.00	*Vibrio gazogenes/alfacsensis/salilacus*
ASV_15901	0.00	0.00	0.00	0.00	0.00	0.00	0.00	0.88	0.00	*Vibrio europaeus/alfacsensis/marinisediminis/gangliei*

Table 7. Best hit species for ASVs classified as belonging to genus Vibrio; relative abundance (%) of each ASV in each sample.

Treatment strategy for infected corals

Four experimental groups were tested on diseased coral fragments: untreated control, sealant alone (BW4LO1), sealant plus Cipro-loaded film (BW4LO1 + Cipro), and sealant plus Gent-loaded film (BW4LO1 + Gent) (Figure 8A). Films with a P/C ratio of 70/30 were selected for their greater flexibility, essential for application on the highly branched morphology of S. pistillata.

To evaluate therapeutic efficacy under realistic conditions, fragments were monitored for 18 weeks, tracking survival, infection progression, bleaching, necrosis, and overall macroscopic outcomes relative to untreated controls. Final results are summarized in Figure 8B. In the control group, disease advanced rapidly: two of five fragments were dead after six weeks, two remained infected, and only one recovered and resumed growth by the end of the study. In the BW4LO1–DIC group, disease initially appeared slowed—likely due to the physical barrier formed by the sealant—but progression resumed after six weeks. At 18 weeks, four fragments were still infected, and one was healthy, mirroring the control outcomes.

By contrast, fragments treated with BW4LO1–DIC and 70P-30C-Cipro films all recovered fully and maintained a healthy state. In the BW4LO1–DIC + 70P-30C-Gent group, four of five fragments were healthy, while one remained infected.

Chi-square analysis confirmed overall significance (χ^2 (3, N = 20) = 10.30, p = 0.016), with a strong association between treatment type and health outcome (φ = 0.72). When pooling both antibiotic-loaded systems (Cipro and Gent), the overall success rate reached 90%, compared to only 20% in treatments without antibiotics (untreated and sealant-only), which corresponds to the natural recovery capacity of the coral.

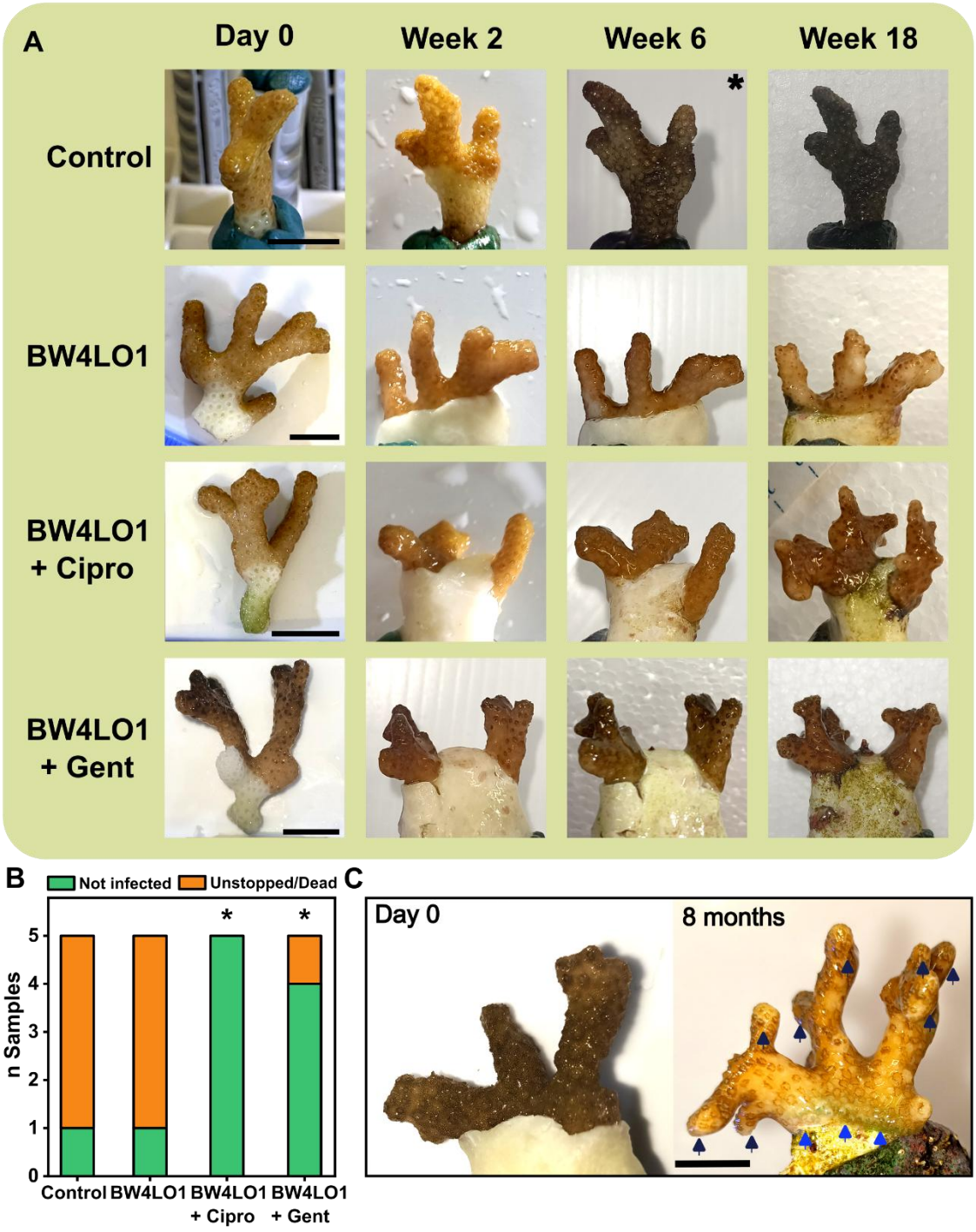

*Figure 4. Application of the two-component system in diseased corals. A, Photographs of infected coral fragments untreated (control), treated with the BW4LO1–DIC, treated with the BW4LO1–DIC + 70P-30C-Cipro, and treated with the BW4LO1–DIC + 70P-30C-Gent over 18 weeks; * time point at which the fragment died. B, a summary of the status of the fragments after 4 months; * = $p < 0.05$ ($\chi^2(3, N = 20) = 10.30$, $p = 0.016$). C, apical and basal growth of a single*

fragment treated with 70P-30C Cipro + BW4LO1–DIC after 8 months; dark blue arrows indicate apical growth, and light blue arrows indicate basal growth. A, C, scale bars of 1 cm.

At eight months post-treatment, new tissue growth was observed macroscopically in surviving fragments, both apically (new branch formation) and basally (enlargement of the colony base) (Figure 8C). Fragments in which the sealant successfully halted disease progression (1 in BW4LO1–DIC, 5 in BW4LO1–DIC + Cipro, and 4 in BW4LO1–DIC + Gent) displayed basal growth. Notably, basal tissue expansion began after three months in fragments treated with Cipro or Gent, whereas the surviving sealant-only fragment showed delayed regrowth, with signs of basal tissue formation first appearing after four months (Figure 8A).

Discussion

Coral diseases represent an increasingly pressing multifactorial problem, often linked to chronic environmental stressors such as pollution, ocean warming, and acidification, all of which severely threaten reef ecosystems (Burke et al., 2023; Miller & Richardson, 2015). In recent decades, outbreaks have become both more frequent and more destructive (Alvarez-Filip et al., 2019). A particularly dramatic case is Stony Coral Tissue Loss Disease (SCTLD), which has reached the scale of a marine pandemic across the Caribbean over the past decade (Precht et al., 2016). While several treatments have been tested to manage and slow SCTLD progression, their overall effectiveness has remained limited (Neely et al., 2020; Neely et al., 2021; Shilling et al., 2021; Walker et al., 2021). Beyond open-reef settings, the lack of effective treatment strategies is also problematic in controlled environments, where coral fragments are propagated *ex situ* or *in situ* and later transplanted as part of restoration programs (Barton et al., 2017; Hughes et al., 2023; Zych et al., 2024). The spread of disease in coral nurseries or aquaculture systems poses a critical threat to such restoration efforts, reinforcing the urgent need for innovative, adaptable therapeutic solutions (Ridlon et al., 2023; Suggett et al., 2023; Vega Thurber et al., 2025).

Currently, antibiotics remain one of the most consolidated approaches for the treatment of bacterial coral diseases (Shilling et al., 2021; Studivan et al., 2023; Sweet et al., 2012). However, their use raises concerns regarding antibiotic resistance and potential alterations in coral microbiome composition (Lupo et al., 2012). Controlled delivery approaches, such as the one presented here, aim to minimize these risks (Cabello, 2006). Similar strategies are well established in pharmaceutics and biomedicine, where engineered drug delivery vehicles concentrate therapeutic agents at the target site, reducing the overall dosage required to achieve efficacy while limiting off-target effects and the emergence of resistance (Gao et al., 2011; Kalhapure et al., 2015). Applying these principles of controlled release and precision delivery to coral diseases offers a promising path forward.

Conventional treatments, including silicon-based ointments and chlorinated–epoxy resin matrices, are typically applied as free-standing monolayers (Favero M, 2020; Forrester et al., 2024; Neely et al., 2020; Neely et al., 2021; Shilling et al., 2021; Walker et al., 2021). When used underwater, these formulations allow drug diffusion in two directions: toward the coral tissue and toward the surrounding seawater. The release behavior follows Fick's law of diffusion and is influenced by multiple parameters, including drug partition coefficients, swelling and erosion processes, matrix hydrophilicity/hydrophobicity, and drug distribution within the carrier (Ritger & Peppas, 1987a, 1987b; Wijmans & Baker, 1995). Consequently, the material side exposed to open seawater experiences continuous solvent turnover and high erosion, favoring drug loss into the environment. Conversely, the side in contact with coral tissue is exposed to far less water, leading to lower drug release. This asymmetry results in intensive drug diffusion into seawater and reduced delivery to the infected coral tissue (Figure 9A) (Contardi et al., 2020). For effective therapy, however, the infected site requires maintenance of antibiotic levels above the Minimal Inhibitory Concentration (MIC) for a sufficient duration to eradicate pathogenic bacteria (Topaz et al., 2021).

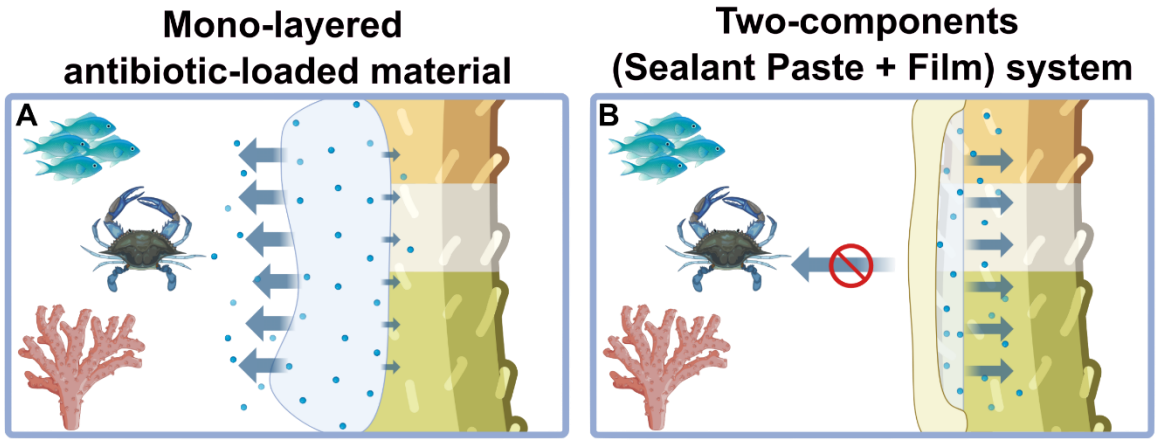

Figure 5. Schematic representation of the sea environment/material/coral-infected site interface. The application and drug diffusion of a currently used mono-layered antibiotic-loaded material (A) and the two-component antibiotic-loaded system described in this work (B). The size and direction of the arrows indicate the release intensity of the drug (small blue dots) from the materials based on the osmotic pressure given by the water.

To overcome these limitations, we proposed a two-component system designed to treat coral infections locally while preventing antibiotic dispersion into the surrounding water (Figure 9B) (Tian et al., 2024). This system is composed of a beeswax/plant-oil-based sealant and a hydrophilic polymeric film made of polyvinylpyrrolidone (PVP), chitosan, and antibiotics. Gentamicin (Gent) and Ciprofloxacin (Cipro) were selected as broad-spectrum antibiotics, and their MIC values against *Vibrio coralliilyticus*, a major coral pathogen (Munn, 2015; Vizcaino et al., 2010), were determined as 32.0 µg/mL and 0.5 µg/mL, respectively. Notably, earlier studies reported Cipro as ineffective

against *V. coralliilyticus* (Vizcaino et al., 2010), but solubility issues may have compromised drug availability. In contrast, in our study, Cipro was solubilized in acetic acid, greatly enhancing its antibacterial activity (Contardi et al., 2017).

The developed films, incorporating PVP and chitosan in varying ratios with polyglycerol as a plasticizer, were loaded with antibiotics at a polymer-to-drug ratio of 100:1 (w/w). Importantly, this represents a significantly lower antibiotic load compared to previously tested formulations, such as amoxicillin-silicone pastes with ratios up to 8:1 (w/w) (Neely et al., 2020; Neely et al., 2021). The films were transparent, homogeneous, ductile, and stretchable, ensuring both effective drug dispersion and adaptability for application onto irregular coral surfaces.

The sealant was produced by melt-mixing beeswax with two plant-derived oils, followed by rapid solidification. Among the candidates, BW4LO1–DIC was selected as the most suitable due to its semi-crystalline structure, which conferred thermoresponsive mechanical properties. As corals typically inhabit waters between 25–28 °C, the sealant must remain solid at this range while still being moldable during underwater application. Dynamic Mechanical Thermal Analysis (DMTA) confirmed that BW4LO1–DIC exhibited a reversible transition from rigidity to malleability simply by manual rubbing, both in air and underwater. This represents a significant technological advance compared to earlier sealants, such as a polycaprolactone–p-coumaric acid copolymer, which required heating to 45–50 °C for application, restricting its use to controlled laboratory or aquarium environments (Contardi et al., 2020).

The two-component system was validated in a transwell setup that mimicked the seawater–coral interface. Results confirmed its capacity for unidirectional diffusion of antibiotics exclusively toward the coral-infected site, ensuring effective drug delivery while preventing environmental release. Moreover, the system allowed sufficient working time for underwater application before drug leakage occurred, making it a practical and eco-friendly therapeutic option. In this sense, the technology operates as a precise *in situ* treatment, akin to a “first-aid kit” for corals, with applicability in both controlled aquaria and open-sea environments.

As proof of concept, the system effectively eradicated high concentrations of *V. coralliilyticus in vitro* (Figure 6C). It was further tested *in vivo* on *Stylophora pistillata* fragments affected by a tissue necrosis-like disease, likely associated with *Vibrio harveyi* based on microbiome analyses. For these trials, BW4LO1–DIC was combined with either 70P-30C-Cipro or 70P-30C-Gent films, chosen for their flexibility and slower initial release, which facilitated application to branched corals. Across 18 weeks of monitoring, the antibiotic-loaded two-component system successfully halted disease progression in 90% of treated fragments, a dramatic improvement over the 20% natural recovery

observed in untreated controls. Following infection arrest, corals resumed apical and basal tissue growth, with the basal overgrowth ultimately incorporating the sealant into the skeleton.

Biodegradability tests (BOD assay, 30 days) confirmed that all components were degradable. While laboratory conditions accelerate degradation (days to months), previous fieldwork by our group demonstrated that such biocomposites degrade much more slowly in natural seawater, over months to years (Contardi et al., 2021; Zych et al., 2024). After 18 weeks *in vivo*, the sealant remained macroscopically intact, providing sufficient stability for coral tissue to overgrow the material. Additionally, antifouling behavior was observed: biofouling of the hydrophobic sealant began only after six weeks, comparable to antifouling benchmarks such as PDMS (2–8 weeks in seawater) (Kolle et al., 2022).

The natural origin of both components supports the eco-friendly profile of this therapeutic system. Nonetheless, further studies are needed to evaluate potential interactions with fish and other marine organisms.

In conclusion, we developed a novel, easy-to-use, two-component system for coral disease treatment. The first component, a natural thermoresponsive and biodegradable sealant, enables underwater application and protection of the second component: a flexible, transparent film composed of PVP, chitosan, and polyglycerol, loaded with Cipro or Gent. Together, they enabled highly efficient infection control, halting disease in 90% of cases while using one-tenth of the antibiotic amounts required in previous strategies, and simultaneously supporting coral regrowth over the applied materials. This versatile system can be implemented in aquaria, nurseries, and natural reef environments, illustrating how interdisciplinary approaches—combining pharmaceutics, materials science, and marine ecology—can yield transformative solutions to protect coral reef ecosystems.

Chapter 4 – Assessment of an antibiotic-based two-step system on a new coral disease-induced model

Introduction

Vibrio coralliilyticus is a globally distributed, Gram-negative marine bacterium that has been repeatedly implicated in temperature-associated coral diseases and mass tissue loss events (Ben-Haim et al., 2003). Different isolates of *V. coralliilyticus* show clear phenotypic and genotypic heterogeneity: some strains produce rapid bleaching and tissue lysis in branching corals as seawater temperatures rise, while others show either lower temperature sensitivity or different host spectra (Ushijima et al., 2014). Temperature acts as a key modulator of pathogenicity in many *V. coralliilyticus* strains, altering expression of secreted proteases, secretion systems, and other virulence determinants that control the timing and severity of disease (Kimes et al., 2012).

That heterogeneity at the strain level is mirrored by genomic and proteomic variation: comparative genomics and whole-genome sequencing studies reveal a large pan-genome, frequent horizontal gene transfer and acquisition/loss of pathogenicity islands and accessory genes among *V. coralliilyticus* isolates (Kehlet-Delgado et al., 2020; Lin et al., 2018; Mass et al., 2024; Raymann et al., 2013). Those differences underlie variable repertoires of secretion systems (including T6SS/T3SS), metalloproteases, and small-molecule secondary metabolites that modulate host interactions, interbacterial competition, and environmental persistence-factors that directly influence both virulence and how a strain responds to antimicrobial agents (Mass et al., 2024; Ushijima et al., 2020; Wang et al., 2022).

Studies that have tested antimicrobial interventions against *V. coralliilyticus* and report highly variable susceptibilities across strains and contexts (Ushijima et al., 2020; Vizcaino et al., 2010). Another work has documented intrinsic and acquired resistance traits in some isolates, as well as the ability of strains to withstand antimicrobial activity produced by resident coral-associated microbiota (Vizcaino et al., 2010). This variability means that an antibiotic that suppresses one *V. coralliilyticus* isolate *in vitro* or in an aquarium model may fail against another strain or may only transiently control disease while selecting for resistant variants.

Applied treatments on corals—ranging from topical antibiotic pastes and bath treatments in aquaria to small-scale interventions in reef restoration trials—have produced mixed outcomes and raised ecological and ethical concerns (Forrester et al., 2024; Sweet et al., 2014). Recent experimental investigations and field trials underscore two recurrent themes: (1) antibiotics can reduce tissue loss in some cases but are not universally effective, and (2) broad-spectrum application risks collateral damage to beneficial microbiota, selection for multi-drug resistant Vibrionaceae, and unknown downstream effects on holobiont recovery and reef microbiome structure (Cohen et al., 2013; Xu et

al., 2024). These findings have motivated exploration of more targeted approaches (for example, strain-specific phages, controlled-release matrices, and localized delivery) that aim to minimize off-target impacts while improving efficacy against the infecting genotype (Cohen et al., 2013; Scribano et al., 2025).

Taken together, the literature frames a working hypothesis that underpins this chapter: antibiotic treatment outcomes in an experimentally infected coral model are expected to differ depending on the infecting *V. coralliilyticus* strain, because the strain-level differences determine baseline virulence, intrinsic susceptibility or resistance mechanisms, and the ecological context of the coral holobiont shapes drug efficacy and recovery (Ushijima et al., 2020; Vizcaino et al., 2010). Therefore, this chapter situates strain variability and documented antimicrobial susceptibility into the biology of *V. coralliilyticus* infections, and it discusses the features that a drug-delivery system must have to be useful in practice: the ability to deliver therapeutically relevant concentrations at the site, minimize the disturbance to the surrounding beneficial microbiota, and enable an adaptive response to strain.

Materials and methods

Materials

Epoxidized soybean oil acrylate (ESOA), lauroyl peroxide, sepiolite, calcium stearate, chitosan, polyvinylpyrrolidone (360 kDa), acetic acid, ciprofloxacin, and gentamicin sulfate were purchased from Sigma-Aldrich. Para-toluidine ethoxylate tertiary amine, commercialized with the name of Bisomer PTE, was kindly provided by GEO Speciality Chemicals. Polyglycerol-10 was kindly donated by SPIGA NORD (batch no. PG10_20221021_0945). V. coralliilyticus (strains H1, YB2, OCN014) were kindly donated by Professor Ushijima Blake (Department of Biology and Marine Biology, University of North Carolina Wilmington, NC 28403, USA).

Methods

Antibiotic-loaded film and sealant were prepared as described in (Scribano et al., 2025) and (Zych et al., 2024), respectively.

Shortly, the film was prepared by mixing polyvinylpyrrolidone and chitosan (1,470:630 mg, respectively) in an 8% acetic acid aqueous solution (20 mL). Then, 8.4 mL of a polyglycerol-10 solution at a concentration of 50 mg/mL (8% v/v acetic acid aqueous solution) and 2.542 mL of antibiotic solution 10mg/mL (either Ciprofloxacin or Gentamicin) were added to the polymer solution. The final volume was brought to 35 mL by adding 8% v/v acetic acid aqueous solution, and then was homogenized and left stirring for 2 h at 55°C. Finally, the solution was cast on a square Petri dish (120 × 120 mm^2), previously covered with Polydimethylsiloxane, and left to dry in an aspirated

hood for 48 hours. The final composition of the film was 57.75% (w/w) of P, 24.75% (w/w) of C, 16.50% (w/w) of polyglycerol-10, and 1% (w/w) of drug.

Instead, the sealant was prepared as a bicomponent paste, and the exact quantities and composition cannot be disclosed because it is under patenting. Shortly, the process was designed to produce the same paste, differentiating only for the accelerator/initiator (Bisomer PTE and Lauroyl peroxide) component. Either 0.4% w/w of the radical initiator was homogenized with 49.6% w/w of ESOA (for component A) or 0.3% w/w of the accelerator with 49.7% w/w of ESOA (for component B) using a THINKY mixer. Then, Calcium carbonate and sepiolite were added in the same quantities to the two pastes. Ideally, the two components will be mixed manually in a ratio of 1:1 and applied over the film to seal drug leakage from the film; the paste will quickly crosslink (within 30 min) and set a new substrate for coral regrowth.

Coral maintenance

90 fragments (about 2 x 2 cm each) of *Porites sp.*, coming from the same quarantine aquarium, were subdivided into 9 aquaria (n = 10) of 200L each (Figure 1). Corals were fed 3 times/week with ground frozen *Artemia sp.* or phytoplankton, and parameters were monitored one time per week (pH 8.1±0.1, Calcium 410±30, Magnesium 1320±140, Alkalinity 8±0.5, Phosphates 0.065±0.035, Ammonia <0, Nitrites <0.15, Nitrates 2.5±1.5). Temperature (24-27 °C) and salinity (32-35 ppm) were monitored daily. Aquaria were cleaned weekly, and 10% of the total water volume was replaced with fresh artificial seawater (35g/L). Corals were provided with 12h of light and 12h of dark.

Experimental setup

The fragments were acclimatized for 2 weeks at 25±1 °C, then the temperature was increased by 0.5 °C/day up to 31±0.5 °C (2 weeks) to simulate an environmental stressor event. The fragments were then scratched using a micropipette tip and causing a wound of about 0.5 cm x 0.2 cm. The fragments were immersed and incubated in three 3-liter tanks having a total concentration of 10^6 CFU/mL of *Vibrio coralliilyticus* (30 fragments per strain: H1, YB2, OCN014) for 2 hours at a temperature of 31 °C (Figure 2). Afterward, fragments were moved back into the aquaria and daily observed to monitor disease progression. When the first signs of disease were noticed (after 9 days from inoculation), fragments were treated with either Ciprofloxacin-loaded film and sealant (TC), or Gentamicin-loaded film and sealant (TG) or left Untreated (UT). Another 10 fragments per tank were added to the experiment to evaluate the condition of the just-stressed corals (no scratch and no inoculation).

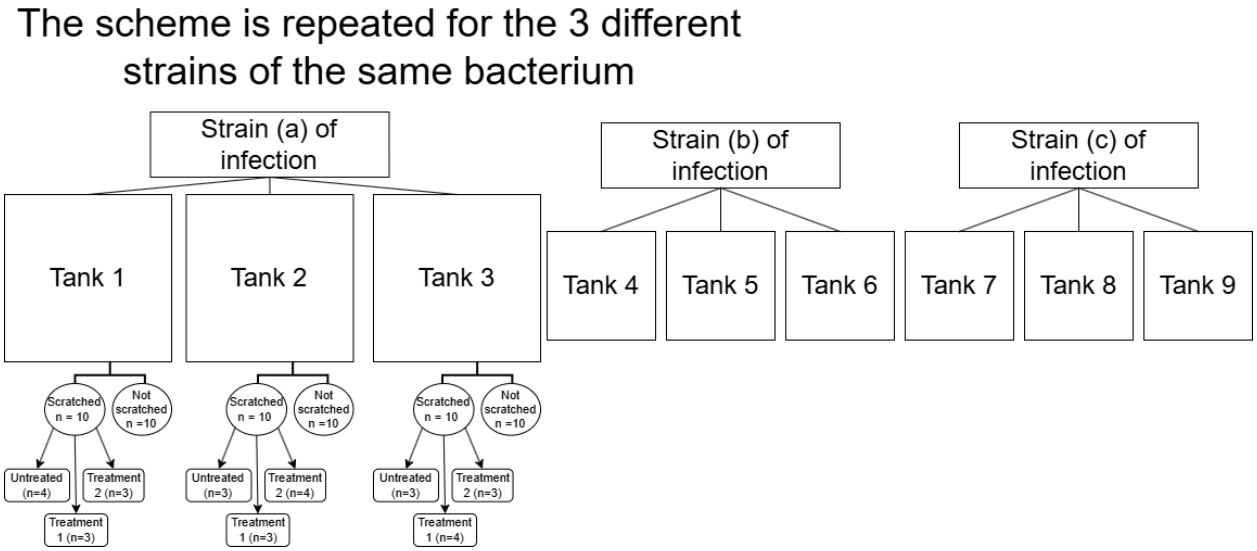

Figure 1. Scheme organizational chart of the experiment setup

An area of 0.5 x 1 cm of either film with Ciprofloxacin or Gentamicin, weighing 13.8±3.1 mg or 16.9 ±6.3 mg, respectively, was applied to cover the scratched area. Then, 0.5 g of sealant (0.25 g of each component) was used to cover and seal the film. After treatment, 2 apparently healthy fragments of *Porites sp.* per tank (size 2 x 2 cm) were added to help restore the Symbiodinaceae in the inoculated fragments. Corals were constantly monitored, and pictures were collected 2 times per week for the following 2 months after treatment. Small pieces of coral fragments were fixed in ethanol for future molecular analysis, and the rest was fixed using Mirsky's fixative to analyze the coral tissue.

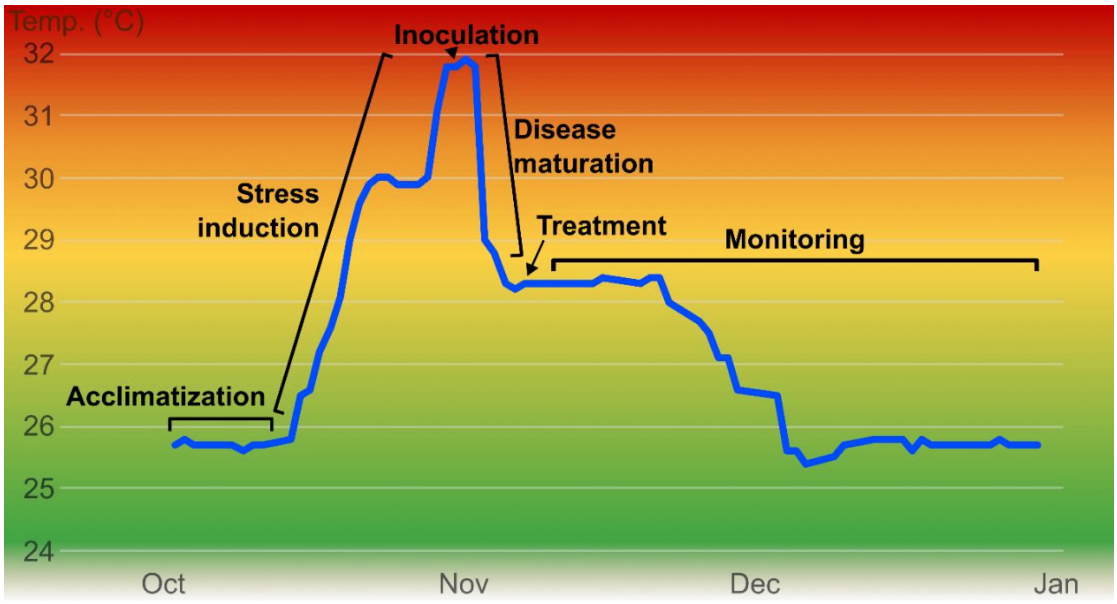

Figure 2. Temperature chart of the experimental setup.

Morphological health area measurement

Morphological analysis on the fragments was performed by measuring the reduced non-diseased/necrotic area of each coral piece over time using the ImageJ tool. The color threshold plugin

was used to separate the healthy/bleached tissue from the diseased/necrotic tissue in the pictures collected over the 2 months of monitoring. The percentage of healthy tissue after two months compared to the day of the treatment was evaluated, and statistical analysis was performed.

Tissue fixation, decalcification, and staining

Samples were fixed in Mirsky's fixative for 48 hours, then washed with PBS 1x pH 7.0 and embedded in 1.5% agar. To decalcify coral skeletons, fragments were immersed in EDTA 0.5M, pH 8.0, and the solution was refreshed every two days until fully decalcified. Processing was done using an automatic tissue processor (Leica TP1020), going through serial dehydration steps (70, 90, 100, 100%), then cleaning xylene with multiple washings (3 times) before paraffin infiltration (3 steps). 10 µm slices were then collected and stained with Hematoxylin and Eosin (H&E) staining. H&E were stained following (Feldman & Wolfe, 2014).

Statistical analysis

Statistical analyses were performed using the Origin software. One-way ANOVA was performed, followed by Bonferroni post-hoc ($n = 10$, $\alpha = 0.05$).

Results and discussions

To reduce the amount of stress to the treated coral fragments, a minimal amount of antibiotic-loaded film was used to cover the lesion. At the end of the monitoring period, the treated fragments demonstrated various responses, from the apparent recovery of the coral, which produced even coral growth in some cases (Figure 3B), to the inability to treat the disease and the continuous progression of this latter/the prevalence of other parasitic microorganisms that may have taken advantage of the altered condition of the fragments. The evaluation of the percentage of recovery/loss of healthy tissue in the fragments was performed by measuring the amount of healthy tissue before applying the treatment and at the end of the two monitoring months.

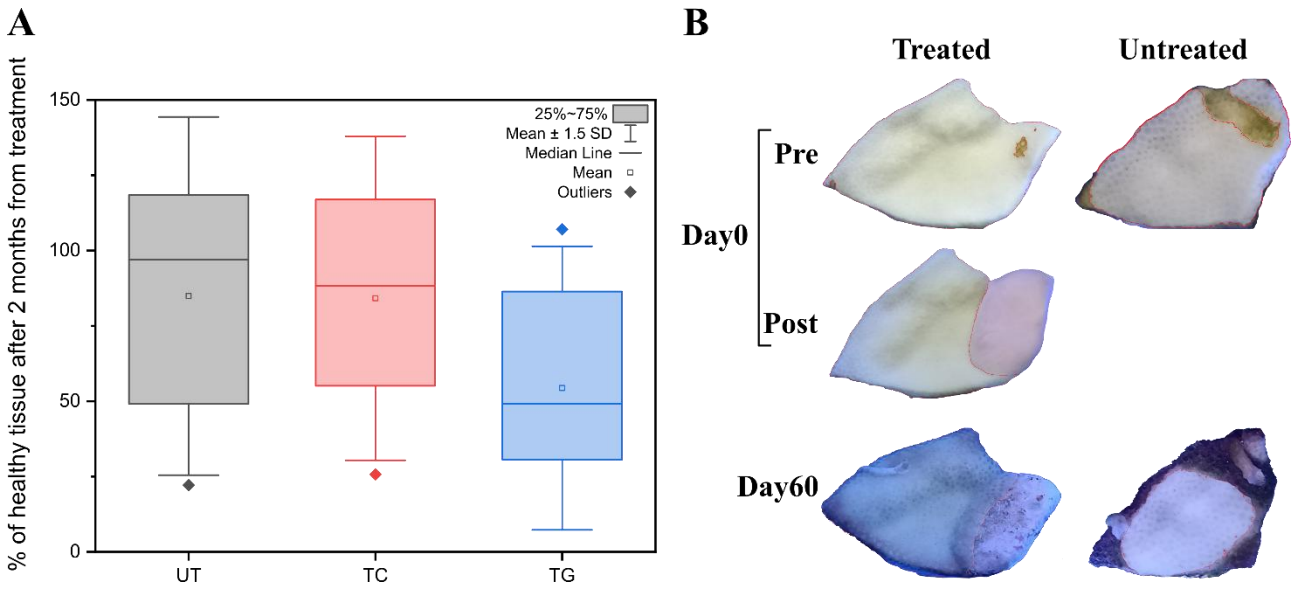

Figure 3. A, the box plot indicates the mean, the median, the error bars (1.5 St. Dev.) and the outliers of the treatment in H1 V. coralliilyticus infected fragments (n = 10). One-way ANOVA, Bonferroni post-hoc; no significance among the groups considered. B, an example of the progression before and after the 2 months of treatment in treated and untreated coral fragments.

So far, 10 samples per condition were measured in the fragments treated with the strain H1. One-way ANOVA test, followed by Bonferroni post-hoc did not reveal any significance among the conditions considered (UT vs TC p = 1, TG vs TC p = 0.16687, TG vs UT p = 0.06326), however, it is observable how the administration of antibiotics increased the variability among the samples, very likely due to the induction of imbalance in the microbiome (Figure 3A).

The tissue analysis further confirmed the condition observed in the morphological analysis.

In the untreated samples that spontaneously recovered from the infection and that looked apparently healthy, the epidermis seems to be intact, but the mesoglea is swollen, which, on its own, could be a sign of an indicative state of growth (Hawthorn et al., 2023) (Figure 4A-C). In the bleached corals examined (Treated and untreated), the necrosis is much more evident (Figure 4D-F, 4J-L). To also note that the untreated diseased fragment presented swelling and disruption of the epidermis, other than internal coagulative necrosis, indicating a diseased condition compared to apparently healthy samples (Figure 4D-F).

The treated samples were more difficult to analyze due to the hardness of the sealing paste. To note how, on top of the sealing paste, in the healthy treated fragment, a layer of coral tissue is expanding, indicative of coral growth (Figure 4G-I). Finally, the diseased treated sample, despite presenting some necrosis, also presents some areas where the cells are still intact (below the film), highlighted by the presence of all the cells still compact in the region observed and all the nuclei intact in that region (Figure 4J-L).

Taken together, these preliminary results seem to indicate that the antibiotic system administered may affect the microbiome, possibly through the induction of some form of dysbiosis. This may also favor

other parasitic microorganisms, inducing further coral infection. However, the damage observed on a tissue level indicates that the coral host is more preserved when treated.

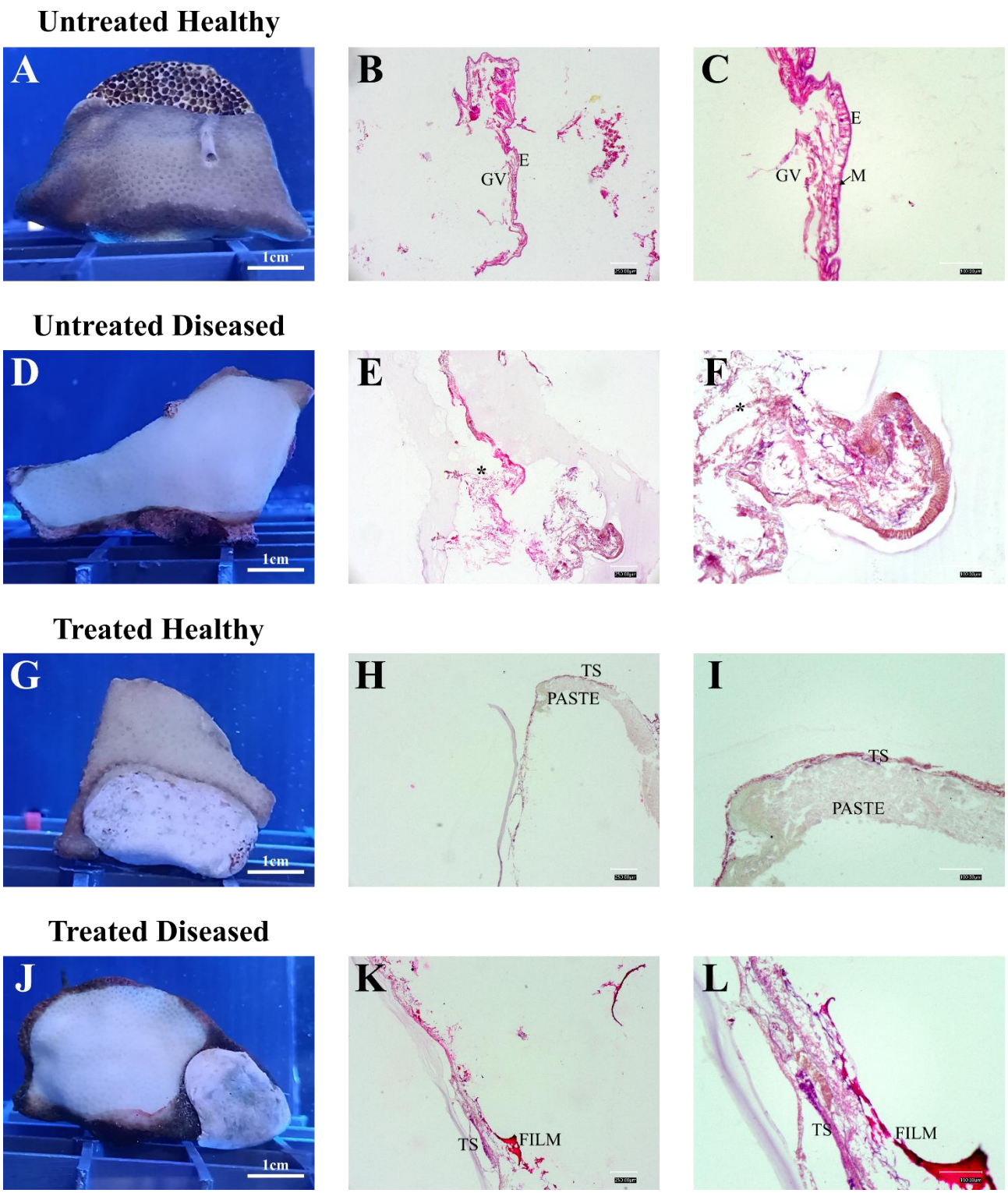

*Figure 4. A,D,G,J, the pictures of the fragments analyzed; B,E,H,K, the H&E tissue staining; C,F,I,L, the magnification of the middle column. Legend: * = necrosis, TS = tissue, PASTE = Sealant, FILM = antibiotic-loaded film, E = epithelium, GV = gastrovascular space, M = mesoglea.*

Future perspectives

The complete analysis of the morphological progression of the disease on the fragments will provide a more comprehensive idea of the differences among the *V. coralliilyticus* strain examined. Moreover, performing molecular analysis on coral samples, such a quantitative real-time PCR, will provide more detailed information about the efficacy of the treatment and the causes of the diseased fragments. Finally, a more detailed description of the tissues analyzed, accompanied by the other supportive staining, such as the Gram staining, and a larger number of samples need to be characterized to properly identify the causes of the disease at the tissue level and observe the presence/absence of bacteria in the treated regions.

Chapter 5 – Advanced alternatives to antibiotics for the treatment of coral diseases

Introduction

Coral diseases have emerged as one of the most serious and least controllable threats, increasingly contributing to mass mortality events and long-term reef degradation. Disease outbreaks are becoming more frequent and widespread, exacerbated by rising ocean temperatures and anthropogenic pollution, both of which disrupt coral immune responses and alter the balance of coral-associated microbial communities (Vega Thurber et al., 2025). A major obstacle to disease management lies in the complexity and ambiguity of coral pathogenesis: the same visible lesion can result from multiple pathogens, and the same pathogen may manifest differently under varying environmental contexts (Meyer et al., 2025; Sweet & Bulling, 2017; Vega Thurber et al., 2025). Consequently, disease diagnosis and pathogen-specific treatment in reef environments are often impractical or impossible. There is therefore an urgent need for broad-spectrum, non-invasive, and environmentally benign therapeutic approaches that can be applied *in situ* to mitigate disease progression without harming the surrounding ecosystem.

One innovative and promising direction lies in photothermal therapy (PTT): a technique in which light-absorbing nanoparticles are used to locally convert electromagnetic radiation into heat, thereby eradicating pathogens through controlled hyperthermia (Liu et al., 2023; Thangudu & Su, 2025). Photothermal therapy is well established in biomedical and antimicrobial research, where it offers a means of sterilizing infected tissues or destroying cancer cells with high spatial precision and minimal systemic toxicity (Liu et al., 2023; Xu et al., 2022; Zhu et al., 2024). The translation of this concept to coral disease treatment, however, represents a frontier yet to be explored.

Other studies already evaluated the use of NIR irradiation, mostly focusing on infrared light presenting a range within the 700 and 900 nm, as higher wavelengths would cover the range of absorption of water (Kuo et al., 2022). To excite underwater nanostructures the efficacy the major factors influencing the PTT activity seems to be attributed to light power density, time of excitation and concentration of the structures in the excited solution (Zhang et al., 2024).

In this context, Iron Oxide NanoCubes (IONCs) offer an attractive photothermal platform: they combine strong photothermal conversion efficiency, chemical stability, and magnetic responsiveness with an excellent safety and biodegradation profile (Espinosa et al., 2016; Guardia et al., 2012; Lartigue et al., 2013). The specific IONCs present a mean diameter of approximately 15 nm, synthesized by Teresa Pellegrino's group at the Italian Institute of Technology, and are particularly suitable because of their uniform shape, low variability in size distribution, and surface functionality that promotes enhanced magnetic response (compared to spherical nanoparticles), aqueous

dispersibility, and biocompatibility (Gavilán et al., 2023; Mai et al., 2019; Mekseriwattana et al., 2025).

For instance, Citric acid coating plays a key role in stabilizing iron oxide nanoparticles in aqueous and physiological environments (Dheyab et al., 2020; Răcuciu et al., 2006). The negatively charged carboxylate groups not only improve colloidal stability but also prevent aggregation and oxidation of the Fe_3O_4 core, ensuring long-term durability and consistent optical and magnetic properties (Mikelashvili et al., 2023). Moreover, citric acid is a naturally occurring, non-toxic molecule that further enhances the biocompatibility of the nanoparticles, minimizing potential ecotoxicological risks in marine applications (Arienzo & Ferrara, 2022; Mikelashvili et al., 2023).

Importantly, the IONCs' therapeutic effect derives purely from localized photothermal conversion. When exposed to a suitable light source—such as near-infrared (NIR) illumination, which penetrates water effectively—these NanoCubes absorb energy and dissipate it as heat (Espinosa et al., 2016). The resulting localized temperature increase can be sufficient to inactivate a broad spectrum of pathogenic microorganisms, including bacteria, fungi, and protozoans, while minimizing chemical inputs and avoiding the induction of antimicrobial resistance.

To ensure precise and environmentally safe deployment on coral colonies, these nanoparticles will be entrapped within a biocompatible hydrogel matrix composed of chitosan and alginate. This polymeric combination, long utilized in biomedical and environmental applications, offers multiple advantages (Saberian et al., 2024; Yadav & Dutta, 2024). Chitosan, a cationic polysaccharide mostly derived from processed crustacean exoskeleton, provides antimicrobial and film-forming properties as well as strong adhesion to biological tissues. Alginate, an anionic polysaccharide extracted from brown algae, contributes structural stability and gel-forming ability in aqueous environments. Together, chitosan and alginate form a polyelectrolyte complex hydrogel that is mechanically robust, highly hydrated, and capable of conforming to irregular surfaces, such as corals (Li et al., 2009). This matrix not only immobilizes the nanoparticles at the treatment site, reducing the risk of environmental dispersal, but also allows close thermal coupling between the lesion and the photothermal agents (Ding et al., 2022; Veloso et al., 2023). Additionally, both polymers are biodegradable and non-toxic to marine organisms, ensuring that the matrix itself poses minimal ecological impact.

The broad-spectrum and non-specific nature of photothermal disinfection addresses one of the most persistent challenges in coral disease management: the need to identify and target specific pathogens (Meyer et al., 2025). Conventional interventions, such as antibiotic pastes or chemical sealants, depend on pathogen-specific action and can contribute to microbial resistance or collateral damage to beneficial microbiota (Forrester et al., 2024; Sweet et al., 2014). In contrast, a physical mechanism like photothermal therapy bypasses the need for etiological identification altogether. The same

thermal treatment can be applied to a wide range of diseases (bacterial, fungal, or else), effectively stepping over the limitations of current diagnostic-dependent strategies. In addition, the chitosan–alginate hydrogel delivery system enables site-specific treatment that can be tuned in duration, intensity, and frequency, making it adaptable to diverse disease severities and coral species.

From an environmental standpoint, this strategy offers substantial advantages. Both the nanoparticles and the hydrogel components are composed of materials with low ecological persistence and toxicity. Iron oxide gradually dissolves or transforms into environmentally benign iron species (Estelrich & Busquets, 2018), and the absence of heavy metals or synthetic polymers reduces long-term contamination risks (Dedman, 2022). Furthermore, the use of light as an activation trigger eliminates the need for continuous chemical exposure, limiting the intervention to precisely controlled periods. Such an approach aligns well with the principles of sustainable marine biotechnology, minimizing the ecological footprint while maximizing therapeutic efficacy.

The integration of IONCs into a chitosan–alginate hydrogel introduces a new class of localized, controllable, and eco-friendly treatment platform for underwater use. When applied directly onto diseased coral tissue, the hydrogel can act as a physical barrier protecting the lesion while enabling light transmission. Upon illumination, the embedded NanoCubes generate heat that diffuses into the adjacent tissue, reaching temperatures sufficient to inactivate or weaken pathogens. Because seawater has high thermal conductivity, heat dissipates rapidly beyond the target area, providing an intrinsic safeguard against overheating of surrounding healthy tissue.

Finally, the novelty of this approach lies in uniting the principles of nanomedicine, photothermal physics, and coral ecology into a single, deployable treatment platform. While the separate components (IONCs and chitosan–alginate hydrogels) have each been independently studied, their combination in this context represents a unique and innovative intersection of materials science and marine conservation. To date, no published work has reported the use of coated-IONCs embedded in a biopolymeric hydrogel for underwater photothermal treatment of coral disease.

If successfully optimized, this system could provide a universal therapeutic tool for coral disease management, holding great promise for mitigating the impacts of coral disease outbreaks while preserving the integrity of the reef environment.

Materials and methods

Materials

Chitosan (CAS: 9012-76-4, product code: 448869), Sodium alginate (CAS: 9005-38-3, product code: 180947) were provided by Sigma-Aldrich. Marine Broth 2216 (Product No.: 76448-500g) was purchased from Millipore and used as recommended.

Materials for the IONCs synthesis are the following: 1-Octanol (anhydrous, ≥99%; Sigma-Aldrich, cat. no. 297887), Hexadecylamine HAD (98%; Sigma-Aldrich, cat. no. 445312)-aliphatic amine, Oleic acid OA (≥99%, GC; Sigma-Aldrich, cat. no. 364525)-surfactant, Iron pentacarbonyl (>99.99%; Sigma-Aldrich, cat. no. 481718) iron precursor, Benzaldehyde (≥99%, ReagentPlus; Sigma-Aldrich, cat. no. 418099) shape-directing agent, tetramethylammonium hydroxide (TMAOH) pentahydrate (≥97%, Ligand; Merck, cat. no. T7505-5G), Citric acid (ACS reagent grade, ≥99.5%, crystals; Sigma-Aldrich, cat. no. 251275), Triethylamine (99.5%, base; Merck, cat. no. T0886), Ethanol Absolute Anhydrous (99.9%; Carlo Erba, cat. no. 308602), Milli-Q water filtered through 0.22 μm pore size hydrophilic filters (18.2 MΩ cm) (supplied by a Milli-Q Integral Water Purification System), Gallic polyethylene glycol (PEG-GA, produced according to reference (Guardia et al., 2014)), Chloroform (Carlo Erba, 99.8%), Toluene (Carlo Erba, 99.7%).

Methods

Iron Oxide NanoCubes (IONCs) synthesis

Iron oxide nanocubes (IONCs) used in this study were synthesized and provided by Dr. Teresa Pellegrino's research group and produced following the protocol described in Gavilán et al (Gavilán et al., 2023).

Shortly, A homogeneous solution was prepared by mixing the OA surfactant (1.9 mmol), HAD aliphatic amine (0.8 mmol), and 1-Octanol (7.8 mL) and stirring at 60 °C for 30 min. After cooling to room temperature (25–28 °C), the metal precursor (8.8 mmol) and benzaldehyde (19.6 mmol) were successively added, and the mixture was stirred for an additional 30 min to yield the final stock solution.

The solution was transferred into a 25 mL autoclave filled to 46% of its total volume (adjusted by solvent volume) and heated at 200 °C for 4-6 h under autogenous pressure (~20–30 bar). After cooling to RT, the reaction mixture was collected and distributed into 45 mL Falcon tubes containing $CHCl_3$. The suspension was sonicated for 5 min, followed by the addition of acetone (30 mL per tube) and centrifugation at 3,893 × g for 20 min to isolate the nanoparticles. The resulting product was redispersed in $CHCl_3$ for future use.

IONCs functionalization

To improve IONCs' water redispersion, two different hydrophilic surface coatings were evaluated to study their potential influence on nanoparticle–bacteria interactions: gallic acid–acid-polyethylene glycol (GA–PEG) and citric acid.

The surface functionalization with GA-PEG was performed using the following protocol.

A chloroform dispersion of 15 nm nanocubes ([Fe] = 4 mg/mL, 0.5 mL) was mixed with 2.8 mL of a PEG–GA chloroform solution (0.05 M) and 0.28 mL of trimethylamine, corresponding to a ligand excess of approximately 500 L/nm² relative to the nanocube surface area. The mixture was stirred overnight at room temperature (RT) on an orbital shaker. The resulting chloroform solution was transferred to a separating funnel containing water (100 mL) and toluene (40 mL) and shaken to form an emulsion. Acetone (100 mL) was then added to induce phase separation, after which the aqueous phase containing the nanocubes was collected. Residual organic solvents were removed by purging with nitrogen for 2 h. The sample was concentrated under reduced pressure using a rotary evaporator at 40 °C to a final volume of 100 mL. The nanoparticle dispersion was then concentrated and washed by centrifugation in membrane tubes (Amicon® Ultra, 100 kDa MWCO, 15 mL) (1500 rpm, 10 min, repeated as needed) until reaching a final volume of 0.5 mL. Finally, the aqueous nanocube suspension was sonicated for 30 min at 65 °C.

For the functionalization with citric acid, the 17 nm iron oxide nanocubes dispersed in chloroform were transferred to water using tetramethylammonium hydroxide (TMAOH) as an intermediate ligand, following (Gavilán et al., 2023). Next, 80 mg of citric acid dissolved in 0.5 mL of Milli-Q water was added to 1 mL of TMAOH-coated iron oxide nanocubes ([Fe]= 1.4 mg/mL). The mixture was heated at 80°C for 1h. Afterwards, 3 mL of Milli-Q water was added, and the dispersion was washed by centrifugal ultrafiltration (Amicon® Ultra, 100 kDa MWCO, 5 mL) at 1500 rpm for 10 min. The washing step was repeated at least three additional times to remove excess ligands. The nanoparticles were finally dispersed in 1 mL of Milli-Q for future characterization.

Hydrogel fabrication

For nanoparticle immobilization and stabilization in seawater, a biopolymeric matrix composed of chitosan and alginate was developed. Chitosan (2.75% w/v, low molecular weight) (pH 1) and alginate (2.4% w/v) water (MilliQ) solutions were combined in different weight ratios (4:1, 3:2, 1:1, 2:3, and 1:4) to identify the most suitable formulation for injectability and stability.

The hydrogels were prepared by simple mixing of the two solutions, followed by mechanical disruption through agitation to homogenize the hydrogel.

The dispersibility of nanoparticles within each polymer solution was qualitatively assessed by simply mixing the IONCs in the solution of chitosan or alginate. Two types of injectable hydrogel formulations were then prepared, each loaded with either GA-PEG-coated or citric acid-coated IONCs (0.05 g/L Fe).

Swelling capacity

Film-forming properties of the chitosan–alginate hydrogel were also evaluated. A 1:1 chitosan–alginate hydrogel was cast onto a Teflon mold and dried for two days to produce thin films. Circular disks (8 mm diameter, n = 3) were cut and immersed for four hours in two different solutions: Milli-Q water and filtered seawater. Weight changes were monitored to evaluate swelling behavior.

Transmission electron microscopy (TEM)

TEM analyses were performed using a JEOL JEM-1011 instrument with an acceleration voltage of 100 kV. Sample preparation was performed by drop-casting of few drops of diluted sample solution on a 400 mesh ultra-thin carbon-coated copper grid, followed by water evaporation.

Minimal inhibitory concentration (MIC)

MIC tests were carried out in 24-well plates, each containing 1 mL of sterilized marine broth inoculated with *Vibrio coralliilyticus* at 1.7×10^6 CFU ($OD_{600} = 0.01$). IONCs were added in various concentrations ranging from 0.1 to 0.001 g/L Fe. After 24 hours of incubation at 28 °C with constant shaking (100 rpm), bacterial growth was observed.

Dynamic Light Scattering (DLS)

Dynamic light scattering (DLS) measurements were performed for each nanoparticle type dispersed in both Milli-Q water and 0.22 µm-filtered seawater (Collected at the "old harbor" of Genova, Italy) to evaluate aggregation and precipitation behaviors.

Photothermal activity (PTA)

Photothermal properties of the IONCs were examined by irradiating suspensions of EHNC37–GA–PEG nanoparticles (100 µL) at varying concentrations (0.5, 1.0, and 3.4 g Fe/L) using an 808 nm laser at two power densities (0.3 W/cm² and 1 W/cm²). Temperature profiles were recorded over 10 min of irradiation, and the thermal responses were visually monitored with an infrared thermal camera before and after treatment. Nanoparticle-loaded hydrogels (100 µL of loaded hydrogel plus 50 µL of seawater) were also irradiated for testing of photothermal efficiency post-immobilization.

Results and discussions

The obtained iron oxide nanocubes with a core size of 15 and 17 nm (Figure 1A, 1C), after being coated with GA-PEG and Citric acid, respectively, displayed a hydrodynamic size of 49.4 and 86.9 nm with corresponding zeta potentials of 27.5 and 31.4 mV, respectively (Figure 1B, 1D).

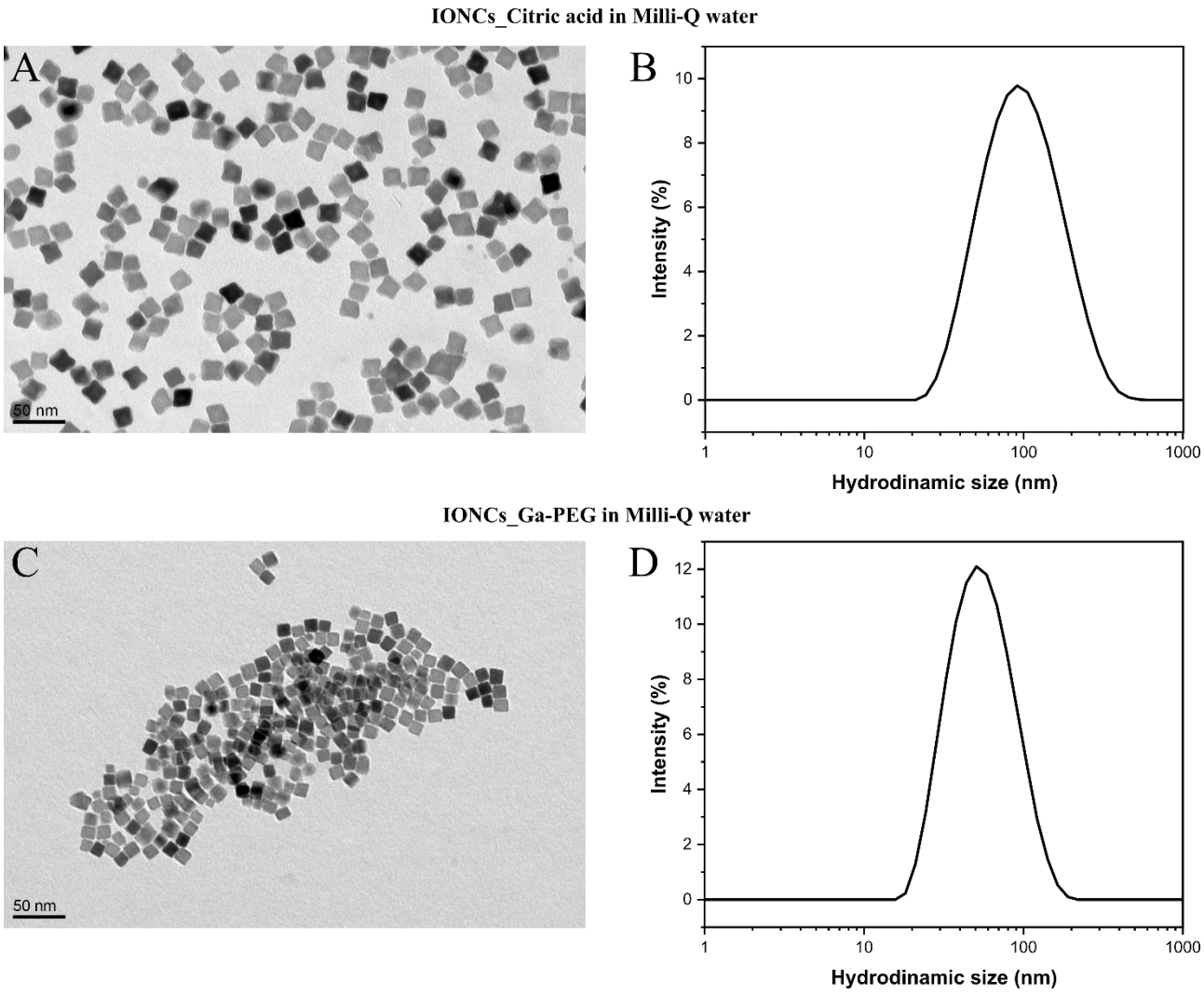

Figure 1. A,C TEM observation and, B,D, Dynamic Light Scattering of the IONCs: A,B, the Citric acid functionalized IONCs, C,D, the GA-PEG IONCs.

During the MIC, the two IONCs formulations in the marine broth exhibited distinct physicochemical behaviors, probably depending on their surface coating. The IONCs_GA–PEG nanoparticles showed the greatest colloidal stability in Marine broth, maintaining dispersion at concentrations even at 0.1 mg/mL (Figure 2C). In contrast, IONCs_Citric Acid nanoparticles demonstrated significant aggregation and sedimentation under the same conditions (Figure 2D). MIC assays performed against *Vibrio coralliilyticus* revealed no bactericidal effect at the tested concentrations, suggesting that higher nanoparticle concentrations or combined photothermal activation might be necessary to achieve antimicrobial efficacy.

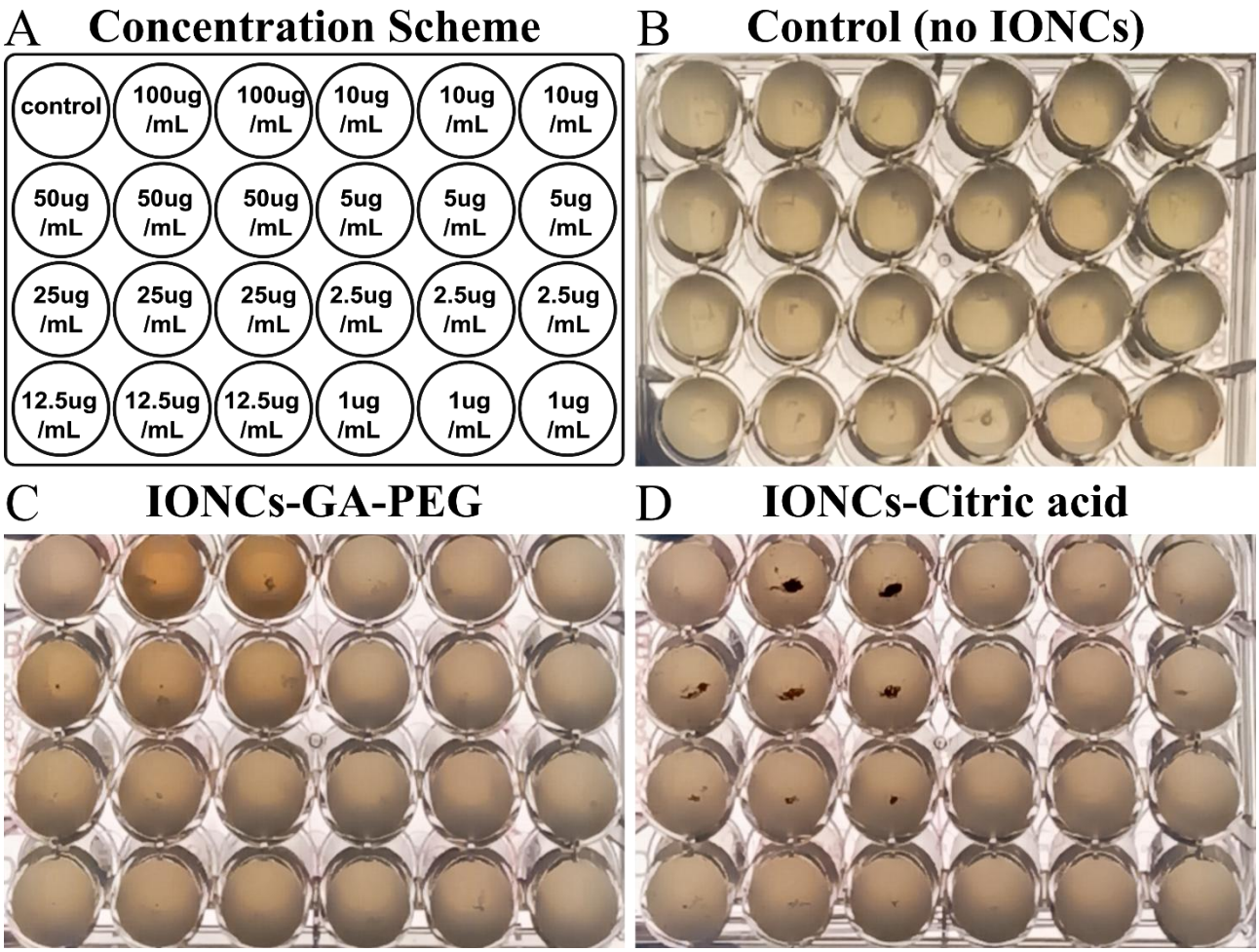

Figure 2. Minimal Inhibitory concentration of the IONCs against V. coralliilyticus at 28°C. A, the scheme of the nanoparticle concentration added to the medium; B, the control where the growth of V. coralliilyticus was assessed without any treatment; C, the treatment with IONCs functionalized with GA-PEG at different concentrations; D, the treatment at different concentrations with IONCs functionalized with Citric acid.

DLS analyses confirmed that, although IONCs are highly stable in MilliQ water, they tend to aggregate in seawater, probably due to high ionic strength and the presence of multivalent cations, which screen electrostatic repulsion between particles (Chekli et al., 2013). Even in the absence of bacteria, visible precipitation was observed for all formulations, indicating that seawater composition significantly compromises nanoparticle stability (Figure 3).

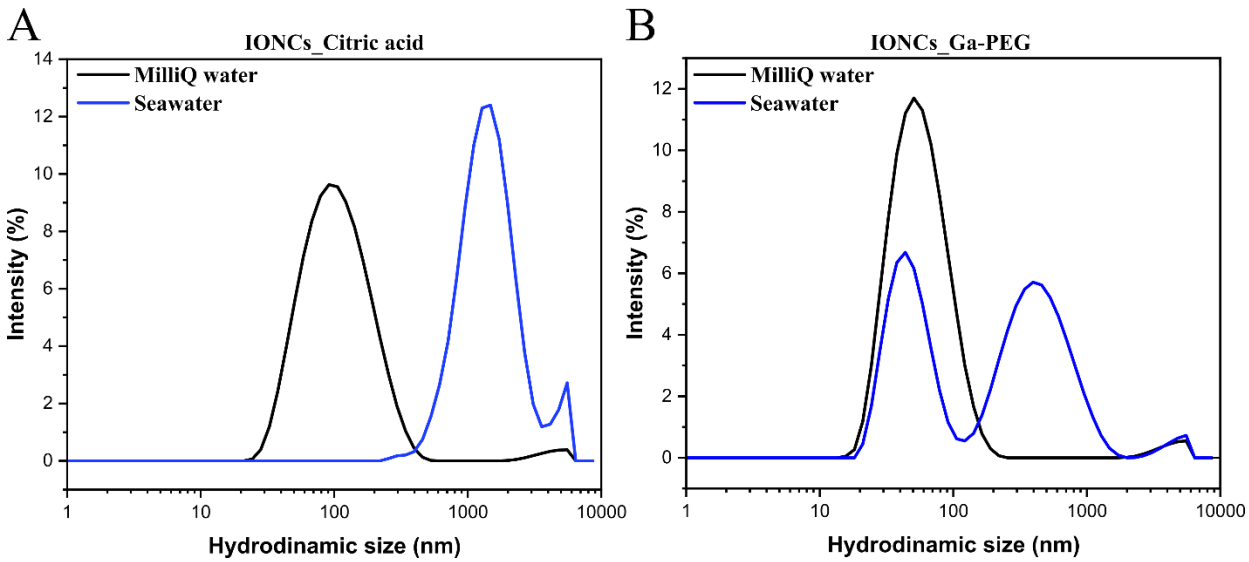

Figure 3. Dynamic Light Scattering of the nanoparticles in MilliQ water and seawater; A, the percentage of IONCs_Citric acid in function of the hydrodynamic size; B, the percentage of IONCs_GA-PEG in function of the hydrodynamic size.

Photothermal heating experiments demonstrated a strong dependence on both laser power (Figure 4) and nanoparticle concentration (Figure 5). IONCs_GA–PEG were selected because of their higher stability in seawater to perform the photothermal experiments. Irradiation of IONCs_GA–PEG dispersions in MilliQ water with an 808 nm laser resulted in rapid temperature increases proportional to the applied power density (Figure 4A) and particle concentration (Figure 5A). However, upon irradiation in seawater, visible aggregation and precipitation occurred (Figure 5D-G), suggesting that while the photothermal conversion remained effective, colloidal instability limited the potential for repeated or prolonged use.

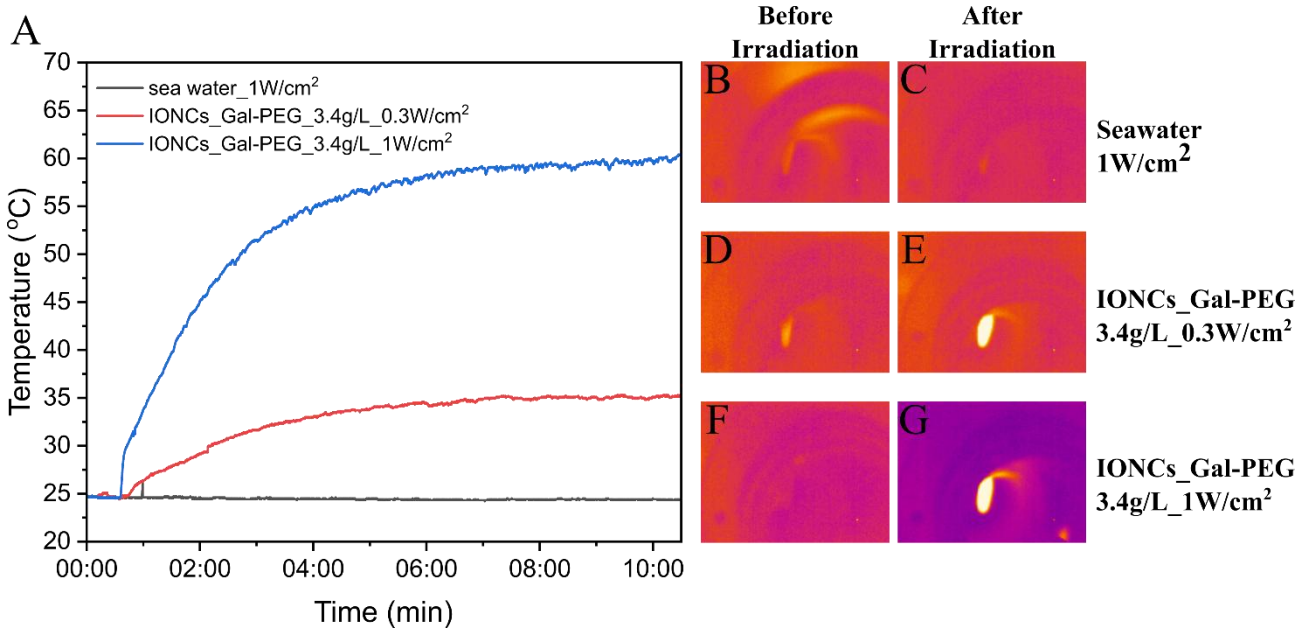

Figure 4. A, the thermal profiles of IONCs-Gal-PEG (Grey control) under irradiation with different laser powers (Red 0.3 W/cm², Blue 1W/cm²); B,C, IR camera showing before (B) and after (C) seawater laser irradiation; D,E, IR camera showing before (D) and after

(E) IONCs_GA-PEG 0.3W/cm² laser irradiation; F,G, IR camera showing before (F) and after (G) IONCs_GA-PEG 1.0W/cm² laser irradiation.

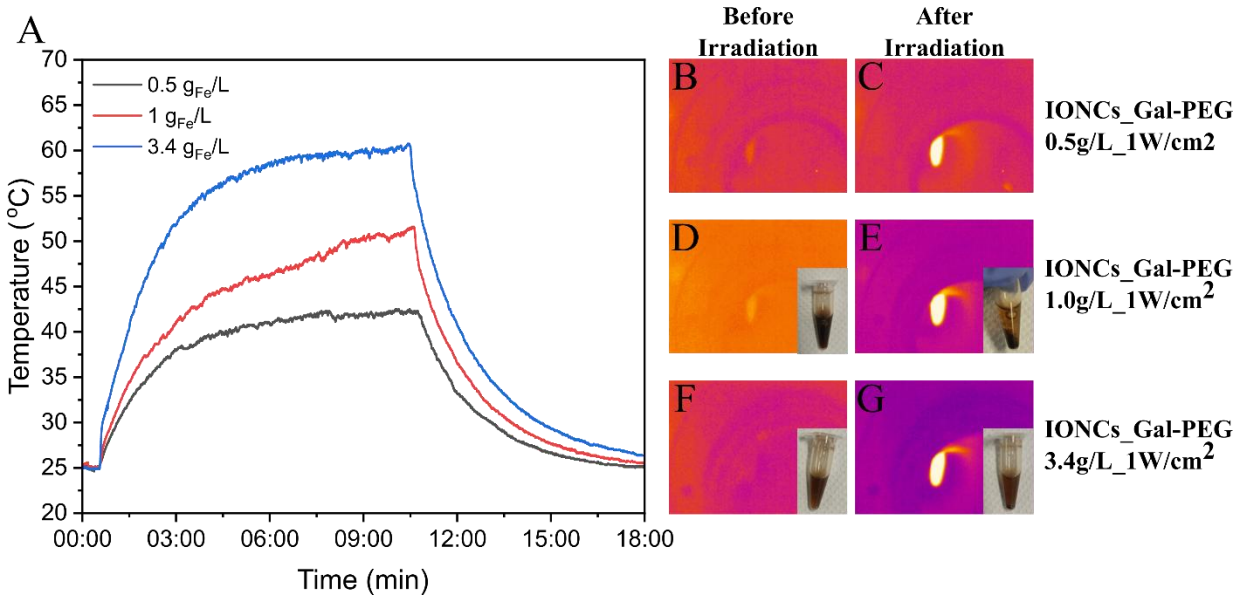

Figure 5. A, the thermal profiles of IONCs-Gal-PEG under irradiation with different concentration (Grey 0.5 g$_{Fe}$/L, Red 1 g$_{Fe}$/L, Blue 3.4 g$_{Fe}$/L); B,C, IR camera showing before (B) and after (C) seawater laser irradiation; D,E, IR camera showing before (D) and after (E) IONCs_GA-PEG 1.0 g$_{Fe}$/L; F,G, IR camera showing before (F) and after (G) IONCs_GA-PEG 3.4 g$_{Fe}$/L. D-G insertions are the pictures in natural light.

To overcome nanoparticle dispersion issues in seawater, a chitosan–alginate hydrogel system was developed as a biocompatible immobilization matrix. Both polymers were selected for their biocompatibility and opposite charges, which enable ionic crosslinking.

Varying the chitosan-to-alginate ratio significantly affected gel consistency and injectability (Figure 6). Ratios of 1:1, 3:2 and 4:1 yielded homogenous and easily injectable gels (Figure 6C, 6D, 6E), whereas higher chitosan contents produced rigid, poorly flowable hydrogels. Mechanical homogenization through a syringe proved superior to tip sonication, which overly disrupted the polymeric network and caused dispersion of the gel upon seawater contact. The optimized hydrogel exhibited mild adhesive properties and could be successfully injected or cast as films.

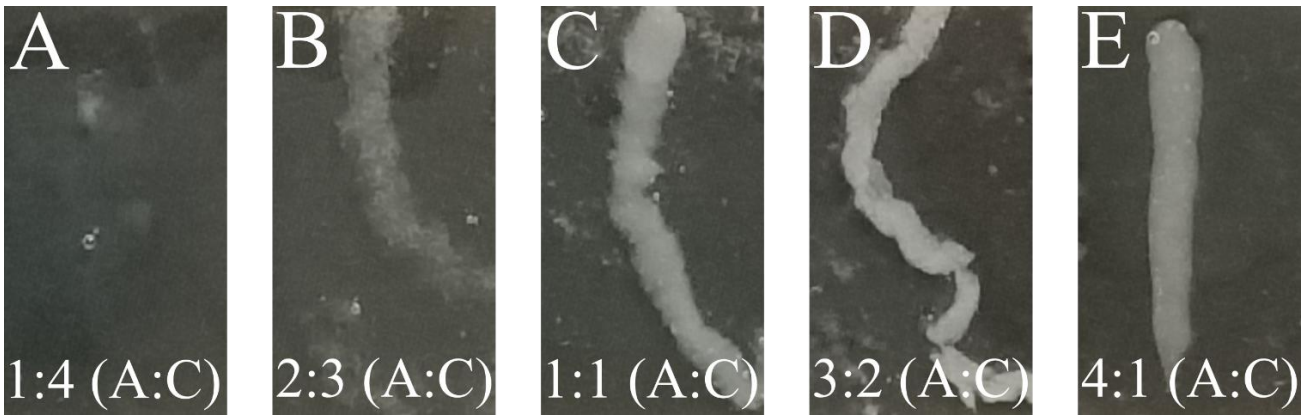

Figure 6. Injectability of the alginate-chitosan hydrogel at different w/w ratios. A, 1 to 4 ratio in weight/weight of the two solutions alginate-chitosan; B, 2 to 3 ratio in weight/weight of the two solutions alginate-chitosan; C, 1 to 1 ratio in weight/weight of the two solutions alginate-chitosan; D, 3 to 2 ratio in weight/weight of the two solutions alginate-chitosan; E, 4 to 1 ratio in weight/weight of the two solutions alginate-chitosan.

Swelling tests demonstrated that the chitosan-alginate films maintained their integrity in seawater, increasing in mass by 237 ± 30% after four hours without disintegration (Figure 7A, 7B). Films immersed in Milli-Q water, however, dissolved completely after a few minutes, indicating that natural ionic crosslinking from seawater (Mg^{2+}, Ca^{2+}, $Fe^{2+/3+}$) provided optimal and fundamental stability (Figure 7C).

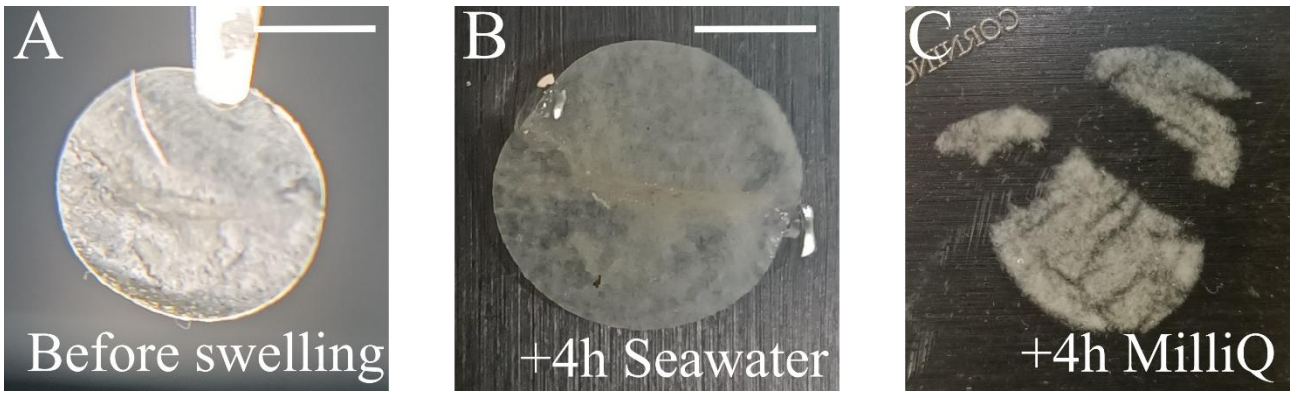

Figure 7. Chitosan-hydrogel films swelling test. A, alginate-chitosan (1:1) 8mm film disk before swelling; B, alginate-chitosan (1:1) 8mm film disk after 4 hours swelling in seawater; C, alginate-chitosan (1:1) 8mm film disk afer 4 hours swelling in MilliQ. Scale bar is 5 mm.

Incorporation of IONCs into the chitosan phase yielded uniform nanoparticle distribution, whereas dispersion in alginate resulted in aggregation, confirming the preference of the iron oxide surface for the cationic chitosan matrix (Figure 8).

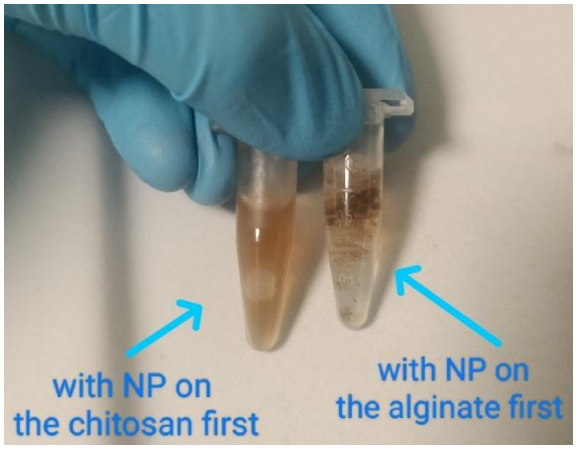

Figure 8. Incorporation of the IONCs with the chitosan solution (left) or with the alginate solution (right).

After the evaluation of the nanoparticle instability in seawater, the IONCs (functionalized with GA-PEG or Citric Acid) were incorporated in the Chitosan-alginate hydrogel (conc. 0.05 g/L Fe), and the photothermal activity was evaluated through laser irradiation (1W/cm^2). 100 µL of loaded hydrogel was mixed with 50 µL of micron-filtered seawater to favor crosslinking. An unloaded hydrogel was irradiated, as well as a control. As expected, the gel alone did not exhibit significant heating, whereas the IONCs-loaded hydrogels showed measurable heating: IONCs-Gal-PEG produced a temperature increase of ~2.5 °C, compared to ~1.3 °C for IONCs-Citric acid (Figure 9A). Moreover, the matrix remained stable after the irradiation, demonstrating the efficacy of the delivery treatment (Figure 9B-G). These results indicate that IONCs remain effective at generating heat even when embedded within a matrix.

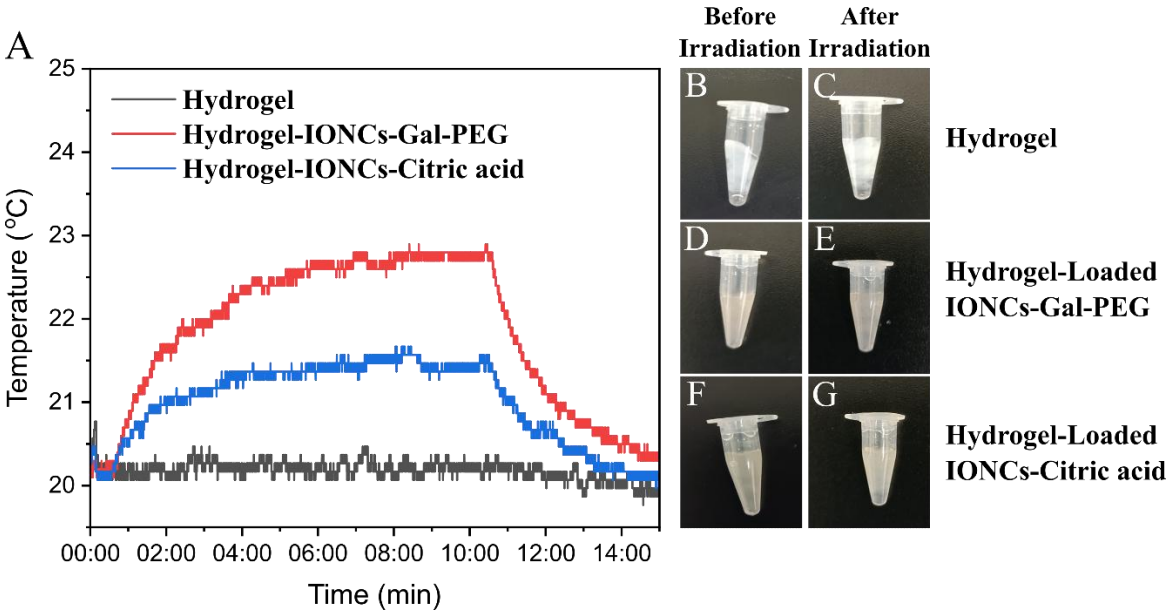

Figure 9. A, Thermal profiles of hydrogel alone (Grey), hydrogel loaded with IONCs-Gal-PEG (0.05 g/L) (Red), and hydrogel incorporated with IONCs-citric acid (0.05 g/L) (Blue) obtained under laser irradiation for 10 min with a laser power of 1 W/cm^2; B,C, the hydrogel samples before (B) and after (C) laser irradiation; D,E, the hydrogel-loaded with IONCs_GA-PEG samples before

(D) and after (E) laser irradiation; F,G, the hydrogel-loaded with IONCs_Citric acid samples before (F) and after (G) laser irradiation;

Future perspectives

From the results so far, this system seems to be the right direction to produce a potential universal therapeutic tool for coral disease. However, to demonstrate real efficacy, further tests need to be performed.

To begin, future experiments will include increasing the concentrations of nanoparticles embedded in the hydrogels to further boost the heating efficiency. The evaluation of the photothermal activity against *Vibrio coralliilyticus* is a required feature that still needs to be assessed. Moreover, the biocompatibility of the gel with coral tissue is still to be addressed. Finally, given the impracticality of laser use directly on corals in potential *in vivo* applications, a torch light emitting at 850 nm was identified as an alternative light source for further testing, which will be assessed in future studies.

Chapter 6 - Bioadhesive development as a versatile tool from the treatment of coral diseases to various underwater applications

Introduction

With the advancement of technologies for the utilization of marine resources, adhesives are gaining a crucial role in many applications. Classic adhesives as cyanoacrylates, lack proper performance underwater or in wet conditions compared to dry conditions (Taghizadeh et al., 2022). The application of underwater sensors and cameras, treatments for mariculture (e.g., coral aquacultures), treatments for coral disease (as described in Chapter 3), and marine soft robotics requires a reversible wet adhesion that would allow the easy attachment/detachment directly underwater (Cheng et al., 2022; Kerrison et al., 2018; C. Lee et al., 2023). However, developing a good adhesive for underwater applications is challenging. Water molecules and relative ions in it can quickly cover the surface, creating a layer between the adhesive and the substrate (Maier et al., 2015). Moreover, if we are considering the usage of adhesive in seawater, we must also take into account the strong ionic strength that further weakens interfacial interactions (H-bonds, Van der Waals, and electrostatic interactions), preventing good adhesion to the substrate (Israelachvili, 2011). Finally, the long exposure of the adhesive to seawater may favor the water and ions penetration causing swelling, oxidation, and erosion of the adhesive (Fan, 2023).

Despite all these challenges, successful examples of underwater adhesives are present in nature. Animals such as mussels, barnacles, octopuses, and remoras found different ways to adhere to various underwater surfaces. These could primarily be distinct by physical and chemical adhesions (C. Lee et al., 2023) where physical adhesives mostly rely on mechanical or electromagnetic actuation that permits easy attachment/detachment (Frey et al., 2022; C. Lee et al., 2023), whereas chemicals focus more on the usage of specific catechol/gallol-based molecules (Cheng et al., 2022; Fan, 2023; Hofman et al., 2018; C. Lee et al., 2023; Taghizadeh et al., 2022) that tend to produce cement-like adhesives, allowing a one-time super-strong adhesion.

An intermediate type of adhesive that may allow easy removability, instant tacking (no curing time), and potential biocompatibility and sustainability, as well as the simplicity of the application and production (no actuators), are the pressure-sensitive adhesives (PSAs) (Abu Bakar et al., 2024). PSAs high viscoelasticity permits immediate adhesion on rough surfaces, almost independently of the substrate type (Abu Bakar et al., 2024; Liu et al., 2025). In the last five years, several PSAs have been developed, always paying more attention to the sustainability of the product and their capacity to degrade under certain conditions (Badía et al., 2020; Chen et al., 2020; Gabriel & Dubé, 2023; Jeong et al., 2023; Paul et al., 2023). However, so far, the scientific literature is lacking articles discussing

bio-based pressure-sensitive adhesives that work well in seawater and that present easy multiple attachment/detachment on multiple surfaces.

Taking inspiration from precedent publications (Chen et al., 2020; Fan et al., 2024; Hu et al., 2024; Khosravi et al., 2024; Lee et al., 2020; Lee et al., 2021; S.-J. Lee et al., 2023; Lei et al., 2020; Qie et al., 2024; Gudrun Schmidt et al., 2023; Schmidt et al., 2025; Shao et al., 2025; Tang et al., 2024; Tiu et al., 2019) of bio-inspired adhesives, I followed three main lines of research for the development of a new potential bio-based and bio-inspired underwater adhesive: (1) the production of stable emulsions of zein/tannic acid complex mixed with an oleogel of carnauba wax and castor oil, (2) a two-component precipitating system made of Poly Vinyl Alcohol (PVA)-Fe and Alginate-Tannic acid, and (3) a thermally pre-cured PSAs composed of Epoxidized Linseed Oil (ELO) (Nardi et al., 2024) and phenol-based acids. This work prioritized the underwater handling and the in-water stability rather than absolute adhesive strength.

The three projects presented focus on the usage of catechol/gallol-based molecules as tackifiers, then mixed with different matrices using different methods for the production of new, improved underwater adhesives. The qualitative outcomes show tradeoffs between immediate tack and long-term retention, highlighting key chemical and formulation controls (polyphenol size, metal coordination kinetics, matrix hydrophobicity).

Materials and methods

Materials

Zein (CAS: 9010-66-6, product code: Z3625-500G), Poly(vinyl alcohol) (PVA) low Mw (≈9–10 kDa) (CAS: 9002-89-5, product code: 360627-500G) and medium Mw (30–70 kDa) (CAS: 9002-89-5, product code: P8136-1KG), Sodium alginate (SA) (CAS: 9005-38-3, product code: 180947-500G), Tannic acid (TA) (CAS: 1401-55-4, product code: 403040-100G), Caffeic acid (CA) (CAS: 331-39-5, product code: C0625), Gallic acid (GA) (CAS: 149-91-7, product code: G7384-100G), trans-ferulic acid (FA) (CAS: 537-98-4, product code: 128708-100G), p-coumaric acid (p-CA) (CAS: 501-98-4, product code: C9008-25G), $FeCl_3$ (CAS: 10025-77-1, product code: 236489-5G), Castor oil (CAS: 8001-79-4, product code: 259853-1L), Carnauba wax (CAS: 8015-86-9, product code: 243213-250G), , Ethanol (CAS: 64-17-5, product code: 24105-M-2.5L) were all bought from Sigma-Aldrich. Epoxidized Linseed oil (ELO) (under the trade name Lankroflex™ L with Mw = 947.5 g/mol and average number of epoxy groups per ELO of 5.6 was kindly provided by Valtris Specialty Chemicals, UK), MilliQ water was produced through the Milli-Q Advantage A10 ultrapure water purification system (Merck-Millipore, Darmstadt, Germany).

Methods

Three complementary strategies were chosen to probe the adhesive production:

Emulsion preparation and handling tests

Zein/TA solutions were mixed into preheated oil/wax matrices and ultrasonicated (30 s at 30 kHz, 50% power, repeated 3×). Emulsions were inspected for coalescence and ease of injectability.

Two-component mixes

One part (PVA + Fe^{3+}) and the other (SA + TA) were stored separately and mixed at the point of use. Qualitative handling (plastic precipitate formation, smearability), underwater retention, and mode of failure (adhesive vs cohesive) were preliminary tested.

Thermal pre-curing reactions

ELO mixed stoichiometrically with phenolic acids and heated in closed conditions to form viscous, tacky materials; handling and tack were judged qualitatively.

Reaction table

ID	Reaction name	Reagents & concentrations (% in w/w)	Preparation modality	Conditions	Outcome notes
1	Zein–TA emulsification (Matrix: Wax 10% / Oil 90%)	5% Wax, 45% Oil, 50% Zein-TA sol (21.6% Zein, 29.4% TA, 49% H_2O/EtOH 40/60)	Melt wax in oil (~90 °C), add aqueous zein/TA, ultrasonicate 3×30 s (30 kHz, 50% power)	Hot mixing then cooling	If properly emulsified: Injectable paste; stability depends on surfactant capacity of oil & sonication; good underwater persistence
2	Zein–TA emulsification (Matrix: Wax 25% / Oil 75%)	12.5% Wax, 37.5% Oil, 50% Zein-TA sol (21.6% Zein, 29.4% TA, 49% H2O/EtOH 40/60)	Melt wax in oil (~90 °C), add aqueous zein/TA, ultrasonicate 3×30 s (30 kHz, 50% power)	Hot mixing then cooling	Higher wax increases stiffness; Injectability decreases with higher wax
3	TA → CA substitution (same OH equivalents) in W/O emulsion	Replace TA with CA at the equivalent −OH content in reaction 1	Melt wax in oil (~90 °C), add aqueous zein/CA, ultrasonicate 3×30 s (30 kHz, 50% power)	Hot mixing then cooling	Higher dry lap-shear for CA sample but CA leaches in seawater → loss of underwater adhesion
4	PFAT — Part A: PVA + Fe (low Mw)	0.4 mL PVA 20% in H_2O + 0.04 mL $FeCl_3$ 25% in H_2O	Prepare and store as a separate Part A	Ambient storage until mixing	Part A alone is liquid; designed to be mixed with Part B at point-of-use

5	PFAT — Part B: SA + TA	0.4 mL SA 20% in H_2O + 0.4 mL TA 20% in H_2O	Prepare and store as a separate Part B	Ambient storage until mixing	Part B liquid; on mixing with Part A, forms plastic precipitate
6	PFAT mixing (low-Mw PVA variant)	Part A + Part B	Point-of-use mixing	Ambient; immediate precipitation	Plastic precipitate forms; ductile mass; underwater-stable for days; Self-healing properties
7	PFAT mixing (high-Mw PVA variant)	Part A + Part B	Point-of-use mixing	Ambient; immediate precipitation	Plastic precipitate forms; more cohesive failure compared to PVA low-Mw; Self-healing properties
8	ELO + Caffeic acid (ELOCA) — epoxide–acid thermal reaction	2 g ELO + 0.7099 g CA Equivalent ELO Epoxy: Reactive groups CA = 1:1	Mix on Teflon plate; oven at 142 °C; closed oxygen	142 °C; reaction time up to ~5 h	Viscosity increase: tacky/PSA-like material after extended heating; slowest among tested acids
9	ELO + Gallic acid (ELOGA) — epoxide–acid thermal reaction	2 g ELO + 0.5324 g GA Equivalent ELO Epoxy: Reactive groups GA = 1:1	Mix on Teflon plate; oven at 142 °C; closed oxygen	142 °C; reaction time up to 2.5 h	Viscosity increase: tacky/PSA-like material after extended heating
10	ELO + p-coumaric acid (ELOp-CA) — epoxide–acid thermal reaction	2 g ELO + 0.9696 g p-CA Equivalent ELO Epoxy: Reactive groups p-CA = 1:1	Mix on Teflon plate; oven at 142 °C; closed oxygen	142 °C; reaction time up to ~2.5 h	Viscosity increase: tacky/PSA-like material after extended heating
11	ELO + trans-ferulic acid (ELOFA) — epoxide–acid thermal reaction	2 g ELO + 1.1477 g FA Equivalent ELO Epoxy: Reactive groups FA = 1:1	Mix on Teflon plate; oven at 142 °C; closed oxygen	142 °C; reaction time up to ~2 h	Viscosity increase: tacky/PSA-like material after extended heating
12	ELO + Tannic acid (ELOTA) — epoxide–acid thermal reaction	2 g ELO + 0.804.4 g TA Equivalent ELO Epoxy: Reactive groups TA = 1:1	Mix on Teflon plate; oven at 142 °C; closed oxygen	142 °C; short reaction time noted (~20 min)	Rapid curing reaction; fully cured after 20 min (142°C); to evaluate milder temperatures

Lap shear test

Preliminary lap shear strength was measured using a dual-column Instron 3365 universal testing machine (2 kN cell load) at a strain rate of 5 mm*min^{-1}. Aluminum sheets (6061) with dimensions of 100 mm × 25 mm × 1 mm were washed with soap and 2-propanol. The tested adhesives were placed on the aluminum sheets submerged in seawater and attached underwater using gentle pressure. Tests were conducted after 24h or 48h from adhesion.

Minimal Inhibitory concentration (MIC)

MIC tests were carried out in 24-well plates, each containing 1 mL of sterilized marine broth inoculated with *Vibrio coralliilyticus* at 1.7 × 10^6 CFU (OD_{600} = 0.01). Gallic acid, Tannic acid, Caffeic acid, and p-coumaric acid were added in various concentrations, depending also on the solvent used to dissolve them (either Ethanol or EtOH, or MilliQ water or MilliQ). After 24 hours of incubation at 28 °C with constant shaking (100 rpm), bacterial growth was observed.

Results and discussions

Adhesion under aqueous conditions remains a significant scientific and engineering challenge due to the presence of interfacial water, which physically and energetically impedes direct contact between adhesive and substrate. The hydration layers on surfaces and water's high dielectric constant screen electrostatic and hydrogen bonding interactions, leading to drastically reduced adhesion strength compared to dry environments (Fan, 2023; Li et al., 2022). Recent efforts have drawn heavily from biological systems—particularly mussels, sandcastle worms, and barnacles—whose adhesive proteins demonstrate strong, non-toxic, and repeatable adhesion in seawater through coacervation and catechol chemistry (Stewart et al., 2011). Recent literature shows a clear shift toward bio-derived PSAs, produced from renewable or naturally occurring precursors such as cellulose, lignin, chitosan, or polyphenols. These materials often mimic the catechol (DOPA) and amine functionalities of mussel adhesive proteins to promote underwater adhesion (Hu et al., 2024; Khosravi et al., 2024; Lee et al., 2020; Gudrun Schmidt et al., 2023; Tang et al., 2024).

Cellulose-based PSAs functionalized with catechols or gallols have already demonstrated measurable adhesion in both deionized and seawater environments. Tang and colleagues (Tang et al., 2024) reported a cellulose-catechol coacervate system capable of achieving lap-shear strengths of 0.16 MPa on steel in seawater, confirming the potential of natural polymer backbones as water-compatible carriers. Similarly, protein–polyphenol systems (e.g., zein/tannic acid combinations) have shown tunable tack and cohesive energy depending on pH and salinity (Gudrun Schmidt et al., 2023).

Another example coming from nature that has been taken into consideration for the design of underwater adhesives is the method applied by sandcastle worms: they secrete oppositely charged polyphosphoproteins that coacervate upon contact with seawater, forming a malleable glue that later solidifies via metal-ion bridging (Taghizadeh et al., 2022). Similarly, mussel foot proteins (mfps), rich in DOPA and lysine, form single-component coacervates that spread and adhere under seawater salinity (Costa et al., 2021; Taghizadeh et al., 2022).

Unlike hydraulic or epoxy cements, which require curing and yield rigid, permanent bonds, underwater PSAs and coacervates provide reversible, low-stress, and conformal adhesion (Abu Bakar et al., 2024). Cementitious adhesives are ideal for structural and load-bearing applications (bridges, hull repair), but PSAs excel in dynamic, flexible, and temporary scenarios—such as sensor mounting, marine robotics, or biomedical patches. Whereas cement systems depend on chemical hardening and high modulus, PSAs rely on viscoelastic dissipation and non-covalent bonding, allowing easy detachment and reusability.

Despite significant progress, achieving simultaneous instant adhesion, high strength, biocompatibility, and environmental resilience in seawater remains an active frontier.

With this project, I wanted to explore three different syntheses of underwater adhesives, focusing on the biocompatibility and environmental respect: the coacervation (1), the mix-on-use method (2), and the covalent bonding of tacky molecules on bio-based polymers (3).

Hereafter, I will explore the results of each mini project individually:

(1) Molecular size and hydrophobic confinement emerged as the principal determinants of underwater retention. Smaller phenolics such as caffeic acid and gallic acid enhanced initial dry tack, producing up to twice the lap shear strength of equivalent tannic acid systems, but these gains evaporated in seawater as the small molecules leached rapidly from hydrophilic matrices. Larger polyphenols, such as tannic acid, proved more resistant to washout and preserved adhesion underwater (Figure 1).

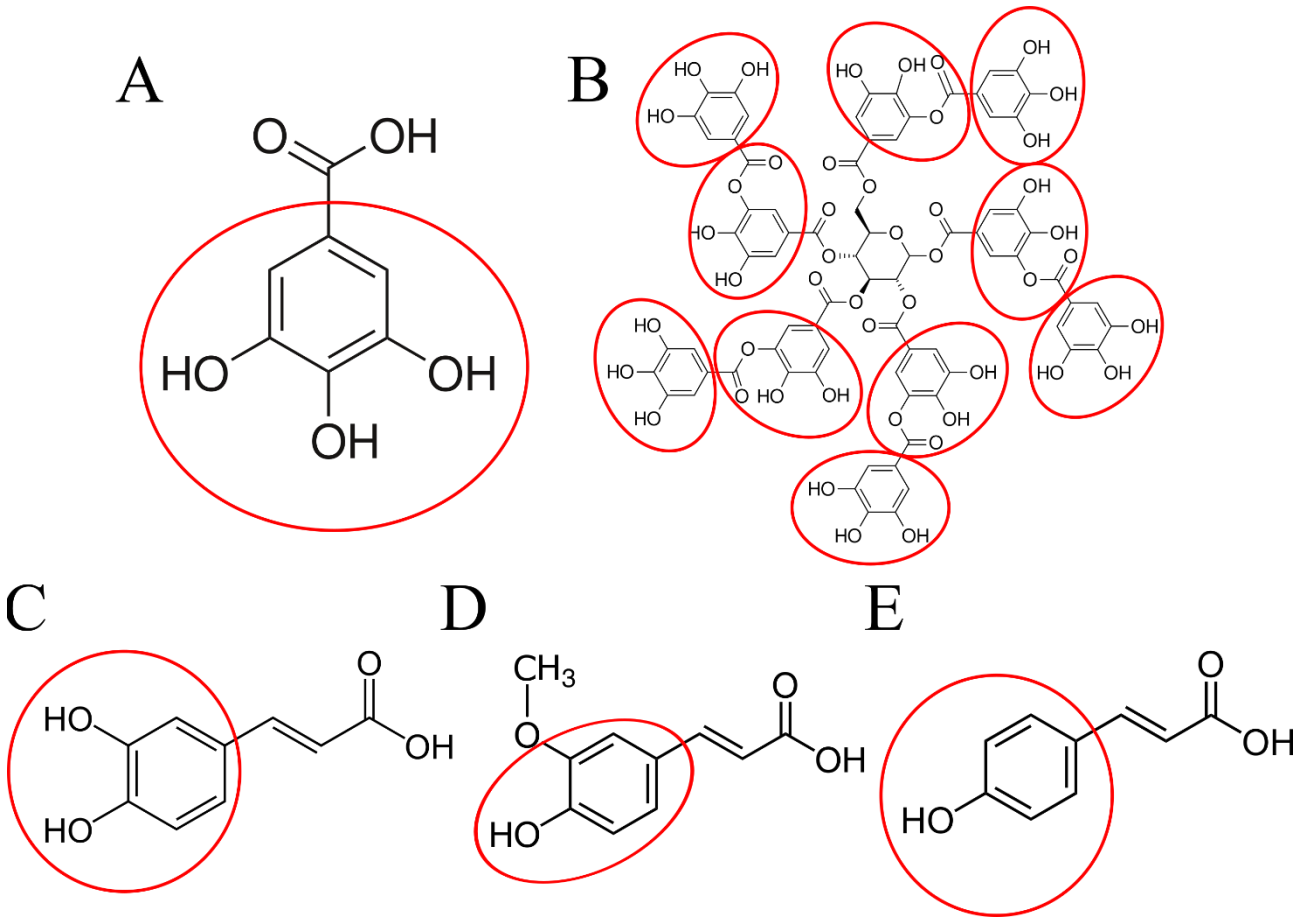

Figure 1. Molecular structure of the polyphenols used: A, Gallic acid (GA); B, Tannic acid (TA); C, Caffeic acid (CA); D, ferulic-acid (FA); E, p-coumaric acid (p-CA). Red circles indicate the phenol-based tacking groups.

These phenols also demonstrated antibacterial properties if dissolved in the right solvent, such as ethanol (Bhattacharya & Mandal, 2025; Chen et al., 2024). In particular, caffeic acid, gallic acid, and p-coumaric acid dissolved in ethanol demonstrated an antibacterial capacity against *V. coralliilyticus* already at concentrations of 0.5, 0.25, and 0.5 mg/mL, respectively (Figure 2B, 2E, 2F). Due to the reduced solubility of caffeic acid and p-coumaric acid in water, the gallic acid and the tannic acid were the only molecules to be tested using MilliQ water. The tannic acid did not present any antibacterial activity at the tested concentration, but instead flocculated, forming aggregates, possibly due to the presence of biofilms that formed even in the MilliQ control (Figure 2H). Even if in smaller quantities, this behavior was also pursued in the gallic acid dissolved in the MilliQ test, but this latter presented an antibacterial activity at the concentration of 2mg/mL (Figure 2I), which could be attributed to the decrease in pH determined by the intrinsic properties of the acid (Farid & Larsen, 1981). The higher antibacterial activity observed in the presence of ethanol instead could be assigned to a synergistic activity with the toxic activity derived from the solvent that was necessary to solubilize the molecules considered.

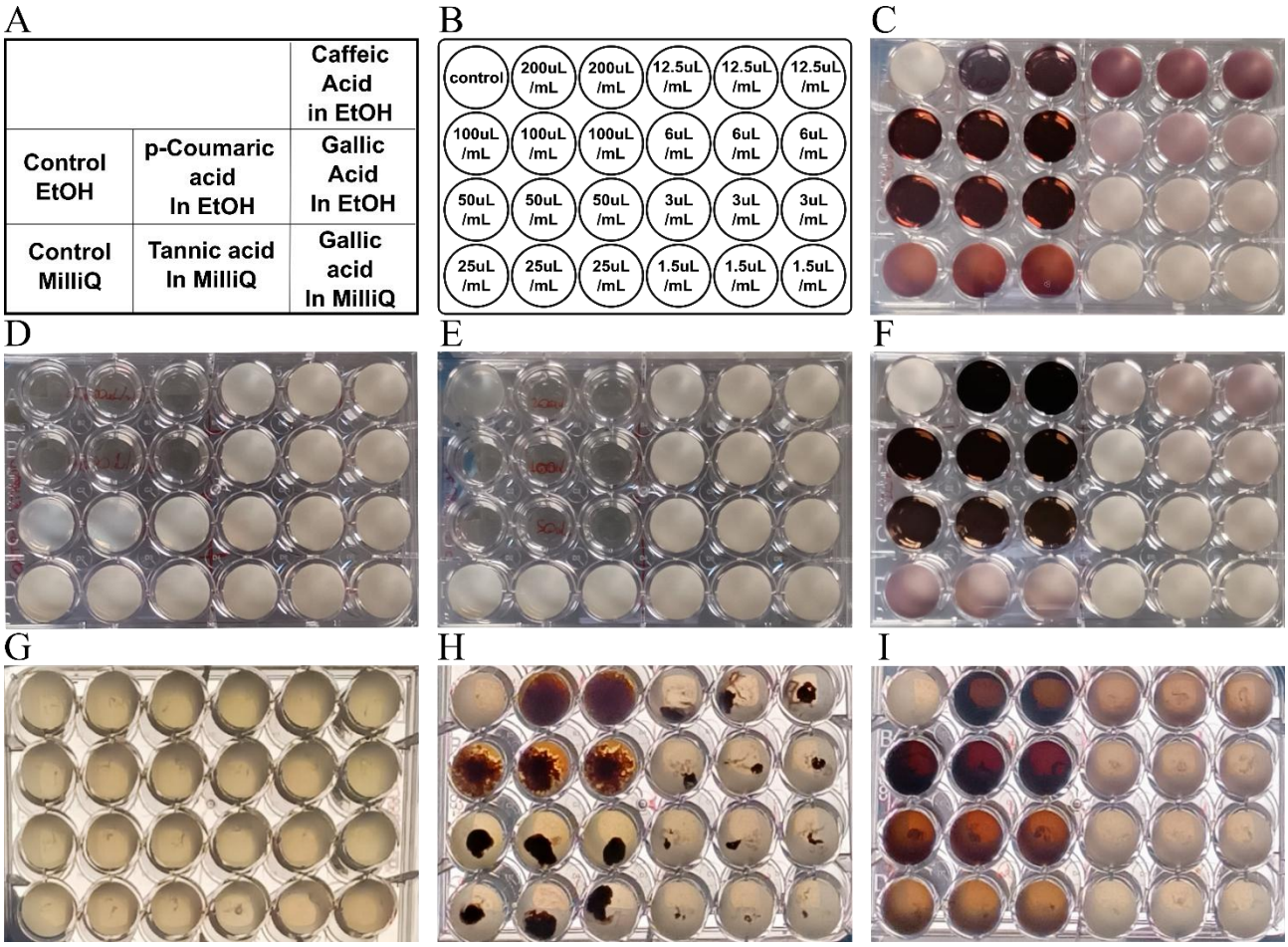

Figure 2. Test of the antibacterial capacity of caffeic acid, gallic acid, tannic acid, and p-coumaric acid dissolved in ethanol or in MilliQ water. A, the legend of the MIC shown; B, the scheme volume ratio of solution tested; C, caffeic acid solution in ethanol: initial solution concentration of 10mg/mL, tested concentrations 2 – 0.01mg/mL; D, Ethanol control; E, p-coumaric acid solution in ethanol: initial solution concentration of 10mg/mL, tested concentrations 2 – 0.01mg/mL; F, gallic acid solution in ethanol: initial solution concentration of 10mg/mL, tested concentrations 1 – 0.005 mg/ml; G, MilliQ water control; H, tannic acid solution in MilliQ: initial solution concentration of 10mg/mL, tested concentrations 2 – 0.01mg/ml; I, gallic acid solution in MilliQ: initial solution concentration of 10mg/mL, tested concentrations 2 – 0.01mg/ml;

Embedding reactive polyphenols in zein-based oil/wax emulsions generated physically stable, injectable materials capable of forming conformal coatings on aluminum and coral substrates. However, the adhesive capacity of these emulsions was highly reduced compared to the scientific standard used (Figure 3A)(Schmidt et al., 2025), probably by the presence of the wax that induced the prevalence of the cohesive forces over the adhesive ones (Figure 3C) (Park et al., 2006). Their main limitation was emulsion stability and phenolic retention, but the hydrophobic matrix effectively slowed leaching and suggested an accessible route for field application.

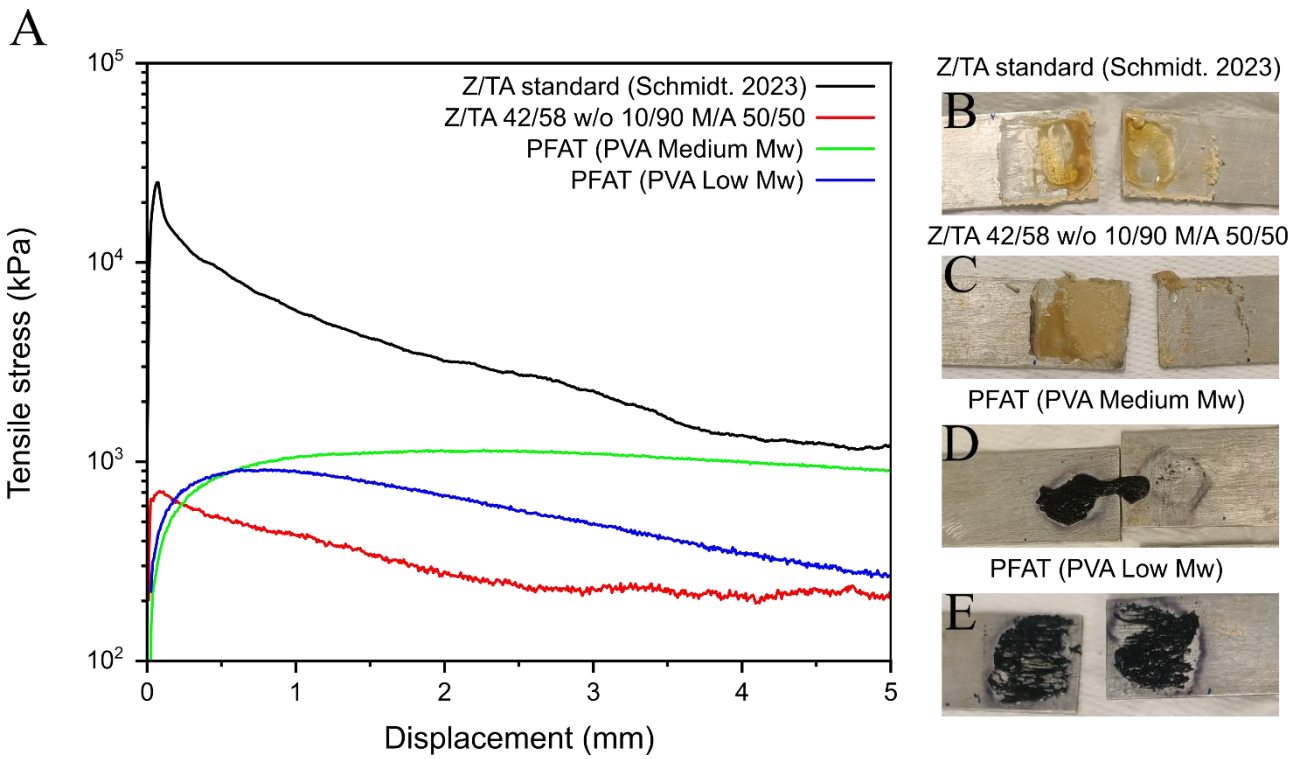

Figure 3. A, the graph represents the tensile stress of the adhesives tested and compared with the standard (G. Schmidt et al., 2023); B, Zein-Tannic acid standard adhesive stress after the shear lap; C, Zein-Tannic acid emulsion in Carnauba wax and castor oil adhesive stress after the shear lap; D, PFAT (medium Molecular weight) adhesive stress after the shear lap; E, PFAT (low Molecular weight) adhesive stress after the shear lap.

(2) Parallel development of the PFAT system, a two-component aqueous formulation of poly(vinyl alcohol)–Fe^{3+} and alginate–tannic acid, highlighted a contrasting yet complementary strategy. PFAT mixed easily at the point of use to yield a ductile, plastic precipitate that remained coherent underwater for several days and resisted hydrodynamic detachment. Its mechanical response under shear was characterized by a broad stress plateau rather than brittle failure, indicating energy-dissipative plasticity ideal for dynamic underwater environments (Figure 3A). Variations in polymer molecular weight revealed a tunable failure mode: higher-molecular-weight PVA promoted adhesive failure at the substrate interface, while low-molecular-weight chains produced cohesive internal fracture, offering a practical control over adhesion versus cohesion balance (Figure 3D, 3E).

(3) Preliminary thermal reactions between epoxidized linseed oil and polyphenolic acids opened a pressure-sensitive route, yielding tacky, crosslinked oils whose adhesion could be activated by heat rather than water chemistry. However, the reaction needs to be controlled: if fully cured, the mix of phenolics and epoxidized oils is known to form strong thermoset adhesives that can present underwater resistance but cannot be applied underwater (Figure 4B, 4D) (Nardi et al., 2024).

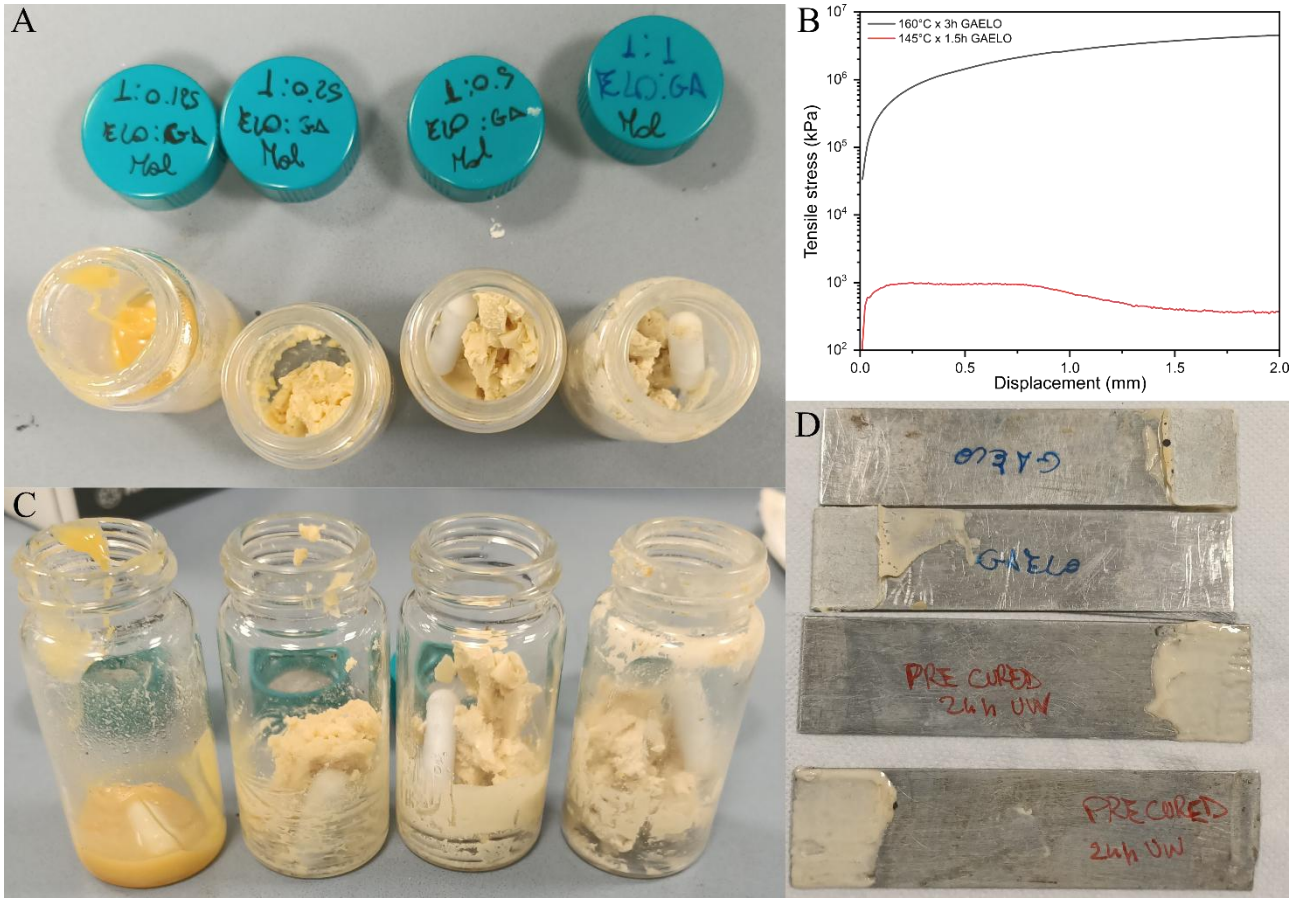

Figure 4. A,C, the production of one of the pressure-sensitive adhesives (ELOCA) is testing different ratios in equivalent mols; A, Top view, C, Lateral view of the vials; B, two different conditions of induced crosslinking show the variability in adhesivity between precured (145°C x 1.5h) and fully cured (160°C x 3h);D, the aluminum plates of the B experiment shown in B after the shear lap test: the top two plates are from the fully cured adhesive (160°C x 3h), the bottom two plates are from the precured adhesive (145°C x 1.5h).

This reaction has been proven to be proficient by a maintained adhesivity of the ELOCA composition even after 7 days of immersion in seawater. A possible theorized explanation for this behavior would be that ELO reacts with polyphenolic acids under heat (at ~140 °C), the epoxide rings of the triglyceride chains open to form ester and ether linkages with the carboxylic acid or hydroxyl groups of the phenolic compounds (Li et al., 2024). This explanation could be indirectly proven by the increased crosslinking of the PSA with the increase of phenols in the overall composition (Figure 4A, 4C), resulting in a crosslinked or grafted polyester network that retains long aliphatic chains from linseed oil, making the bulk matrix highly hydrophobic. If some of the phenolic units are not fully reacted through all hydroxyl groups, a fraction of their catechol moieties will remain chemically active but physically confined within the hydrophobic oil network. These “buried” catechols are sterically shielded from water and oxygen, reducing oxidation to quinones and limiting solubilization in aqueous environments (Hofman et al., 2018).

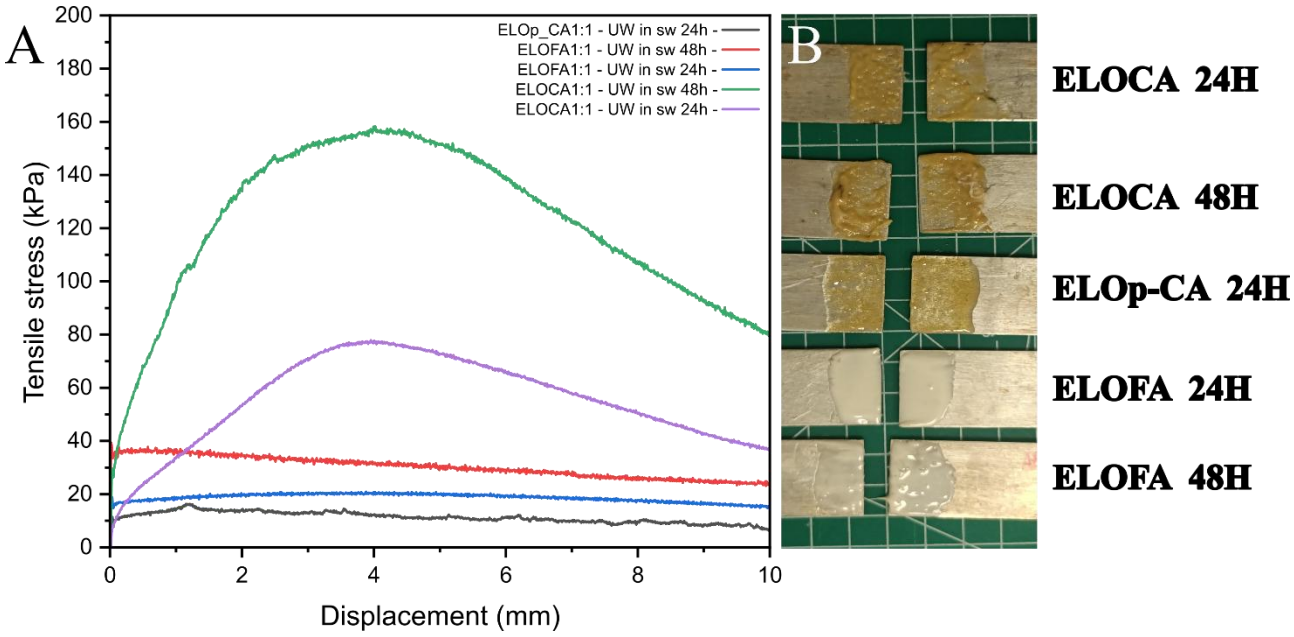

Figure. 5. A, the graph represents the tensile stress of the PSAs tested after 24/48h immersed in seawater. B, the plates of the experiment A after the shear-lap test.

A preliminary underwater adhesion screening of the PSAs produced showed that ELOGA did not maintain adhesivity after 24h of immersion, whereas ELOTA was over-crosslinked and not usable. On the other hand, ELOp-CA, ELOFA, and ELOCA maintained their adhesivity as shown in Figure 5. This could be due to the intrinsic water solubility properties of the acid used for the different compositions. Indeed, gallic acid is soluble in water, whereas the *p*-coumaric, *trans*-ferulic, and caffeic acids are hardly soluble or insoluble in water (Furia et al., 2021). In particular, it is worth noting how the PSA obtained by mixing epoxidized linseed oil and caffeic acid stands out from the other compositions in adhesivity, providing an adhesion of 3,5 kPa (Figura 5A). This level of adhesion underwater in seawater is already notable for a PSA; however, there is still margin to further optimize the fabrication procedure and hence the adhesivity of the pressure-sensitive adhesive.

Across these experiments, several unifying conclusions emerged: reactivity must be moderated rather than maximized to achieve homogeneous, usable films, and hydrophobic encapsulation or polymer entrapment of polyphenols is essential for long-term adhesion in seawater.

Future perspectives

A quantification and standardization of the adhesion performances under controlled underwater conditions and across multiple substrate types will be relevant to real-world marine environments, plus a thorough characterization of the chemical-physical reaction occurring during the adhesive production will be needed. Generally, despite qualitative tests revealing indicative key behaviors,

further quantitative data, obtained through tests such as lap shear, peel, and tack strengths, will be needed to measure essential features of the adhesives here produced.

Moreover, future research should address long-term durability and ecological safety, including leaching studies, biodegradation pathways, and interactions with the marine environment. Demonstrating that these materials remain stable over weeks or months in seawater, without releasing toxic byproducts, will be essential for regulatory acceptance and real-world deployment. The combination of renewable sourcing, tunable adhesion, and environmental compatibility positions these bio-based underwater adhesives at the intersection of green chemistry and marine technology. Continued refinement—through systematic mechanical testing, kinetic control, and field validation—can thus transform them from experimental curiosities into reliable tools for underwater repair, monitoring, and biomaterial integration in marine and biomedical systems.

Chapter 7 – Conclusions

Over the past three years, I have investigated the causes of coral diseases and developed potential solutions for their treatment. My research began with the use of broad-spectrum antibiotics and later evolved toward exploring more environmentally sustainable approaches.

In the first stage of my work, I conducted a comprehensive review of the literature on the causes and treatment methods of coral diseases. Building on this foundation, I proposed an innovative underwater drug delivery system utilizing broad-spectrum antibiotics as a potential therapeutic approach. My focus was on developing a system capable of targeting specific sites, thereby reducing the quantity of antibiotics required and minimizing environmental dispersion. This novel concept not only demonstrated the effectiveness of targeted antibiotic delivery underwater but also opened the door to broader applications beyond coral disease management. Despite the great achievement obtained with this product, several limitations were presented, such as the inconsistency of the paste (which varied based on the batch of beeswax used), the lack of adhesivity of the film and the specificity of the antibiotic loaded in the film. To address these limitations, I developed other products, each one focused on the optimization of one of these features, with the aim of perfecting the system produced. I evaluated the system's performance against different strains of *Vibrio coralliilyticus*, a highly virulent coral pathogen known for its strain-dependent variability in antibiotic resistance. Preliminary results indicated that the two-step delivery system did not significantly improve disease treatment outcomes, highlighting the limitations of antibiotic-based approaches in this context, but where the treatment demonstrated its efficacy, the coral exploited the sealant properties and, in two monitored months, managed to regrow and cover the treatment.

These findings led me to explore alternative treatments capable of overcoming both the challenges of pathogen identification and the constraints associated with antibiotic use underwater. In this regard, the application of photothermal activity emerged as a potentially transformative method for treating coral diseases directly in situ, even at the reef scale. This technology would potentially overcome the problem of pathogen identification but may face other issues, such as the scalability at the industrial level and the scattering of the light at elevated distances.

Finally, I developed a bioadhesive incorporating naturally derived phenol-based molecules, which exhibit both adhesive and antibacterial properties. This bioadhesive represents a promising tool for the treatment of bacterial coral diseases and demonstrates remarkable versatility. Its formulation, based entirely on natural materials, offers significant potential for a wide range of applications, including the attachment of sensors to mobile marine organisms and possible use in biomedical contexts. Moreover, the fully natural composition and the ease in production may favor the scalability and commercialization of this product. Among the limitations, however, it has to be considered the

necessity of a substrate and the potential colonization by other marine organisms (e.g., fouling), which may remain entrapped on the adhesive if exposed to the environment.

Overall, throughout this doctoral research, I have designed and developed several potential tools for treating coral diseases both in aquaculture settings and in the field. Each tool embodies distinct features and a high degree of adaptability, all sharing the common goal of minimizing environmental impact while enhancing treatment efficiency. Together, these advances contribute to the optimization of targeted therapeutic approaches and represent meaningful progress toward sustainable coral disease management.

Bibliography

Abu Bakar, R., Keddie, J. L., & Roth, P. J. (2024). New Chemistries for Degradable Pressure-Sensitive Adhesive Networks. *Chempluschem*, *89*(6), e202400034. https://doi.org/10.1002/cplu.202400034

Adebisi, Y. A. (2023). Balancing the risks and benefits of antibiotic use in a globalized world: the ethics of antimicrobial resistance. *Globalization and Health*, *19*(1), 27. https://doi.org/10.1186/s12992-023-00930-z

Aeby, G. S., Work, T. M., Runyon, C. M., Shore-Maggio, A., Ushijima, B., Videau, P., Beurmann, S., & Callahan, S. M. (2015). First Record of Black Band Disease in the Hawaiian Archipelago: Response, Outbreak Status, Virulence, and a Method of Treatment. *Plos One*, *10*(3), e0120853. https://doi.org/10.1371/journal.pone.0120853

Akmal, K. F., Shahbudin, S., Abdul Muhaimin, Z., Shah, M. D., & Chong, W. S. (2023). Application of Biotechnology in White Syndrome Coral Disease Identification. In M. D. Shah, J. Ransangan, & B. A. Venmathi Maran (Eds.), *Marine Biotechnology: Applications in Food, Drugs and Energy* (pp. 271-297). Springer Nature Singapore. https://doi.org/10.1007/978-981-99-0624-6_13

Alvarez-Filip, L., Estrada-Saldívar, N., Pérez-Cervantes, E., Molina-Hernández, A., & González-Barrios, F. J. (2019). A rapid spread of the stony coral tissue loss disease outbreak in the Mexican Caribbean. *PeerJ*, *7*, e8069. https://doi.org/10.7717/peerj.8069

Ambrosini, R., Corti, M., Franzetti, A., Caprioli, M., Rubolini, D., Motta, V. M., Costanzo, A., Saino, N., & Gandolfi, I. (2019). Cloacal microbiomes and ecology of individual barn swallows. *FEMS Microbiology Ecology*, *95*(6). https://doi.org/10.1093/femsec/fiz061

Andersson, D. I., & Hughes, D. (2014). Microbiological effects of sublethal levels of antibiotics. *Nat Rev Microbiol*, *12*(7), 465-478. https://doi.org/10.1038/nrmicro3270

Apprill, A. (2017). Marine Animal Microbiomes: Toward Understanding Host-Microbiome Interactions in a Changing Ocean. *Frontiers in Marine Science*, *4*. https://doi.org/10.3389/fmars.2017.00222

Apprill, A., Weber, L. G., & Santoro, A. E. (2016). Distinguishing between Microbial Habitats Unravels Ecological Complexity in Coral Microbiomes. *Msystems*, *1*(5). https://doi.org/10.1128/mSystems.00143-16

Arienzo, M., & Ferrara, L. (2022). Environmental Fate of Metal Nanoparticles in Estuarine Environments. *Water*, *14*(8). https://doi.org/10.3390/w14081297

Atad, I., Zvuloni, A., Loya, Y., & Rosenberg, E. (2012). Phage therapy of the white plague-like disease of Favia favus in the Red Sea. *Coral Reefs*, *31*(3), 665-670. https://doi.org/10.1007/s00338-012-0900-5

Badía, A., Agirre, A., Barandiaran, M. J., & Leiza, J. R. (2020). Removable Biobased Waterborne Pressure-Sensitive Adhesives Containing Mixtures of Isosorbide Methacrylate Monomers. *Biomacromolecules*, *21*(11), 4522-4531. https://doi.org/10.1021/acs.biomac.0c00474

Bajzek, T. J. (2005). Thermocouples: A sensor for measuring temperature. *Ieee Instrumentation & Measurement Magazine*, *8*(1), 35-40. https://doi.org/10.1109/Mim.2005.1405922

Barreto, M. M., Ziegler, M., Venn, A., Tambutte, E., Zoccola, D., Tambutte, S., Allemand, D., Antony, C. P., Voolstra, C. R., & Aranda, M. (2021). Effects of Ocean Acidification on Resident and Active Microbial Communities of. *Frontiers in Microbiology*, *12*. https://doi.org/10.3389/fmicb.2021.707674

Barton, J. A., Bourne, D. G., Humphrey, C., & Hutson, K. S. (2020). Parasites and coral-associated invertebrates that impact coral health. *Reviews in Aquaculture*, *12*(4), 2284-2303. https://doi.org/10.1111/raq.12434

Barton, J. A., Willis, B. L., & Hutson, K. S. (2017). Coral propagation: a review of techniques for ornamental trade and reef restoration. *Reviews in Aquaculture*, *9*(3), 238-256. https://doi.org/10.1111/raq.12135

Beeden, R., Maynard, J., Puotinen, M., Marshall, P., Dryden, J., Goldberg, J., & Williams, G. (2015). Impacts and Recovery from Severe Tropical Cyclone Yasi on the Great Barrier Reef. *Plos One*, *10*(4). https://doi.org/10.1371/journal.pone.0121272

Beloe, C. J., Browne, M. A., & Johnston, E. L. (2022). Plastic Debris As a Vector for Bacterial Disease: An Interdisciplinary Systematic Review. *Environmental Science & Technology*, *56*(5), 2950-2958. https://doi.org/10.1021/acs.est.1c05405

Ben-Haim, Y., Thompson, F. L., Thompson, C. C., Cnockaert, M. C., Hoste, B., Swings, J., & Rosenberg, E. (2003). Vibrio coralliilyticus sp. nov., a temperature-dependent pathogen of the coral Pocillopora damicornis. *International Journal of Systematic and Evolutionary Microbiology*, *53*(1), 309-315. https://doi.org/10.1099/ijs.0.02402-0

Beurmann, S., Runyon, C. M., Videau, P., Callahan, S. M., & Aeby, G. S. (2017). Assessment of disease lesion removal as a method to control chronic white syndrome. *Diseases of Aquatic Organisms*, *123*(2), 173-179. https://doi.org/10.3354/dao03088

Beurmann, S., Ushijima, B., Videau, P., Svoboda, C. M., Smith, A. M., Rivers, O. S., Aeby, G. S., & Callahan, S. M. (2017). Pseudoalteromonas piratica strain OCN003 is a coral pathogen that causes a switch from chronic to acute Montipora white syndrome in Montipora capitata. *Plos One*, *12*(11), e0188319. https://doi.org/10.1371/journal.pone.0188319

Bhattacharya, M., & Mandal, S. (2025). Antibacterial activity of caffeic acid from plant sources: A review based on in silico, in vitro and in vivo approaches. *The Microbe*, *8*, 100541. https://doi.org/10.1016/j.microb.2025.100541

Bourne, D. G., Garren, M., Work, T. M., Rosenberg, E., Smith, G. W., & Harvell, C. D. (2009). Microbial disease and the coral holobiont. *Trends in Microbiology*, *17*(12), 554-562. https://doi.org/10.1016/j.tim.2009.09.004

Brandt, M. E., Smith, T. B., Correa, A. M. S., & Vega-Thurber, R. (2013). Disturbance Driven Colony Fragmentation as a Driver of a Coral Disease Outbreak. *Plos One*, *8*(2). https://doi.org/10.1371/journal.pone.0057164

Briggs, F., Browne, D., & Asuri, P. (2022). Role of Polymer Concentration and Crosslinking Density on Release Rates of Small Molecule Drugs. *International Journal of Molecular Sciences*, *23*(8). https://doi.org/10.3390/ijms23084118

Browne, M. A., Underwood, A. J., Chapman, M. G., Williams, R., Thompson, R. C., & van Franeker, J. A. (2015). Linking effects of anthropogenic debris to ecological impacts. *Proceedings of the Royal Society B-Biological Sciences*, *282*(1807). https://doi.org/10.1098/rspb.2014.2929

Bruckner, A. (2002). *Priorities for Effective Management of Coral Diseases*. NOAA Technical Memorandum NMFS-OPR-22

Bruckner, A., & Bruckner, R. (1999). Rapid assessment of coral reef condition and short-term changes to corals affected by disease in Curacao, Netherlands Antilles. Int. Conf. Sci. Aspects Coral Reef Assessment, Monitoring and restoration Abstract,

Burke, S., Pottier, P., Lagisz, M., Macartney, E. L., Ainsworth, T., Drobniak, S. M., & Nakagawa, S. (2023). The impact of rising temperatures on the prevalence of coral diseases and its predictability: A global meta-analysis. *Ecology Letters*. https://doi.org/10.1111/ele.14266

Byers, J. E. (2021). Marine Parasites and Disease in the Era of Global Climate Change. *Ann Rev Mar Sci*, *13*, 397-420. https://doi.org/10.1146/annurev-marine-031920-100429

Cabello, F. C. (2006). Heavy use of prophylactic antibiotics in aquaculture: a growing problem for human and animal health and for the environment. *Environmental Microbiology*, *8*(7), 1137-1144. https://doi.org/10.1111/j.1462-2920.2006.01054.x

Callahan, B. J., McMurdie, P. J., Rosen, M. J., Han, A. W., Johnson, A. J. A., & Holmes, S. P. (2016). DADA2: High-resolution sample inference from Illumina amplicon data. *Nature Methods*, *13*(7), 581-583. https://doi.org/10.1038/nmeth.3869

Cervino, J. M., Thompson, F. L., Gomez-Gil, B., Lorence, E. A., Goreau, T. J., Hayes, R. L., Winiarski-Cervino, K. B., Smith, G. W., Hughen, K., & Bartels, E. (2008). The core group induces yellow band disease in Caribbean and Indo-Pacific reef-building corals. *Journal of Applied Microbiology*, *105*(5), 1658-1671. https://doi.org/10.1111/j.1365-2672.2008.03871.x

Chekli, L., Phuntsho, S., Roy, M., Lombi, E., Donner, E., & Shon, H. K. (2013). Assessing the aggregation behaviour of iron oxide nanoparticles under relevant environmental conditions using a multi-method approach. *Water Research*, *47*(13), 4585-4599. https://doi.org/10.1016/j.watres.2013.04.029

Chen, T. T. D., Carrodeguas, L. P., Sulley, G. S., Gregory, G. L., & Williams, C. K. (2020). Bio-based and Degradable Block Polyester Pressure-Sensitive Adhesives. *Angewandte Chemie International Edition*, *59*(52), 23450-23455. https://doi.org/10.1002/anie.202006807

Chen, X., Lan, W., & Xie, J. (2024). Natural phenolic compounds: Antimicrobial properties, antimicrobial mechanisms, and potential utilization in the preservation of aquatic products. *Food Chemistry*, *440*, 138198. https://doi.org/10.1016/j.foodchem.2023.138198

Cheng, B., Yu, J., Arisawa, T., Hayashi, K., Richardson, J. J., Shibuta, Y., & Ejima, H. (2022). Ultrastrong underwater adhesion on diverse substrates using non-canonical phenolic groups. *Nat Commun*, *13*(1), 1892. https://doi.org/10.1038/s41467-022-29427-w

Cohen, Y., Joseph Pollock, F., Rosenberg, E., & Bourne, D. G. (2013). Phage therapy treatment of the coral pathogen Vibrio coralliilyticus. *MicrobiologyOpen*, *2*(1), 64-74. https://doi.org/doi.org/10.1002/mbo3.52

Connelly, M. T., McRae, C. J., Liu, P. J., Martin, C. E., & Traylor-Knowles, N. (2022). Antibiotics Alter Coral-Symbiodiniaceae Bacteria Interactions and Cause Microbial Dysbiosis During Heat Stress. *Frontiers in Marine Science*, *08*. https://doi.org/10.3389/fmars.2021.814124

Connelly, M. T., Snyder, G., Palacio-Castro, A. M., Gillette, P. R., Baker, A. C., & Traylor-Knowles, N. (2023). Antibiotics reduce coral-associated bacteria diversity, decrease holobiont oxygen consumption and activate immune gene expression. *Molecular Ecology*, *32*(16), 4677-4694. https://doi.org/10.1111/mec.17049

Contardi, M., Ayyoub, A. M. M., Summa, M., Kossyvaki, D., Fadda, M., Liessi, N., Armirotti, A., Fragouli, D., Bertorelli, R., & Athanassiou, A. (2022). Self-Adhesive and Antioxidant Poly(vinylpyrrolidone)/Alginate-Based Bilayer Films Loaded with Extracts as Potential Skin Dressings. *Acs Applied Bio Materials*, *5*(6), 2880-2893. https://doi.org/10.1021/acsabm.2c00254

Contardi, M., Fadda, M., Isa, V., Louis, Y. D., Madaschi, A., Vencato, S., Montalbetti, E., Bertolacci, L., Ceseracciu, L., Seveso, D., Lavorano, S., Galli, P., Athanassiou, A., & Montano, S. (2023). Biodegradable Zein-Based Biocomposite Films for Underwater Delivery of Curcumin Reduce Thermal Stress Effects in Corals. *ACS Appl Mater Interfaces*, *15*(28), 33916-33931. https://doi.org/10.1021/acsami.3c01166

Contardi, M., Heredia-Guerrero, J. A., Guzman-Puyol, S., Summa, M., Benítez, J. J., Goldoni, L., Caputo, G., Cusimano, G., Picone, P., Di Carlo, M., Bertorelli, R., Athanassioua, A., & Bayer, I. S. (2019). Combining dietary phenolic antioxidants with polyvinylpyrrolidone: transparent biopolymer films based on p-coumaric acid for controlled release. *Journal of Materials Chemistry B*, *7*(9), 1384-1396. https://doi.org/10.1039/c8tb03017k

Contardi, M., Heredia-Guerrero, J. A., Perotto, G., Valentini, P., Pompa, P. P., Spanò, R., Goldoni, L., Bertorelli, R., Athanassiou, A., & Bayer, I. S. (2017). Transparent ciprofloxacin-povidone antibiotic films and nanofiber mats as potential skin and wound care dressings. *European Journal of Pharmaceutical Sciences*, *104*, 133-144. https://doi.org/10.1016/j.ejps.2017.03.044

Contardi, M., Montano, S., Galli, P., Mazzon, G., Ayyoub, A. M. M., Seveso, D., Saliu, F., Maggioni, D., Athanassiou, A., & Bayer, I. S. (2021). Marine Fouling Characteristics of Biocomposites in a Coral Reef Ecosystem. *Advanced Sustainable Systems*, *5*(9), 2100089. https://doi.org/10.1002/adsu.202100089

Contardi, M., Montano, S., Liguori, G., Heredia-Guerrero, J. A., Galli, P., Athanassiou, A., & Bayer, I. S. (2020). Treatment of Coral Wounds by Combining an Antiseptic Bilayer Film and an Injectable Antioxidant Biopolymer. *Scientific Reports*, *10*(1), 988. https://doi.org/10.1038/s41598-020-57980-1

Contardi, M., Russo, D., Suarato, G., Heredia-Guerrero, J. A., Ceseracciu, L., Penna, I., Margaroli, N., Summa, M., Spanò, R., Tassistro, G., Vezzulli, L., Bandiera, T., Bertorelli, R., Athanassiou, A., & Bayer, I. S. (2019). Polyvinylpyrrolidone/hyaluronic acid-based bilayer constructs for sequential delivery of cutaneous antiseptic and antibiotic. *Chemical Engineering Journal*, *358*, 912-923. https://doi.org/10.1016/j.cej.2018.10.048

Costa, P. M., Learmonth, D. A., Gomes, D. B., Cautela, M. P., Oliveira, A. C. N., Andrade, R., Espregueira-Mendes, J., Veloso, T. R., Cunha, C. B., & Sousa, R. A. (2021). Mussel-Inspired Catechol Functionalisation as a Strategy to Enhance Biomaterial Adhesion: A Systematic Review. *Polymers (Basel)*, *13*(19). https://doi.org/10.3390/polym13193317

Costanzo, A., Ambrosini, R., Franzetti, A., Romano, A., Cecere, J. G., Morganti, M., Rubolini, D., & Gandolfi, I. (2022). The cloacal microbiome of a cavity-nesting raptor, the lesser kestrel (Falco naumanni). *PeerJ*, *10*, e13927. https://doi.org/10.7717/peerj.13927

Cotas, J., Leandro, A., Monteiro, P., Pacheco, D., Figueirinha, A., Gonçalves, A. M. M., da Silva, G. J., & Pereira, L. (2020). Seaweed Phenolics: From Extraction to Applications. *Marine drugs*, *18*(8), E384. https://doi.org/10.3390/md18080384

Davis, J. R. (2004). *Tensile testing*. ASM international.

Dedman, C. J. (2022). Nano-ecotoxicology in a changing ocean. *SN Applied Sciences*, *4*(10), 264. https://doi.org/10.1007/s42452-022-05147-0

Delgadillo-Ordoñez, N., Garcias-Bonet, N., Raimundo, I., García, F. C., Villela, H., Osman, E. O., Santoro, E. P., Curdia, J., Rosado, J. G. D., Cardoso, P., Alsaggaf, A., Barno, A., Antony, C. P., Bocanegra, C., Berumen, M. L., Voolstra, C. R., Benzoni, F., Carvalho, S., & Peixoto, R. S. (2024). Probiotics reshape the coral microbiome in situ without detectable off-target effects in the surrounding environment. *Communications Biology*, *7*(1), 434. https://doi.org/10.1038/s42003-024-06135-3

Demko, A. M., Sneed, J. M., Houk, L. J., Vekich, T., & Paul, V. J. (2025). The effects of probiotics and stony coral tissue loss disease exposure on coral recruits. *Coral Reefs*, *44*(2), 411-422. https://doi.org/10.1007/s00338-024-02610-9

Denner, E. B. M., Smith, G. W., Busse, H.-J., Schumann, P., Narzt, T., Polson, S. W., Lubitz, W., & Richardson, L. L. (2003). Aurantimonas coralicida gen. nov., sp. nov., the causative agent of white plague type II on Caribbean scleractinian corals. *International Journal of Systematic and Evolutionary Microbiology*, *53*(4), 1115-1122. https://doi.org/10.1099/ijs.0.02359-0

Dheyab, M. A., Aziz, A. A., Jameel, M. S., Noqta, O. A., Khaniabadi, P. M., & Mehrdel, B. (2020). Simple rapid stabilization method through citric acid modification for magnetite nanoparticles. *Scientific Reports*, *10*(1), 10793. https://doi.org/10.1038/s41598-020-67869-8

Ding, F., Zhang, L., Chen, X., Yin, W., Ni, L., & Wang, M. (2022). Photothermal nanohybrid hydrogels for biomedical applications [Review]. *Frontiers in Bioengineering and Biotechnology*, *Volume 10 - 2022*. https://doi.org/10.3389/fbioe.2022.1066617

Donald, A. M. (2003). The use of environmental scanning electron microscopy for imaging wet and insulating materials. *Nature Materials*, *2*(8), 511-516. https://doi.org/10.1038/nmat898

Dörr, M., Barno, A. R., Villela, H., García, F. C., Garcias-Bonet, N., Voolstra, C. R., & Peixoto, R. S. (2025). Microbial-Based Therapies to Restore and Rehabilitate Disrupted Coral Health. In R. S. Peixoto & C. R. Voolstra (Eds.), *Coral Reef Microbiome* (pp. 181-195). Springer Nature Switzerland. https://doi.org/10.1007/978-3-031-76692-3_13

Espinosa, A., Di Corato, R., Kolosnjaj-Tabi, J., Flaud, P., Pellegrino, T., & Wilhelm, C. (2016). Duality of Iron Oxide Nanoparticles in Cancer Therapy: Amplification of Heating Efficiency by Magnetic Hyperthermia and Photothermal Bimodal Treatment. *ACS Nano*, *10*(2), 2436-2446. https://doi.org/10.1021/acsnano.5b07249

Estelrich, J., & Busquets, M. A. (2018). Iron Oxide Nanoparticles in Photothermal Therapy. *Molecules*, *23*(7). https://doi.org/10.3390/molecules23071567

The European Committee on Antimicrobial Susceptibility Testing - EUCAST 2025. Retrieved 2025 from https://www.eucast.org/newsiandr

Fan, H. (2023). Getting glued in the sea. *Polym J*, *55*(6), 653-664. https://doi.org/10.1038/s41428-023-00769-6

Fan, S., Yang, Q., Wang, D., Zhu, C., Wen, X., Li, X., Richel, A., Fauconnier, M.-L., Yang, W., Hou, C., & Zhang, D. (2024). Zein and tannic acid hybrid particles improving physical stability, controlled release properties, and antimicrobial activity of cinnamon essential oil loaded Pickering emulsions. *Food Chemistry*, *446*, 138512. https://doi.org/10.1016/j.foodchem.2024.138512

Farid, A. F., & Larsen, J. L. (1981). Growth of Vibrio alginolyticus: Interacting effects on pH, temperature, salt concentration, and incubation time. *Zentralblatt für Bakteriologie Mikrobiologie und Hygiene: I. Abt. Originale C: Allgemeine, angewandte und ökologische Mikrobiologie*, *2*(1), 68-75. https://doi.org/10.1016/S0721-9571(81)80019-1

Favero M, C. K. (2020). *Creation and Release Profiles of Novel Biodegradable Ointments for Lesion Based and Whole Colony Treatment Methods to be Utilized in the Response to Stony Coral Tissue Loss*

Disease (SCTLD). https://floridadep.gov/rcp/coral/documents/creation-release-profiles-ointments-treatment-methods-be-utilized-sctld-response

Feldman, A. T., & Wolfe, D. (2014). Tissue Processing and Hematoxylin and Eosin Staining. In C. E. Day (Ed.), *Histopathology: Methods and Protocols* (pp. 31-43). Springer New York. https://doi.org/10.1007/978-1-4939-1050-2_3

Forrester, G. E., Arton, L., Horton, A., & Aeby, G. (2024). The relative effectiveness of chlorine and antibiotic treatments for stony coral tissue loss disease [Brief Research Report]. *Frontiers in Marine Science*, *Volume 11 - 2024*. https://doi.org/10.3389/fmars.2024.1465173

Fox-Kemper, B., Hewitt, H. T., Xiao, C., Aðalgeirsdóttir, G., Drijfhout, S. S., Edwards, T. L., Golledge, N. R., Hemer, M., Kopp, R. E., Krinner, G., Mix, A., Notz, D., Nowicki, S., Nurhati, I. S., Ruiz, L., Sallée, J.-B., Slangen, A. B. A., & Yu, Y. (2021). Ocean, Cryosphere and Sea Level Change. In C. Intergovernmental Panel on Climate (Ed.), *Climate Change 2021 – The Physical Science Basis: Working Group I Contribution to the Sixth Assessment Report of the Intergovernmental Panel on Climate Change* (pp. 1211-1362). Cambridge University Press. https://doi.org/10.1017/9781009157896.011

Frey, S. T., Haque, A. B. M. T., Tutika, R., Krotz, E. V., Lee, C., Haverkamp, C. B., Markvicka, E. J., & Bartlett, M. D. (2022). Octopus-inspired adhesive skins for intelligent and rapidly switchable underwater adhesion [Article]. *Science Advances*, *8*(28), Article eabq1905. https://doi.org/10.1126/sciadv.abq1905

Furia, E., Beneduci, A., Malacaria, L., Fazio, A., La Torre, C., & Plastina, P. (2021). Modeling the Solubility of Phenolic Acids in Aqueous Media at 37 °C. *Molecules*, *26*(21). https://doi.org/10.3390/molecules26216500

Gabriel, V. A., & Dubé, M. A. (2023). Toward a Fully Biobased Pressure-Sensitive Adhesive. *Industrial & Engineering Chemistry Research*, *62*(1), 478-488. https://doi.org/10.1021/acs.iecr.2c03756

Gao, P., Nie, X., Zou, M. J., Shi, Y. J., & Cheng, G. (2011). Recent advances in materials for extended-release antibiotic delivery system. *Journal of Antibiotics*, *64*(9), 625-634. https://doi.org/10.1038/ja.2011.58

Garcias-Bonet, N., Villela, H., García, F. C., Duarte, G. A. S., Delgadillo-Ordoñez, N., Raimundo, I., El-Khaled, Y. C., Santoro, E. P., Bennett-Smith, M., Nieuwenhuis, B. O., Curdia, J., Zgliczynski, B., Edwards, C., Sandin, S., Osman, E. O., Sicat, R., Przybysz, A., Rosado, A. S., Jones, B. H., . . . Peixoto, R. S. (2025). The Coral Probiotics Village: An Underwater Laboratory to Tackle the Coral Reefs Crisis. *Ecology and Evolution*, *15*(7), e71558. https://doi.org/10.1002/ece3.71558

Gavilán, H., Rizzo, G. M. R., Silvestri, N., Mai, B. T., & Pellegrino, T. (2023). Scale-up approach for the preparation of magnetic ferrite nanocubes and other shapes with benchmark performance for magnetic hyperthermia applications. *Nature Protocols*, *18*(3), 783-809. https://doi.org/10.1038/s41596-022-00779-3

Gleason, F. H., Gadd, G. M., Pitt, J. I., & Larkum, A. W. D. (2017). The roles of endolithic fungi in bioerosion and disease in marine ecosystems. II. Potential facultatively parasitic anamorphic ascomycetes can cause disease in corals and molluscs. *Mycology*, *8*(3), 216-227. https://doi.org/10.1080/21501203.2017.1371802

Guardia, P., Di Corato, R., Lartigue, L., Wilhelm, C., Espinosa, A., Garcia-Hernandez, M., Gazeau, F., Manna, L., & Pellegrino, T. (2012). Water-Soluble Iron Oxide Nanocubes with High Values of Specific Absorption Rate for Cancer Cell Hyperthermia Treatment. *ACS Nano*, *6*(4), 3080-3091. https://doi.org/10.1021/nn2048137

Guardia, P., Riedinger, A., Nitti, S., Pugliese, G., Marras, S., Genovese, A., Materia, M. E., Lefevre, C., Manna, L., & Pellegrino, T. (2014). One pot synthesis of monodisperse water soluble iron oxide nanocrystals with high values of the specific absorption rate [10.1039/C4TB00061G]. *Journal of Materials Chemistry B*, *2*(28), 4426-4434. https://doi.org/10.1039/C4TB00061G

Haapkylä, J., Unsworth, R. K. F., Flavell, M., Bourne, D. G., Schaffelke, B., & Willis, B. L. (2011). Seasonal Rainfall and Runoff Promote Coral Disease on an Inshore Reef. *Plos One*, *6*(2). https://doi.org/10.1371/journal.pone.0016893

Han, X. H., Xue, Y. W., Lou, R., Ding, S. Q., & Wang, S. R. (2023). Facile and efficient chitosan-based hygroscopic aerogel for air dehumidification. *International Journal of Biological Macromolecules*, *251*. https://doi.org/10.1016/j.ijbiomac.2023.126191

Harvell, D., Altizer, S., Cattadori, I. M., Harrington, L., & Weil, E. (2009). Climate change and wildlife diseases: When does the host matter the most? *Ecology*, *90*(4), 912-920. https://doi.org/10.1890/08-0616.1

Hawthorn, A., Berzins, I. K., Dennis, M. M., Kiupel, M., Newton, A. L., Peters, E. C., Reyes, V. A., & Work, T. M. (2023). An introduction to lesions and histology of scleractinian corals. *Veterinary Pathology*, *60*(5), 529-546. https://doi.org/10.1177/03009858231189289

Heron, S. F., Willis, B. L., Skirving, W. J., Eakin, C. M., Page, C. A., & Miller, I. R. (2010). Summer Hot Snaps and Winter Conditions: Modelling White Syndrome Outbreaks on Great Barrier Reef Corals. *Plos One*, *5*(8). https://doi.org/10.1371/journal.pone.0012210

Hofman, A. H., van Hees, I. A., Yang, J., & Kamperman, M. (2018). Bioinspired Underwater Adhesives by Using the Supramolecular Toolbox. *Adv Mater*, *30*(19), e1704640. https://doi.org/10.1002/adma.201704640

Howells, E. J., Abrego, D., Meyer, E., Kirk, N. L., & Burt, J. A. (2016). Host adaptation and unexpected symbiont partners enable reef-building corals to tolerate extreme temperatures. *Global Change Biology*, *22*(8), 2702-2714. https://doi.org/doi.org/10.1111/gcb.13250

Hu, O., Lu, M., Cai, M., Liu, J., Qiu, X., Guo, C. F., Zhang, C. Y., & Qian, Y. (2024). Mussel-Bioinspired Lignin Adhesive for Wearable Bioelectrodes. *Advanced Materials*, *36*(38), 2407129. https://doi.org/10.1002/adma.202407129

Hudson, J. (2000). First aid for massive corals infected with black band disease, Phormidium corallyticum: An underwater aspirator and post-treatment sealant to curtail reinfection.

Huggett, M. J., & Apprill, A. (2019). Coral microbiome database: Integration of sequences reveals high diversity and relatedness of coral-associated microbes. *Environ Microbiol Rep*, *11*(3), 372-385. https://doi.org/10.1111/1758-2229.12686

Hughes, T. P., Baird, A. H., Morrison, T. H., & Torda, G. (2023). Principles for coral reef restoration in the anthropocene. *One Earth*, *6*(6), 656-665. https://doi.org/10.1016/j.oneear.2023.04.008

Inkson, B. J. (2016). 2 - Scanning electron microscopy (SEM) and transmission electron microscopy (TEM) for materials characterization. In G. Hübschen, I. Altpeter, R. Tschuncky, & H.-G. Herrmann (Eds.), *Materials Characterization Using Nondestructive Evaluation (NDE) Methods* (pp. 17-43). Woodhead Publishing. https://doi.org/10.1016/B978-0-08-100040-3.00002-X

Israelachvili, J. N. (2011). 17 - Adhesion and Wetting Phenomena. In J. N. Israelachvili (Ed.), *Intermolecular and Surface Forces (Third Edition)* (pp. 415-467). Academic Press. https://doi.org/10.1016/B978-0-12-375182-9.10017-X

Jeong, H., Hong, S.-J., Yuk, J. S., Lee, H., Koo, H., Park, S. H., & Shin, J. (2023). Renewable and Degradable Triblock Copolymers Produced via Metal-Free Polymerizations: From Low Sticky Pressure-Sensitive Adhesive to Soft Superelastomer. *ACS Sustainable Chemistry & Engineering*, *11*(12), 4871-4884. https://doi.org/10.1021/acssuschemeng.3c00312

Kadeřábková, N., Mahmood, A. J. S., & Mavridou, D. A. I. (2024). Antibiotic susceptibility testing using minimum inhibitory concentration (MIC) assays. *npj Antimicrobials and Resistance*, *2*(1), 37. https://doi.org/10.1038/s44259-024-00051-6

Kalhapure, R. S., Suleman, N., Mocktar, C., Seedat, N., & Govender, T. (2015). Nanoengineered Drug Delivery Systems for Enhancing Antibiotic Therapy. *Journal of Pharmaceutical Sciences*, *104*(3), 872-905. https://doi.org/10.1002/jps.24298

Kehlet-Delgado, H., Häse, C. C., & Mueller, R. S. (2020). Comparative genomic analysis of Vibrios yields insights into genes associated with virulence towards C. gigas larvae. *BMC Genomics*, *21*(1), 599. https://doi.org/10.1186/s12864-020-06980-6

Kellogg, C. A., Piceno, Y. M., Tom, L. M., DeSantis, T. Z., Gray, M. A., Zawada, D. G., & Andersen, G. L. (2013). Comparing Bacterial Community Composition between Healthy and White Plague-Like Disease States in Orbicella annularis Using PhyloChip™ G3 Microarrays. *Plos One*, *8*(11), e79801. https://doi.org/10.1371/journal.pone.0079801

Kerrison, P. D., Stanley, M. S., & Hughes, A. D. (2018). Textile substrate seeding of Saccharina latissima sporophytes using a binder: An effective method for the aquaculture of kelp. *Algal Research*, *33*, 352-357. https://doi.org/10.1016/j.algal.2018.06.005

Khodzori, F. A., Roger, N. A. A., Nor'ashikin, A. Z., Azseri, A., Misi, L. L., Mazni, M. A., Hisham, H. K., Shah, M. D., & Chong, W. S. (2024). Coral Aquaculture: A Review of In Situ and Ex Situ Culture Systems, Conditions, Applications, and Challenges. In *Essentials of Aquaculture Practices* (pp. 239-265). https://doi.org/10.1007/978-981-97-6699-4_12

Khosravi, Z., Kharaziha, M., Goli, R., & Karimzadeh, F. (2024). Antibacterial adhesive based on oxidized tannic acid-chitosan for rapid hemostasis. *Carbohydrate Polymers*, *333*, 121973. https://doi.org/10.1016/j.carbpol.2024.121973

Kimes, N. E., Grim, C. J., Johnson, W. R., Hasan, N. A., Tall, B. D., Kothary, M. H., Kiss, H., Munk, A. C., Tapia, R., Green, L., Detter, C., Bruce, D. C., Brettin, T. S., Colwell, R. R., & Morris, P. J. (2012). Temperature regulation of virulence factors in the pathogen Vibrio coralliilyticus. *The ISME Journal*, *6*(4), 835-846. https://doi.org/10.1038/ismej.2011.154

Kolle, S., Ahanotu, O., Meeks, A., Stafslien, S., Kreder, M., Vanderwal, L., Cohen, L., Waltz, G., Lim, C. S., Slocum, D., Greene, E. M., Hunsucker, K., Swain, G., Wendt, D., Teo, S. L. M., & Aizenberg, J. (2022). On the mechanism of marine fouling-prevention performance of oil-containing silicone elastomers. *Scientific Reports*, *12*(1). https://doi.org/10.1038/s41598-022-15553-4

Kuo, M. Y. J., Murai, S., Kawahara, R., Nobuhara, S., & Nishino, K. (2022). Surface Normals and Shape From Water. *IEEE Transactions on Pattern Analysis and Machine Intelligence*, *44*(12), 9150-9162. https://doi.org/10.1109/TPAMI.2021.3121963

Lamb, J. B., True, J. D., Piromvaragorn, S., & Willis, B. L. (2014). Scuba diving damage and intensity of tourist activities increases coral disease prevalence. *Biological Conservation*, *178*, 88-96. https://doi.org/10.1016/j.biocon.2014.06.027

Lamb, J. B., Wenger, A. S., Devlin, M. J., Ceccarelli, D. M., Williamson, D. H., & Willis, B. L. (2016). Reserves as tools for alleviating impacts of marine disease. *Philosophical Transactions of the Royal Society B-Biological Sciences*, *371*(1689). https://doi.org/10.1098/rstb.2015.0210

Lamb, J. B., Williamson, D. H., Russ, G. R., & Willis, B. L. (2015). Protected areas mitigate diseases of reef-building corals by reducing damage from fishing. *Ecology*, *96*(9), 2555-2567. https://doi.org/10.1890/14-1952.1

Lartigue, L., Alloyeau, D., Kolosnjaj-Tabi, J., Javed, Y., Guardia, P., Riedinger, A., Péchoux, C., Pellegrino, T., Wilhelm, C., & Gazeau, F. (2013). Biodegradation of Iron Oxide Nanocubes: High-Resolution In Situ Monitoring. *ACS Nano*, *7*(5), 3939-3952. https://doi.org/10.1021/nn305719y

Lee, C., Shi, H., Jung, J., Zheng, B., Wang, K., Tutika, R., Long, R., Lee, B. P., Gu, G. X., & Bartlett, M. D. (2023). Bioinspired materials for underwater adhesion with pathways to switchability. *Cell Reports Physical Science*, *4*(10). https://doi.org/10.1016/j.xcrp.2023.101597

Lee, D., Hwang, H., Kim, J.-S., Park, J., Youn, D., Kim, D., Hahn, J., Seo, M., & Lee, H. (2020). VATA: A Poly(vinyl alcohol)- and Tannic Acid-Based Nontoxic Underwater Adhesive. *ACS Applied Materials & Interfaces*, *12*(18), 20933-20941. https://doi.org/10.1021/acsami.0c02037

Lee, J. N., Lee, S. Y., & Park, W. H. (2021). Bioinspired Self-Healable Polyallylamine-Based Hydrogels for Wet Adhesion: Synergistic Contributions of Catechol-Amino Functionalities and Nanosilicate. *ACS Applied Materials & Interfaces*, *13*(15), 18324-18337. https://doi.org/10.1021/acsami.1c02141

Lee, S.-J., Back, J.-H., Kim, J.-S., Yi, M.-B., Han, G.-Y., Kim, Y. D., & Kim, H.-J. (2023). Surface-patterned gallol pressure-sensitive adhesives for strong underwater adhesion. *Materials & Design*, *236*, 112505. https://doi.org/10.1016/j.matdes.2023.112505

Lehner, F. K. (1979). On the validity of Fick's law for transient diffusion through a porous medium. *Chemical Engineering Science*, *34*(6), 821-825. https://doi.org/10.1016/0009-2509(79)85137-4

Lei, Y.-F., Wang, X.-L., Liu, B.-W., Ding, X.-M., Chen, L., & Wang, Y.-Z. (2020). Fully Bio-Based Pressure-Sensitive Adhesives with High Adhesivity Derived from Epoxidized Soybean Oil and Rosin Acid. *ACS Sustainable Chemistry & Engineering*, *8*(35), 13261-13270. https://doi.org/10.1021/acssuschemeng.0c03451

Lesser, M. P., & Jarett, J. K. (2014). Culture-dependent and culture-independent analyses reveal no prokaryotic community shifts or recovery of Serratia marcescens in Acropora palmata with white pox disease. *FEMS Microbiology Ecology*, *88*(3), 457-467. https://doi.org/10.1111/1574-6941.12311

Li, J., Kuang, Y., Li, W., Xu, P., Peng, D., Zhou, P., & Bi, Y. (2024). Preparation and structural characterization of epoxidized soybean oils-based pressure sensitive adhesive grafted with tea polyphenol

palmitate. *International Journal of Biological Macromolecules*, *263*, 130153. https://doi.org/10.1016/j.ijbiomac.2024.130153

Li, S., Ma, C., Hou, B., & Liu, H. (2022). Rational design of adhesives for effective underwater bonding [Mini Review]. *Frontiers in Chemistry*, *Volume 10 - 2022*. https://doi.org/10.3389/fchem.2022.1007212

Li, X., Xie, H., Lin, J., Xie, W., & Ma, X. (2009). Characterization and biodegradation of chitosan–alginate polyelectrolyte complexes. *Polymer Degradation and Stability*, *94*(1), 1-6. https://doi.org/10.1016/j.polymdegradstab.2008.10.017

Liang, F., Sun, C., Li, S., Hou, T., & Li, C. (2021). Therapeutic effect and immune mechanism of chitosan-gentamicin conjugate on Pacific white shrimp (Litopenaeus vannamei) infected with Vibrio parahaemolyticus. *Carbohydrate Polymers*, *269*, 118334. https://doi.org/10.1016/j.carbpol.2021.118334

Lin, H., Yu, M., Wang, X., & Zhang, X.-H. (2018). Comparative genomic analysis reveals the evolution and environmental adaptation strategies of vibrios. *BMC Genomics*, *19*(1), 135. https://doi.org/10.1186/s12864-018-4531-2

Liu, H., Xing, F., Zhou, Y., Yu, P., Xu, J., Luo, R., Xiang, Z., Maria Rommens, P., Liu, M., & Ritz, U. (2023). Nanomaterials-based photothermal therapies for antibacterial applications. *Materials & Design*, *233*, 112231. https://doi.org/10.1016/j.matdes.2023.112231

Liu, J., Singh, P., Wong, T. H., & Lin, S. (2025). Pressure-sensitive in-situ underwater adhesives. *Communications Physics*, *8*(1), 6. https://doi.org/10.1038/s42005-024-01921-1

Liu, Y., Shi, L. Q., Su, L. Z., van der Mei, H. C., Jutte, P. C., Ren, Y. J., & Busscher, H. J. (2019). Nanotechnology-based antimicrobials and delivery systems for biofilm-infection control. *Chemical Society Reviews*, *48*(2), 428-446. https://doi.org/10.1039/c7cs00807d

Liu, Y. W., Wu, H., Shu, Y., Hua, Y. Y., & Fu, P. C. (2024). Symbiodiniaceae and Ruegeria sp. Co-Cultivation to Enhance Nutrient Exchanges in Coral Holobiont. *Microorganisms*, *12*(6). https://doi.org/10.3390/microorganisms12061217

Luna, G. M., Biavasco, F., & Danovaro, R. (2007). Bacteria associated with the rapid tissue necrosis of stony corals. *Environ Microbiol*, *9*(7), 1851-1857. https://doi.org/10.1111/j.1462-2920.2007.01287.x

Luna, G. M., Bongiorni, L., Gili, C., Biavasco, F., & Danovaro, R. (2010). Vibrio harveyi as a causative agent of the White Syndrome in tropical stony corals. *Environmental Microbiology Reports*, *2*(1), 120-127. https://doi.org/10.1111/j.1758-2229.2009.00114.x

Lupo, A., Coyne, S., & Berendonk, T. U. (2012). Origin and Evolution of Antibiotic Resistance: The Common Mechanisms of Emergence and Spread in Water Bodies [Review]. *Frontiers in Microbiology*, *3*. https://doi.org/10.3389/fmicb.2012.00018

MacVittie, S., Doroodian, S., Alberto, A., & Sogin, M. (2024). Microbiome depletion and recovery in the sea anemone, following antibiotic exposure. *Msystems*, *9*(6). https://doi.org/10.1128/msystems.01342-23

Mai, B. T., Balakrishnan, P. B., Barthel, M. J., Piccardi, F., Niculaes, D., Marinaro, F., Fernandes, S., Curcio, A., Kakwere, H., Autret, G., Cingolani, R., Gazeau, F., & Pellegrino, T. (2019). Thermoresponsive Iron Oxide Nanocubes for an Effective Clinical Translation of Magnetic Hyperthermia and Heat-Mediated Chemotherapy. *ACS Applied Materials & Interfaces*, *11*(6), 5727-5739. https://doi.org/10.1021/acsami.8b16226

Maier, G. P., Rapp, M. V., Waite, J. H., Israelachvili, J. N., & Butler, A. (2015). Adaptive synergy between catechol and lysine promotes wet adhesion by surface salt displacement. *Science*, *349*(6248), 628-632. https://doi.org/10.1126/science.aab0556

Mass, S., Cohen, H., Podicheti, R., Rusch, D. B., Gerlic, M., Ushijima, B., van Kessel, J. C., Bosis, E., & Salomon, D. (2024). The coral pathogen Vibrio coralliilyticus uses a T6SS to secrete a group of novel anti-eukaryotic effectors that contribute to virulence. *PLOS Biology*, *22*(9), e3002734. https://doi.org/10.1371/journal.pbio.3002734

Maynard, J., van Hooidonk, R., Eakin, C. M., Puotinen, M., Garren, M., Williams, G., Heron, S. F., Lamb, J., Weil, E., Willis, B., & Harvell, C. D. (2015). Projections of climate conditions that increase coral disease susceptibility and pathogen abundance and virulence. *Nature Climate Change*, *5*(7), 688-+. https://doi.org/10.1038/nclimate2625

Maynard, J. A., Anthony, K. R. N., Harvell, C. D., Burgman, M. A., Beeden, R., Sweatman, H., Heron, S. F., Lamb, J. B., & Willis, B. L. (2011). Predicting outbreaks of a climate-driven coral disease in the Great Barrier Reef. *Coral Reefs*, *30*(2), 485-495. https://doi.org/10.1007/s00338-010-0708-0

Meksériwattana, W., Silvestri, N., Brescia, R., Tiryaki, E., Barman, J., Mohammadzadeh, F. G., Jarmouni, N., & Pellegrino, T. (2025). Shape-Control in Microwave-Assisted Synthesis: A Fast Route to Size-Tunable Iron Oxide Nanocubes with Benchmark Magnetic Heat Losses. *Advanced Functional Materials*, *35*(3), 2413514. https://doi.org/10.1002/adfm.202413514

Mera, H., & Bourne, D. G. (2018). Disentangling causation: complex roles of coral-associated microorganisms in disease. *Environmental Microbiology*, *20*(2), 431-449. https://doi.org/10.1111/1462-2920.13958

Meyer, J. L., Gunasekera, S. P., Scott, R. M., Paul, V. J., & Teplitski, M. (2015). Microbiome shifts and the inhibition of quorum sensing by Black Band Disease cyanobacteria. *The ISME Journal*, *10*(5), 1204-1216. https://doi.org/10.1038/ismej.2015.184

Meyer, J. L., Paul, V. J., Raymundo, L. J., & Teplitski, M. (2017). Comparative Metagenomics of the Polymicrobial Black Band Disease of Corals [Original Research]. *Frontiers in Microbiology*, *Volume 8 - 2017*. https://doi.org/10.3389/fmicb.2017.00618

Meyer, J. L., Sweet, M. J., & Ushijima, B. (2025). When Microbial Interactions Go Wrong: Coral Bleaching, Disease, and Dysbiosis. In R. S. Peixoto & C. R. Voolstra (Eds.), *Coral Reef Microbiome* (pp. 169-180). Springer Nature Switzerland. https://doi.org/10.1007/978-3-031-76692-3_12

Mikelashvili, V., Kekutia, S., Markhulia, J., Saneblidze, L., Maisuradze, N., Kriechbaum, M., & Almásy, L. (2023). Synthesis and Characterization of Citric Acid-Modified Iron Oxide Nanoparticles Prepared with Electrohydraulic Discharge Treatment. *Materials*, *16*(2). https://doi.org/10.3390/ma16020746

Miller, A. W., & Richardson, L. L. (2011). A meta-analysis of 16S rRNA gene clone libraries from the polymicrobial black band disease of corals. *FEMS Microbiology Ecology*, *75*(2), 231-241. https://doi.org/10.1111/j.1574-6941.2010.00991.x

Miller, A. W., & Richardson, L. L. (2015). Emerging coral diseases: a temperature-driven process? *Marine Ecology-an Evolutionary Perspective*, *36*(3), 278-291. https://doi.org/10.1111/maec.12142

Moriarty, T., Leggat, W., Huggett, M. J., & Ainsworth, T. D. (2020). Coral Disease Causes, Consequences, and Risk within Coral Restoration. *Trends in Microbiology*, *28*(10), 793-807. https://doi.org/10.1016/j.tim.2020.06.002

Muller, E. M., Bartels, E., & Baums, I. B. (2018). Bleaching causes loss of disease resistance within the threatened coral species. *Elife*, *7*. https://doi.org/10.7554/eLife.35066

Muller, E. M., & van Woesik, R. (2012). Caribbean coral diseases: primary transmission or secondary infection? *Global Change Biology*, *18*(12), 3529-3535. https://doi.org/10.1111/gcb.12019

Muller, E. M., & van Woesik, R. (2014). Genetic Susceptibility, Colony Size, and Water Temperature Drive White-Pox Disease on the Coral. *Plos One*, *9*(11). https://doi.org/10.1371/journal.pone.0110759

Munn, C. B. (2015). The Role of Vibrios in Diseases of Corals. *Microbiol Spectr*, *3*(4). https://doi.org/10.1128/microbiolspec.VE-0006-2014

Murgia, D., Angellotti, G., Conigliaro, A., Carfi Pavia, F., D'Agostino, F., Contardi, M., Mauceri, R., Alessandro, R., Campisi, G., & De Caro, V. (2020). Development of a Multifunctional Bioerodible Nanocomposite Containing Metronidazole and Curcumin to Apply on L-PRF Clot to Promote Tissue Regeneration in Dentistry. *Biomedicines*, *8*(10). https://doi.org/10.3390/biomedicines8100425

Mydlarz, L. D., Couch, C. S., Weil, E., Smith, G., & Harvell, C. D. (2009). Immune defenses of healthy, bleached and diseased during a natural bleaching event. *Diseases of Aquatic Organisms*, *87*(1-2), 67-78. https://doi.org/10.3354/dao02088

Nancy Knowlton, & Forest Rohwer. (2003). Multispecies Microbial Mutualisms on Coral Reefs: The Host as a Habitat. *The American Naturalist*, *162*(S4), S51-S62. https://doi.org/10.1086/378684

Nardi, M., Ceseracciu, L., Scribano, V., Contardi, M., Athanassiou, A., & Zych, A. (2024). Sustainable adhesives: Exploring boronic ester vitrimers containing lignin microparticles. *Chemical Engineering Journal*, *495*, 153400. https://doi.org/10.1016/j.cej.2024.153400

Neely, K., & Hower, E. (2019). *FY 2018 In Situ Disease Intervention*. Retrieved from https://floridadep.gov/rcp/coral/documents/fy-2018-situ-disease-intervention

Neely, K. L., Macaulay, K. A., Hower, E. K., & Dobler, M. A. (2020). Effectiveness of topical antibiotics in treating corals affected by Stony Coral Tissue Loss Disease. *PeerJ*, *8*, e9289. https://doi.org/10.7717/peerj.9289

Neely, K. L., Nowicki, R. J., Dobler, M. A., Chaparro, A. A., Miller, S. M., & Toth, K. A. (2024). Too hot to handle? The impact of the 2023 marine heatwave on Florida Keys coral. *Frontiers in Marine Science*, *Volume 11 - 2024*. https://doi.org/10.3389/fmars.2024.1489273

Neely, K. L., Shea, C. P., Macaulay, K. A., Hower, E. K., & Dobler, M. A. (2021). Short- and Long-Term Effectiveness of Coral Disease Treatments. *Frontiers in Marine Science*, *8*. https://doi.org/10.3389/fmars.2021.675349

Olio di semi di Girasole Coop. https://www.coop.it/il-prodotto-coop/coop/olio-e-aceto/alimentari-confezionati/olio-di-semi/olio-di-semi-di-girasole-1-l

Pantos, O., Cooney, R. P., Le Tissier, M. D. A., Barer, M. R., O'Donnell, A. G., & Bythell, J. C. (2003). The bacterial ecology of a plague-like disease affecting the Caribbean coral Montastrea annularis. *Environmental Microbiology*, *5*(5), 370-382. https://doi.org/10.1046/j.1462-2920.2003.00427.x

Papke, E., Carreiro, A., Dennison, C., Deutsch, J. M., Isma, L. M., Meiling, S. S., Rossin, A. M., Baker, A. C., Brandt, M. E., Garg, N., Holstein, D. M., Traylor-Knowles, N., Voss, J. D., & Ushijima, B. (2024). Stony coral tissue loss disease: a review of emergence, impacts, etiology, diagnostics, and intervention [Review]. *Frontiers in Marine Science*, *10*. https://doi.org/10.3389/fmars.2023.1321271

Park, Y.-J., Joo, H.-S., Do, H.-S., & Kim, H.-J. (2006). Viscoelastic and adhesion properties of EVA/tackifier/wax ternary blend systems as hot-melt adhesives. *Journal of Adhesion Science and Technology*, *20*(14), 1561-1571. https://doi.org/10.1163/156856106778884244

Paul, A., Laurila, T., Vuorinen, V., Divinski, S. V., Paul, A., Laurila, T., Vuorinen, V., & Divinski, S. V. (2014). Fick's laws of diffusion. *Thermodynamics, diffusion and the kirkendall effect in solids*, 115-139.

Paul, R., Singh, M., V J, V., Manik, G., & Sahoo, S. K. (2023). Bio-based Pressure Sensitive Adhesives Derived from Cardanol, Vanillin, and Sebacic Acid for Removable Nonstructural Applications. *Industrial & Engineering Chemistry Research*, *62*(1), 423-434. https://doi.org/10.1021/acs.iecr.2c03601

Pearson-Lund, A. S., Williams, S. D., Eaton, K. R., Clark, A. S., Holloway, N. H., Ewen, K. A., & Muller, E. M. (2025). Evaluating the effect of amoxicillin treatment on the microbiome of <i>Orbicella faveolata<i> with Caribbean yellow band disease. *Applied and Environmental Microbiology*, *91*(7), e02407-02424. https://doi.org/10.1128/aem.02407-24

Peixoto, R. S., Rosado, P. M., Leite, D. C. d. A., Rosado, A. S., & Bourne, D. G. (2017). Beneficial Microorganisms for Corals (BMC): Proposed Mechanisms for Coral Health and Resilience [Review]. *Frontiers in Microbiology*, *Volume 8 - 2017*. https://doi.org/10.3389/fmicb.2017.00341

Pinzón, J. H., Kamel, B., Burge, C. A., Harvell, C. D., Medina, M., Weil, E., & Mydlarz, L. D. (2015). Whole transcriptome analysis reveals changes in expression of immune-related genes during and after bleaching in a reef-building coral. *Royal Society Open Science*, *2*(4). https://doi.org/10.1098/rsos.140214

Pitts, K. A., Scheuermann, M., Lefcheck, J. S., Ushijima, B., Danek, N., McDonald, E. M., Milanese, A. R., Schul, M. D., Meyer, J. L., Toth, K. A., Ferris, Z., De La Flor, Y. T., DeMarco, T., Noren, H. K. G., Walker, B. K., & Paul, V. J. (2025). Evaluating the effectiveness of field-based probiotic treatments for stony coral tissue loss disease in southeast Florida, USA [Original Research]. *Frontiers in Marine Science*, *Volume 12 - 2025*. https://doi.org/10.3389/fmars.2025.1480966

Pohl, T., Al-Muqdadi, S. W., Ali, M. H., Fawzi, N. A.-M., Ehrlich, H., & Merkel, B. (2014). Discovery of a living coral reef in the coastal waters of Iraq. *Scientific Reports*, *4*(1), 4250. https://doi.org/10.1038/srep04250

Pollock, F. J., Lamb, J. B., van de Water, J. A. J. M., Smith, H. A., Schaffelke, B., Willis, B. L., & Bourne, D. G. (2019). Reduced diversity and stability of coral-associated bacterial communities and suppressed immune function precedes disease onset in corals. *Royal Society Open Science*, *6*(6). https://doi.org/10.1098/rsos.190355

Pollock, F. J., McMinds, R., Smith, S., Bourne, D. G., Willis, B. L., Medina, M., Thurber, R. V., & Zaneveld, J. R. (2018). Coral-associated bacteria demonstrate phylosymbiosis and cophylogeny. *Nat Commun*, *9*(1), 4921. https://doi.org/10.1038/s41467-018-07275-x

Prada, F., Caroselli, E., Mengoli, S., Brizi, L., Fantazzini, P., Capaccioni, B., Pasquini, L., Fabricius, K. E., Dubinsky, Z., Falini, G., & Goffredo, S. (2017). Ocean warming and acidification synergistically increase coral mortality. *Scientific Reports*, *7*. https://doi.org/10.1038/srep40842

Precht, W. F., Gintert, B. E., Robbart, M. L., Fura, R., & van Woesik, R. (2016). Unprecedented Disease-Related Coral Mortality in Southeastern Florida. *Scientific Reports*, *6*(1), 31374. https://doi.org/10.1038/srep31374

Qie, R., Zajforoushan Moghaddam, S., & Thormann, E. (2024). Fully Biobased Adhesive from Chitosan and Tannic Acid with High Water Resistance. *ACS Sustainable Chemistry & Engineering*, *12*(11), 4456-4463. https://doi.org/10.1021/acssuschemeng.3c07306

Răcuciu, M., Creangă, D. E., & Airinei, A. (2006). Citric-acid-coated magnetite nanoparticles for biological applications. *The European Physical Journal E*, *21*(2), 117-121. https://doi.org/10.1140/epje/i2006-10051-y

Raymann, K., Bobay, L.-M., Doak, T. G., Lynch, M., & Gribaldo, S. (2013). A genomic survey of Reb homologs suggests widespread occurrence of R-bodies in proteobacteria. *G3: Genes, Genomes, Genetics*, *3*(3), 505-516. https://doi.org/10.1534/g3.112.005231

Redding, J. E., Myers-Miller, R. L., Baker, D. M., Fogel, M., Raymundo, L. J., & Kim, K. (2013). Link between sewage-derived nitrogen pollution and coral disease severity in Guam. *Marine Pollution Bulletin*, *73*(1), 57-63. https://doi.org/10.1016/j.marpolbul.2013.06.002

Reimer, J. D., Peixoto, R. S., Davies, S. W., Traylor-Knowles, N., Short, M. L., Cabral-Tena, R. A., Burt, J. A., Pessoa, I., Banaszak, A. T., Winters, R. S., Moore, T., Schoepf, V., Kaullysing, D., Calderon-Aguilera, L. E., Wörheide, G., Harding, S., Munbodhe, V., Mayfield, A., Ainsworth, T., . . . Voolstra, C. R. (2024). The Fourth Global Coral Bleaching Event: Where do we go from here? *Coral Reefs*, *43*(4), 1121-1125. https://doi.org/10.1007/s00338-024-02504-w

Reshef, L., Koren, O., Loya, Y., Zilber-Rosenberg, I., & Rosenberg, E. (2006). The Coral Probiotic Hypothesis. *Environmental Microbiology*, *8*(12), 2068-2073. https://doi.org/10.1111/j.1462-2920.2006.01148.x

Rice, M. M., Ezzat, L., & Burkepile, D. E. (2019). Corallivory in the Anthropocene: Interactive Effects of Anthropogenic Stressors and Corallivory on Coral Reefs. *Frontiers in Marine Science*, *5*. https://doi.org/10.3389/fmars.2018.00525

Rice, M. M., Maher, R. L., Thurber, R. V., & Burkepile, D. E. (2019). Different nitrogen sources speed recovery from corallivory and uniquely alter the microbiome of a reef-building coral. *PeerJ*, *7*. https://doi.org/10.7717/peerj.8056

Ridlon, A. D., Grosholz, E. D., Hancock, B., Miller, M. W., Bickel, A., Froehlich, H. E., Lirman, D., Pollock, F. J., Putnam, H. M., Tlusty, M. F., Waters, T. J., & Wasson, K. (2023). Culturing for conservation: the need for timely investments in reef aquaculture. *Frontiers in Marine Science*, *10*. https://doi.org/10.3389/fmars.2023.1069494

Ritger, P. L., & Peppas, N. A. (1987a). A simple equation for description of solute release I. Fickian and non-fickian release from non-swellable devices in the form of slabs, spheres, cylinders or discs. *Journal of Controlled Release*, *5*(1), 23-36. https://doi.org/10.1016/0168-3659(87)90034-4

Ritger, P. L., & Peppas, N. A. (1987b). A simple equation for description of solute release II. Fickian and anomalous release from swellable devices. *Journal of Controlled Release*, *5*(1), 37-42. https://doi.org/10.1016/0168-3659(87)90035-6

Roberts, J. A., Kruger, P., Paterson, D. L., & Lipman, J. (2008). Antibiotic resistance—What's dosing got to do with it? *Critical Care Medicine*, *36*(8). https://doi.org/10.1097/CCM.0b013e318180fe62

Roik, A., Reverter, M., & Pogoreutz, C. (2022). A roadmap to understanding diversity and function of coral reef-associated fungi. *Fems Microbiology Reviews*, *46*(6). https://doi.org/10.1093/femsre/fuac028

Rosado, P. M., Leite, D. C. A., Duarte, G. A. S., Chaloub, R. M., Jospin, G., Nunes da Rocha, U., Saraiva, J. P., Dini-Andreote, F., Eisen, J. A., Bourne, D. G., & Peixoto, R. S. (2019). Marine probiotics: increasing coral resistance to bleaching through microbiome manipulation. *The ISME Journal*, *13*(4), 921-936. https://doi.org/10.1038/s41396-018-0323-6

Rosales, S. M., Miller, M. W., Williams, D. E., Traylor-Knowles, N., Young, B., & Serrano, X. M. (2019). Microbiome differences in disease-resistant vs. susceptible corals subjected to disease challenge assays. *Scientific Reports*, *9*. https://doi.org/10.1038/s41598-019-54855-y

Rubio-Portillo, E., Martin-Cuadrado Ana, B., Caraballo-Rodríguez Andrés, M., Rohwer, F., Dorrestein Pieter, C., & Antón, J. (2020). Virulence as a Side Effect of Interspecies Interaction in Vibrio Coral Pathogens. *mBio*, *11*(4), 10.1128/mbio.00201-00220. https://doi.org/10.1128/mbio.00201-20

Rubio-Portillo, E., Ramos-Esplá, A. A., & Antón, J. (2021). Shifts in marine invertebrate bacterial assemblages associated with tissue necrosis during a heat wave. *Coral Reefs*, *40*(2), 395-404. https://doi.org/10.1007/s00338-021-02075-0

Rubio-Portillo, E., Robertson, S., & Antón, J. (2024). Coral mucus as a reservoir of bacteriophages targeting Vibrio pathogens. *The ISME Journal*, *18*(1), wrae017. https://doi.org/10.1093/ismejo/wrae017

Ruiz-Diaz, C., Andez, C., Mercado-Molina, A., & Sabat, A. (2016). Scraping and extirpating: Two strategies to induce recovery of diseased Gorgonia ventalina sea fans. *Marine Ecology*, *37*. https://doi.org/10.1111/maec.12283

Saberian, M., Safari Roudsari, R., Haghshenas, N., Rousta, A., & Alizadeh, S. (2024). How the combination of alginate and chitosan can fabricate a hydrogel with favorable properties for wound healing. *Heliyon*, *10*(11). https://doi.org/10.1016/j.heliyon.2024.e32040

Sang, V. T., Dat, T. T., Vinh, L. B., Cuong, L. C., Oanh, P. T., Ha, H., Kim, Y. H., Anh, H. L., & Yang, S. Y. (2019). Coral and Coral-Associated Microorganisms: A Prolific Source of Potential Bioactive Natural Products. *Marine drugs*, *17*(8). https://doi.org/10.3390/md17080468

Saranjampour, P., Vebrosky, E. N., & Armbrust, K. L. (2017). Salinity Impacts on Water Solubility and n-Octanol/Water Partition Coefficients of Selected Pesticides and Oil Constituents. *Environmental Toxicology and Chemistry*, *36*(9), 2274-2280. https://doi.org/10.1002/etc.3784

Sato, Y., Bourne, D. G., & Willis, B. L. (2011). Effects of temperature and light on the progression of black band disease on the reef coral, Montipora hispida. *Coral Reefs*, *30*(3), 753-761. https://doi.org/10.1007/s00338-011-0751-5

Schmidt, G., Christ, P. E., Kertes, P. E., Fisher, R. V., Miles, L. J., & Wilker, J. J. (2023). Underwater Bonding with a Biobased Adhesive from Tannic Acid and Zein Protein. *ACS Applied Materials & Interfaces*, *15*(27), 32863-32874. https://doi.org/10.1021/acsami.3c04009

Schmidt, G., Christ, P. E., Kertes, P. E., Fisher, R. V., Miles, L. J., & Wilker, J. J. (2023). Underwater Bonding with a Biobased Adhesive from Tannic Acid and Zein Protein. *ACS Appl Mater Interfaces*, *15*(27), 32863-32874. https://doi.org/10.1021/acsami.3c04009

Schmidt, G., Kitts, L. H., Fisher, R. V., Supasueb, N., & Wilker, J. J. (2025). Plant-Based Underwater Adhesives Developed for Bonding Coral in Sea Water. *ACS Applied Polymer Materials*, *7*(16), 10395-10403. https://doi.org/10.1021/acsapm.5c01029

Scribano, V., Contardi, M., Rinaldi, C., Isa, V., Fiorentini, F., Ceseracciu, L., Gandolfi, I., Ghizzi, I., Lavorano, S., Galli, P., Montano, S., & Athanassiou, A. (2025). Eco-friendly active film and sealant for underwater drug delivery to diseased corals. *One Earth*, *8*(7). https://doi.org/10.1016/j.oneear.2025.101356

Shao, X., Liu, T., Li, Y., Wei, X., Ran, X., Li, J., Yuan, Z., Du, G., & Yang, L. (2025). Recyclable High-Performance Underwater Adhesives Inspired by "Spider Web" Geometric Structure. *ACS Sustainable Chemistry & Engineering*, *13*(27), 10441-10452. https://doi.org/10.1021/acssuschemeng.5c01893

Sheikh, H. I., Najiah, M., Fadhlina, A., Laith, A. A., Nor, M. M., Jalal, K. C. A., & Kasan, N. A. (2022). Temperature Upshift Mostly but not Always Enhances the Growth of Vibrio Species: A Systematic Review [Systematic Review]. *Frontiers in Marine Science*, *9*. https://doi.org/10.3389/fmars.2022.959830

Sheridan, C., Kramarsky-Winter, E., Sweet, M., Kushmaro, A., & Leal, M. C. (2013). Diseases in coral aquaculture: causes, implications and preventions. *Aquaculture*, *396*, 124-135. https://doi.org/10.1016/j.aquaculture.2013.02.037

Shilling, E. N., Combs, I. R., & Voss, J. D. (2021). Assessing the effectiveness of two intervention methods for stony coral tissue loss disease on. *Scientific Reports*, *11*(1). https://doi.org/10.1038/s41598-021-86926-4

Smith, A. W. (2005). Biofilms and antibiotic therapy: Is there a role for combating bacterial resistance by the use of novel drug delivery systems? *Advanced Drug Delivery Reviews*, *57*(10), 1539-1550. https://doi.org/10.1016/j.addr.2005.04.007

Sonawane, M., Shinkar, D., & Ravindrasaudagar. (2017). MUCOADHESIVE BUCCAL DRUG DELIVERY SYSTEM: REVIEW ARTICLE. *International Journal of Current Pharmaceutical Research*, *9*(4), 1-4. https://doi.org/10.22159/ijcpr.2017v9i4.20960

Stewart, R. J., Wang, C. S., & Shao, H. (2011). Complex coacervates as a foundation for synthetic underwater adhesives. *Advances in Colloid and Interface Science*, *167*(1), 85-93. https://doi.org/10.1016/j.cis.2010.10.009

Strathdee, S. A., Hatfull, G. F., Mutalik, V. K., & Schooley, R. T. (2023). Phage therapy: From biological mechanisms to future directions. *Cell*, *186*(1), 17-31. https://doi.org/10.1016/j.cell.2022.11.017

Studivan, M. S., Eckert, R. J., Shilling, E., Soderberg, N., Enochs, I. C., & Voss, J. D. (2023). Stony coral tissue loss disease intervention with amoxicillin leads to a reversal of disease-modulated gene expression pathways. *Molecular Ecology*, *32*(19), 5394-5413. https://doi.org/10.1111/mec.17110

Suggett, D. J., Edwards, M., Cotton, D., Hein, M., & Camp, E. F. (2023). An integrative framework for sustainable coral reef restoration. *One Earth*, *6*(6), 666-681. https://doi.org/10.1016/j.oneear.2023.05.007

Sussman, M., Willis, B. L., Victor, S., & Bourne, D. G. (2008). Coral Pathogens Identified for White Syndrome (WS) Epizootics in the Indo-Pacific. *Plos One*, *3*(6), e2393. https://doi.org/10.1371/journal.pone.0002393

Sweet, M., & Bythell, J. (2012). Ciliate and bacterial communities associated with White Syndrome and Brown Band Disease in reef-building corals. *Environmental Microbiology*, *14*(8), 2184-2199. https://doi.org/10.1111/j.1462-2920.2012.02746.x

Sweet, M., & Bythell, J. (2017). The role of viruses in coral health and disease. *Journal of Invertebrate Pathology*, *147*, 136-144. https://doi.org/10.1016/j.jip.2016.12.005

Sweet, M., Jones, R., & Bythell, J. (2012). Coral diseases in aquaria and in nature. *Journal of the Marine Biological Association of the United Kingdom*, *92*(4), 791-801. https://doi.org/10.1017/S0025315411001688

Sweet, M., Ramsey, A., & Bulling, M. (2017). Designer reefs and coral probiotics: great concepts but are they good practice? *Biodiversity*, *18*(1), 19-22. https://doi.org/10.1080/14888386.2017.1307786

Sweet, M., Villela, H., Keller-Costa, T., Costa, R., Romano, S., Bourne, D. G., Cárdenas, A., Huggett, M. J., Kerwin, A. H., Kuek, F., Medina, M., Meyer, J. L., Müller, M., Pollock, F. J., Rappé, M. S., Sere, M., Sharp, K. H., Voolstra, C. R., Zaccardi, N., . . . Peixoto, R. (2021). Insights into the Cultured Bacterial Fraction of Corals. *Msystems*, *6*(3). https://doi.org/10.1128/mSystems.01249-20

Sweet, M. J., & Bulling, M. T. (2017). On the Importance of the Microbiome and Pathobiome in Coral Health and Disease. *Frontiers in Marine Science*, *4*. https://doi.org/10.3389/fmars.2017.00009

Sweet, M. J., Croquer, A., & Bythell, J. C. (2014). Experimental antibiotic treatment identifies potential pathogens of white band disease in the endangered Caribbean coral Acropora cervicornis. *Proc Biol Sci*, *281*(1788), 20140094. https://doi.org/10.1098/rspb.2014.0094

Taghizadeh, A., Taghizadeh, M., Yazdi, M. K., Zarrintaj, P., Ramsey, J. D., Seidi, F., Stadler, F. J., Lee, H., Saeb, M. R., & Mozafari, M. (2022). Mussel-inspired biomaterials: From chemistry to clinic. *Bioeng Transl Med*, *7*(3), e10385. https://doi.org/10.1002/btm2.10385

Tagliafico, A., Rangel, S., Kelaher, B., Scheffers, S., & Christidis, L. (2018). A new technique to increase polyp production in stony coral aquaculture using waste fragments without polyps. *Aquaculture*, *484*, 303-308. https://doi.org/10.1016/j.aquaculture.2017.09.021

Tagliaro, I., Mariani, M., Akbari, R., Contardi, M., Summa, M., Saliu, F., Nisticò, R., & Antonini, C. (2024). PFAS-free superhydrophobic chitosan coating for fabrics. *Carbohydrate Polymers*, *333*. https://doi.org/10.1016/j.carbpol.2024.121981

Tang, Z., Lin, X., Yu, M., Mondal, A. K., & Wu, H. (2024). Development of Biocompatible Mussel-Inspired Cellulose-Based Underwater Adhesives. *ACS Omega*, *9*(3), 3877-3884. https://doi.org/10.1021/acsomega.3c07972

Tavares-Carreon, F., De Anda-Mora, K., Rojas-Barrera, I. C., & Andrade, A. (2023). Serratia marcescens antibiotic resistance mechanisms of an opportunistic pathogen: a literature review. *PeerJ*, *11*, e14399. https://doi.org/10.7717/peerj.14399

Thangudu, S., & Su, C.-H. (2025). Review of light activated antibacterial nanomaterials in the second biological window. *Journal of Nanobiotechnology*, *23*(1), 293. https://doi.org/10.1186/s12951-025-03333-x

Thatcher, C., Hoj, L., & Bourne, D. G. (2022). Probiotics for coral aquaculture: challenges and considerations. *Current Opinion in Biotechnology*, *73*, 380-386. https://doi.org/10.1016/j.copbio.2021.09.009

Thurber, R. L. V., Burkepile, D. E., Fuchs, C., Shantz, A. A., McMinds, R., & Zaneveld, J. R. (2014). Chronic nutrient enrichment increases prevalence and severity of coral disease and bleaching. *Global Change Biology*, *20*(2), 544-554. https://doi.org/10.1111/gcb.12450

Thurber, R. V., Mydlarz, L. D., Brandt, M., Harvell, D., Weil, E., Raymundo, L., Willis, B. L., Langevin, S., Tracy, A. M., Littman, R., Kemp, K. M., Dawkins, P., Prager, K. C., Garren, M., & Lamb, J. (2020). Deciphering Coral Disease Dynamics: Integrating Host, Microbiome, and the Changing Environment. *Frontiers in Ecology and Evolution*, *8*. https://doi.org/10.3389/fevo.2020.575927

Thurber, R. V., Willner-Hall, D., Rodriguez-Mueller, B., Desnues, C., Edwards, R. A., Angly, F., Dinsdale, E., Kelly, L., & Rohwer, F. (2009). Metagenomic analysis of stressed coral holobionts. *Environmental Microbiology*, *11*(8), 2148-2163. https://doi.org/10.1111/j.1462-2920.2009.01935.x

Tian, Q. R., Zhou, W. Q., Cai, Q., Pan, X. Y., Ma, G. H., & Lian, G. P. (2024). Bi-layered oil encapsulates formed by polydopamine-supported in situ complex coacervation: Investigation of structure formation and sustained release performance. *Colloids and Surfaces a-Physicochemical and Engineering Aspects*, *692*. https://doi.org/10.1016/j.colsurfa.2024.133976

Tiu, B. D. B., Delparastan, P., Ney, M. R., Gerst, M., & Messersmith, P. B. (2019). Enhanced Adhesion and Cohesion of Bioinspired Dry/Wet Pressure-Sensitive Adhesives. *ACS Applied Materials & Interfaces*, *11*(31), 28296-28306. https://doi.org/10.1021/acsami.9b08429

Toledo-Hernández, C., Zuluaga-Montero, A., Bones-González, A., Rodríguez, J. A., Sabat, A. M., & Bayman, P. (2008). Fungi in healthy and diseased sea fans (Gorgonia ventalina): is Aspergillus sydowii always the pathogen? *Coral Reefs*, *27*(3), 707-714. https://doi.org/10.1007/s00338-008-0387-2

Topaz, M., Athamna, A., Ashkenazi, I., Shpitz, B., & Freimann, S. (2021). In-vitro model for bacterial growth inhibition of compartmentalized infection treated by an ultra-high concentration of antibiotics. *Plos One*, *16*(6), e0252724. https://doi.org/10.1371/journal.pone.0252724

Toth, K. A., Buckley, S. F., Noren, H., Neely, K. L., & Walker, B. K. (2024). Broadscale coral disease interventions elicit efficiencies in endemic disease response [Original Research]. *Frontiers in Marine Science*, *10*. https://doi.org/10.3389/fmars.2023.1302697

Ushijima, B., Gunasekera, S. P., Meyer, J. L., Tittl, J., Pitts, K. A., Thompson, S., Sneed, J. M., Ding, Y., Chen, M., Jay Houk, L., Aeby, G. S., Häse, C. C., & Paul, V. J. (2023). Chemical and genomic characterization of a potential probiotic treatment for stony coral tissue loss disease. *Communications Biology*, *6*(1), 248. https://doi.org/10.1038/s42003-023-04590-y

Ushijima, B., Meyer, J. L., Thompson, S., Pitts, K., Marusich, M. F., Tittl, J., Weatherup, E., Reu, J., Wetzell, R., Aeby, G. S., Häse, C. C., & Paul, V. J. (2020). Disease Diagnostics and Potential Coinfections by Vibrio coralliilyticus During an Ongoing Coral Disease Outbreak in Florida. *Frontiers in Microbiology*, *Volume 11 - 2020*. https://doi.org/10.3389/fmicb.2020.569354

Ushijima, B., Videau, P., Burger Andrew, H., Shore-Maggio, A., Runyon Christina, M., Sudek, M., Aeby Greta, S., & Callahan Sean, M. (2014). Vibrio coralliilyticus Strain OCN008 Is an Etiological Agent of Acute Montipora White Syndrome. *Applied and Environmental Microbiology*, *80*(7), 2102-2109. https://doi.org/10.1128/AEM.03463-13

van de Water, J. A. J. M., Lamb, J. B., van Oppen, M. J. H., Willis, B. L., & Bourne, D. G. (2015). Comparative immune responses of corals to stressors associated with offshore reef-based tourist platforms. *Conservation Physiology*, *3*. https://doi.org/10.1093/conphys/cov032

Vega Thurber, R. L., Silva, D., Speare, L., Croquer, A., Veglia, A. J., Alvarez-Filip, L., Zaneveld, J. R., Muller, E. M., & Correa, A. M. S. (2025). Coral Disease: Direct and Indirect Agents, Mechanisms of Disease, and Innovations for Increasing Resistance and Resilience. *Ann Rev Mar Sci*, *17*(1), 227-255. https://doi.org/10.1146/annurev-marine-011123-102337

Veloso, S. R. S., Marta, E. S., Rodrigues, P. V., Moura, C., Amorim, C. O., Amaral, V. S., Correa-Duarte, M. A., & Castanheira, E. M. S. (2023). Chitosan/Alginate Nanogels Containing Multicore Magnetic

Nanoparticles for Delivery of Doxorubicin. *Pharmaceutics*, *15*(9). https://doi.org/10.3390/pharmaceutics15092194

Visan, A. I., Popescu-Pelin, G., & Socol, G. (2021). Degradation Behavior of Polymers Used as Coating Materials for Drug Delivery-A Basic Review. *Polymers*, *13*(8). https://doi.org/10.3390/polym13081272

Vizcaino, M. I., Johnson, W. R., Kimes, N. E., Williams, K., Torralba, M., Nelson, K. E., Smith, G. W., Weil, E., Moeller, P. D. R., & Morris, P. J. (2010). Antimicrobial Resistance of the Coral Pathogen Vibrio coralliilyticus and Caribbean Sister Phylotypes Isolated from a Diseased Octocoral. *Microbial Ecology*, *59*(4), 646-657. https://doi.org/10.1007/s00248-010-9644-3

Voolstra, C. R., Raina, J. B., Dorr, M., Cardenas, A., Pogoreutz, C., Silveira, C. B., Mohamed, A. R., Bourne, D. G., Luo, H., Amin, S. A., & Peixoto, R. S. (2024). The coral microbiome in sickness, in health and in a changing world. *Nat Rev Microbiol*, *22*(8), 460-475. https://doi.org/10.1038/s41579-024-01015-3

Walker, B. K., Turner, N. R., Noren, H. K. G., Buckley, S. F., & Pitts, K. A. (2021). Optimizing Stony Coral Tissue Loss Disease (SCTLD) Intervention Treatments on Montastraea cavernosa in an Endemic Zone [Original Research]. *Frontiers in Marine Science*, *8*. https://doi.org/10.3389/fmars.2021.666224

Wang, W., Tang, K., Wang, P., Zeng, Z., Xu, T., Zhan, W., Liu, T., Wang, Y., & Wang, X. (2022). The coral pathogen Vibrio coralliilyticus kills non-pathogenic holobiont competitors by triggering prophage induction. *Nature Ecology & Evolution*, *6*(8), 1132-1144. https://doi.org/10.1038/s41559-022-01795-y

Ward, J. R., Kim, K., & Harvell, C. D. (2007). Temperature affects coral disease resistance and pathogen growth. *Marine Ecology Progress Series*, *329*, 115-121. https://doi.org/10.3354/meps329115

Wijmans, J. G., & Baker, R. W. (1995). The solution-diffusion model: a review. *Journal of Membrane Science*, *107*(1), 1-21. https://doi.org/10.1016/0376-7388(95)00102-I

Willis, B. L., Page, C. A., & Dinsdale, E. A. (2004). Coral Disease on the Great Barrier Reef. In E. Rosenberg & Y. Loya (Eds.), *Coral Health and Disease* (pp. 69-104). Springer Berlin Heidelberg. https://doi.org/10.1007/978-3-662-06414-6_3

Wójcik-Pastuszka, D., Stawicka, K., Drys, A., & Musial, W. (2023). Influence of HA on Release Process of Anionic and Cationic API Incorporated into Hydrophilic Gel. *International Journal of Molecular Sciences*, *24*(6). https://doi.org/10.3390/ijms24065606

Work, T. M., & Aeby, G. S. (2006). Systematically describing gross lesions in corals. *Diseases of Aquatic Organisms*(0177-5103 (Print)). https://doi.org/10.3354/dao070155

Work, T. M., Weatherby, T. M., Landsberg, J. H., Kiryu, Y., Cook, S. M., & Peters, E. C. (2021). Viral-Like Particles Are Associated With Endosymbiont Pathology in Florida Corals Affected by Stony Coral Tissue Loss Disease [Original Research]. *Frontiers in Marine Science*, *Volume 8 - 2021*. https://doi.org/10.3389/fmars.2021.750658

Wu, P., & Grainger, D. W. (2006). Drug/device combinations for local drug therapies and infection prophylaxis. *Biomaterials*, *27*(11), 2450-2467. https://doi.org/10.1016/j.biomaterials.2005.11.031

Xu, M., Cai, Z., Cheng, K., Chen, G., & Zhou, J. (2024). Mitigation of Vibrio coralliilyticus-induced coral bleaching through bacterial dysbiosis prevention by Ruegeria profundi. *Applied and Environmental Microbiology*, *90*(4), e02274-02223. https://doi.org/10.1128/aem.02274-23

Xu, Y., Chen, H., Fang, Y., & Wu, J. (2022). Hydrogel Combined with Phototherapy in Wound Healing. *Advanced Healthcare Materials*, *11*(16), 2200494. https://doi.org/10.1002/adhm.202200494

Yadav, D., & Dutta, J. (2024). A systematic review on recent development of chitosan/alginate-based polyelectrolyte complexes for wastewater treatment. *International Journal of Environmental Science and Technology*, *21*(3), 3381-3406. https://doi.org/10.1007/s13762-023-05244-6

Zaneveld, J. R., Burkepile, D. E., Shantz, A. A., Pritchard, C. E., McMinds, R., Payet, J. P., Welsh, R., Correa, A. M. S., Lemoine, N. P., Rosales, S., Fuchs, C., Maynard, J. A., & Thurber, R. V. (2016). Overfishing and nutrient pollution interact with temperature to disrupt coral reefs down to microbial scales. *Nature Communications*, *7*. https://doi.org/10.1038/ncomms11833

Zhang, L., Liu, Y., Liu, S., Wang, T., Ouyang, F., Pei, Z., Ren, Y., & Shuai, Q. (2024). NIR-intervened thermally accelerated urease-propelled MOF nanosubmarine for antibiotic-free antibacterial inhibition via

single-wavelength synergistic PDT/PTT. *International Journal of Biological Macromolecules*, *282*, 137367. https://doi.org/https://doi.org/10.1016/j.ijbiomac.2024.137367

Zhu, W., Pan, S., Zhang, J., Xu, J., Zhang, R., Zhang, Y., Fu, Z., Wang, Y., Hu, C., & Xu, Z. (2024). The role of hyperthermia in the treatment of tumor. *Critical Reviews in Oncology/Hematology*, *204*, 104541. https://doi.org/10.1016/j.critrevonc.2024.104541

Zych, A., Contardi, M., Rinaldi, C., Scribano, V., Isa, V., Kossyvaki, D., Gobbato, J., Ceseracciu, L., Lavorano, S., Galli, P., Athanassiou, A., & Montano, S. (2024). Underwater Quick-Hardening Vegetable Oil-Based Biodegradable Putty for Sustainable Coral Reef Restoration and Rehabilitation. *Advanced Sustainable Systems*. https://doi.org/10.1002/adsu.202400110

Acknowledgments

Scientific acknowledgments

The development of this project would not have been possible without the collaboration of many other researchers, whom I desire to cite and thank here:

- Chapter 3: Athanassia Athanassiou Ph.D. (ORCID: 0000-0002-6533-3231), Luca Ceseracciu Ph.D. (ORCID: 0000-0003-3296-8051), Marco Contardi Ph.D. (ORCID: 0000-0003-3877-7985), Professor Paolo Galli (ORCID: 0000-0002-6065-8192), Fabrizio Fiorentini, Ph.D. (ORCID: 0000-0001-8863-5286), Professor Isabella Gandolfi (ORCID: 0000-0002-0267-2412), Isabella Ghizzi (ORCID: 0009-0006-8088-5591), Valerio Isa Ph.D. (0000-0001-8073-7448), Silvia Lavorano Ph.D. (ORCID: 0000-0002-9353-6298), Professor Simone Montano (ORCID: 0000-0002-6612-8731), Camilla Rinaldi (ORCID: 0009-0004-2462-1183).
- Chapter 4: Athanassia Athanassiou Ph.D. (ORCID: 0000-0002-6533-3231), Marco Contardi Ph.D. (ORCID: 0000-0003-3877-7985), Martina Nardi Ph.D. (ORCID: 0000-0002-8857-8813).
- Chapter 5: Athanassia Athanassiou Ph.D. (ORCID: 0000-0002-6533-3231), Camile Avelino, Ph.D. (ORCID: 0000-0002-1442-7289), Triona Barker (ORCID: 0009-0009-9870-2740), Marco Contardi Ph.D. (ORCID: 0000-0003-3877-7985), Professor Paolo Galli (ORCID: 0000-0002-6065-8192), Professor Simone Montano (ORCID: 0000-0002-6612-8731), Professor Michael Sweet (ORCID: 0000-0003-4983-8333), Abigail Yates.
- Chapter 6: Athanassia Athanassiou Ph.D. (ORCID: 0000-0002-6533-3231), Marco Contardi Ph.D. (ORCID: 0000-0003-3877-7985), Nabila Jarmouni Ph.D. (ORCID: 0000-0002-0111-825X), Professor Simone Montano (ORCID: 0000-0002-6612-8731), Teresa Pellegrino Ph.D. (ORCID: 0000-0001-5518-1134), Ecem Tiryaki Ph.D. (ORCID: 0000-0002-9746-0825).

A special thank you goes to Marco Contardi and Simone Montano, who followed me during this journey and guided me to reach the point where I am. Another big thank you goes to Athanassia Athanassiou, who allowed me to work in her group, fund my work, and use their facilities to perform the research I have performed so far. Finally, I would like to thank Professor Michael Sweet, who allowed me to work in his laboratories and facility during my period abroad.

Personal acknowledgments

I cannot avoid speaking up to all the people who, through this doctorate journey, left a mark on my lab book or on my heart.

The first people to thank are my family: I will not be here without their support, motivation, and persuasion to continue my studies. I am extremely grateful for that, thank you, Mum, Dad, Cati, Mari, and Anna.

I want to thank my partner, Rhi, who has been a great support and motivated me, even when everything seemed lost, and my morale was underground. Their rationality pushed me to face challenges that before seemed impossible to go through. I am feeling I have matured so much thanks to you. I am so lucky I met you. Thank you Baba.

I also want to thank a person who may not read this acknowledgment but who definitely deserves it, my therapist. I am really grateful to her for guiding me through some of the traumas and some very difficult moments of my life in these last three years. Thank you.

A massive, gigantic thanks goes to Marco, who has been more of a big brother than a supervisor. He was there at the beginning, inviting me to his famous and amazing dinners, he was there in the middle where the progression of the PhD was tougher, he was there until the very end when I was about to take the last steps of this journey. Despite we did not agree all the times, we also shared awesome ideas and small great joys. I am very grateful I had you next to me in this journey as supervisor and as a friend. Thank you.

Another thank goes to Fabri, friend, colleague, and friend again. I am immensely grateful for all the times you helped me move, from one place to the other, from one life to the other. I want to thank you also for all the nights I called you and you were there to listen, chat and support me, even when I was abroad: on our calls, I allowed a piece of my soul to stay in Genova. Thank you.

A big thank you also goes to Enrico, who, in the last year listened to my complaints and my babbling. Thank you.

I also want to thank my historical friends, Gianki and Brunetta, who have been my primordial boost to push even further and motivated me to go on each time we were meeting. I don’t have words to describe our friendship, is there, it is strong and we all know it. Thank you guys.

A group that has been my second family and that I want to thank is the dance school that hosted me in these last three years, Danza3, and saw me in every possible sauce from drained to hyper energized, and always welcomed me, in- and out-side school. Thank you, Fil, Ila, Ari, Mauri, Manu, Silvia, Ale, Cla, Vale.

I also want to thank Jessica and Sanjana, who, other than colleagues, have been great friends and supporters. I am really grateful for your friendship and our moments reading poetries. Thank you girls.

I finally want to thank all the obstacles, all the people who did not believe in me, all the failed experiments of my life. It is thanks to these challenges that I reached this point, and I have had the opportunity to meet as much wonderful people throughout my life. Thank you.

Overall, my stubbornness allowed me to crash through every wall, and whenever I was unable to get through that barrier, I stepped back just to run faster against it until I smashed through and went forward. I learnt to fail and I would not be here if I was not pushing until now to reach my goals.

A famous singer once said, “I want to thank me for believing in me, I want to thank me for doing all this hard work, I want to thank me for never quitting” and I agree on saying that each one of us should thank first themselves on top of all. Thank me.

Noi non siamo macchine pensanti che si emozionano, ma siamo macchine emotive che pensano. – Antonio Damasio